ALMA MATER STUDIORUM
UNIVERSITÀ DI BOLOGNA

DEPARTMENT OF CIVIL, CHEMICAL, ENVIRONMENTAL, AND MATERIALS ENGINEERING - DICAM

SECOND CYCLE DEGREE

NUMERICAL MODELLING OF PIPE UMBRELLA SYSTEM FOR SHALLOW TUNNELS

Dissertation in Civil Engineering

Supervisor

Prof. Alessio Mentani

Defended by

Lorenzo Sampieri

Co-Supervisor

Prof. Frédéric Collin

Graduation Session July 2026

Academic Year 2025/2026

ALMA MATER STUDIORUM
UNIVERSITÀ DI BOLOGNA

DEPARTMENT OF CIVIL, CHEMICAL, ENVIRONMENTAL, AND MATERIALS ENGINEERING - DICAM

SECOND CYCLE DEGREE

NUMERICAL MODELLING OF PIPE UMBRELLA SYSTEM FOR SHALLOW TUNNELS

Dissertation in Civil Engineering

Supervisor
Prof. Alessio Mentani

Co-Supervisor
Prof. Frédéric Collin

Defended by
Lorenzo Sampieri

Graduation Session July 2026

Academic Year 2025/2026

Acknowledgments

I would like to thank my parents, my family and my friends, who have always been close to me and supported me, despite the physical distance of the past year.

I would also like to thank all the people I met during this new university experience in Liège. Each of them, together with every experience I lived, allowed me to appreciate new perspectives and to grow with greater awareness.

It was not easy to adapt to a new environment, but what I found was a welcoming and human reality, able to make me feel comfortable and appreciated.

A special thanks goes to Professor Collin, for guiding me through the final steps of my university career, and to the company that hosted me in Paris, Amberg Engineering, to whom I owe one of the most formative experiences of my life, both professionally and personally. For this reason, I would like to express my sincere gratitude to all my colleagues at Amberg Engineering and, in particular, to Yves Cojean and Roba Houhou, who supported and advised me during the development of my thesis.

Vorrei ringraziare i miei genitori, la mia famiglia ed i miei amici, che mi sono sempre vicini e che mi sostengono, nonostante la distanza fisica dell'ultimo anno.

Vorrei inoltre ringraziare tutte le persone che ho incontrato in questo nuovo percorso universitario a Liegi. Ognuna di loro, insieme a ogni esperienza vissuta, mi ha permesso di apprezzare nuove prospettive e di crescere con maggiore consapevolezza.

Non è stato facile ambientarsi in un mondo nuovo, ma quello che ho trovato è stata una realtà accogliente ed umana, capace di farmi sentire a mio agio ed apprezzato.

Un ringraziamento speciale va al professor Collin, per avermi guidato nei passi finali della mia carriera universitaria, e all'azienda che mi ha accolto a Parigi, Amberg Engineering, alla quale devo una delle esperienze più formative della mia vita, sia dal punto di vista professionale sia umano. Per questo motivo, vorrei esprimere la mia sincera gratitudine a tutti i miei colleghi di Amberg Engineering e, in particolare, a Yves Cojean e Roba Houhou, che mi hanno seguito e consigliato durante lo sviluppo della mia tesi.

Abstract

Context

Shallow tunnels represent a very delicate condition during excavation. To reinforce the ground, pre-support techniques are therefore often adopted to improve soil stability and reduce deformations. Among these techniques, the pipe umbrella system consists of installing steel pipes in the ground in order to improve the mechanical properties of the soil.

Objectives

The modelling of the pipe umbrella system is a complex problem, for which simplified two-dimensional approaches represent a practical and computationally efficient solution. This thesis aims to investigate and test different 2D strategies to represent the effect of the pipe umbrella in axisymmetric conditions, evaluating their consistency, limitations and relative reliability. Explicit three-dimensional models, although potentially more accurate, require a significantly higher computational cost and are not included within the scope of this work.

Methodology

An analytical model based on the Convergence-confinement method was first developed to define a preliminary tunnel response. Subsequently, a reference problem based on the same assumptions was implemented in the FEM software Lagamine and Plaxis 2D under axisymmetric conditions, modelling different excavation stages. In the numerical models, three simplified equivalent strategies were introduced to represent the behaviour of the soil reinforced with pipes. The three techniques are: linear elastic equivalent volume, anisotropic material and enhanced soil. The results are then compared with each other in terms of stresses, deformations and deconfinement.

Results

The methods produce different deformation responses, depending on the adopted strategy. The linear elastic equivalent volume shows a very high stiffness and may be poorly representative of the real behaviour. The anisotropic material presents a more beam-like behaviour, being able to better capture the greater bending stiffness in the axial direction introduced by the pipes. The enhanced soil shows a less beam-like behaviour, but in terms of deformation magnitude it provides results comparable to those of the anisotropic material.

Conclusions

The results show that some 2D strategies are able to capture part of the global effect of the pipe umbrella system, although they do not directly represent its real three-dimensional nature. As a future perspective, it would be interesting to develop an equivalent 3D model reproducing the same assumptions, conditions and excavation stages. Moreover, it would also be worthwhile to implement the same problems with different initial assumptions, introducing for example anisotropy of the stress state and gravity.

Keywords: shallow tunnel, convergence-confinement method, deconfinement, pipe umbrella system, tunnel reinforcement, axisymmetric modelling, homogenization, Plaxis 2D; Lagamine.

Contents

1 Introduction

1.1 Context and motivation

Tunnel construction has always represented one of the most challenging tasks in civil and geotechnical engineering. Its complexity is related not only to the design of the excavation and support system, but also to the uncertainty associated with ground conditions, the uniqueness of each site, construction logistics, and the interaction with the surrounding environment.

In many cases, tunnels represent the only feasible infrastructure solution, especially in densely urbanised areas where surface space is limited. This is the case, for example, of underground metro lines. In this context, the excavation process must be controlled carefully, since even relatively small ground movements may affect existing buildings, underground utilities and other sensitive structures (Elyasi et al., 2016; Zarei, Moarefvand, & Salmi, 2019). Therefore, the design requirements are strongly linked to serviceability limits, such as limitation of tunnel convergence and ground settlements within acceptable values.

The most critical stage is often associated with the excavation zone close to the advancing face, where the ground has already been disturbed but the final support has not yet fully developed its stabilising effect (Panet & Sulem, 2022). For this reason, tunnelling in weak or deformable ground is frequently combined with pre-support techniques. These systems aim to improve the soil response before excavation and to reduce the deformation during tunnel advance.

Among the possible pre-support measures, this thesis focuses on the pipe umbrella system. This technique consists of installing steel pipes ahead of the excavation, mainly around the crown, so that a reinforced zone is created before the ground is excavated (Figure 1.1). Its purpose is to reduce the deformation that develops before the primary support becomes fully effective (Elyasi et al., 2016; Volkmann & Schubert, 2007; Zarei et al., 2019).

The main mechanical role of the pipe umbrella is to increase the stiffness of the ground above the tunnel crown and to improve load transfer ahead of the excavation face. In this way, the reinforced zone contributes to reducing tunnel convergence and surface settlements during the excavation process (Zarei et al., 2019; Zhang, Li, Liu, Li, & Shi, 2014). This makes the pipe umbrella system particularly useful for shallow tunnels in urban environments, where deformation control is often one of the governing design criteria.

In this context, the present thesis focuses on finding a way to simplify the modelling of a pipe umbrella pre-support system, offering different strategies and possible solutions in a 2D axisymmetric environment, providing a basis for further evaluations. The work starts from an analytical reference model based on the Convergence–Confinement Method and then develops two-dimensional axisymmetric numerical models in Lagamine and Plaxis 2D. The aim is to evaluate how the mechanical effect of the pipe umbrella can be introduced through equivalent properties, and to understand to what extent these simplified models can reproduce the main mechanisms without relying systematically on full three-dimensional analyses.

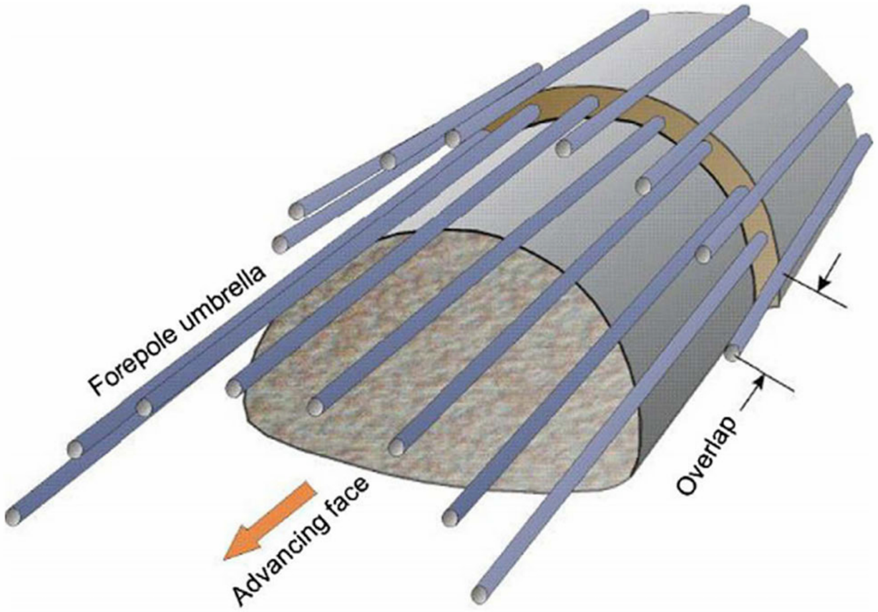

Figure 1.1: Pipe umbrella system simplified scheme. Source: adapted from (Hoek, 2004).

1.2 Research gap and objectives

The process of tunnel excavation is inherently three-dimensional due to the advancing face, construction sequence, and activation of supports and pre-supports (Panet & Sulem, 2022). Among the available modelling approaches, 3D models are indeed able to capture the behaviour of the system more accurately. However, these models are extremely demanding to develop and solve, explaining why some alternatives to 3D modelling have been explored, such as analytical and 2D approaches; these are indeed widely used in engineering practice because of their lower computational cost and their ability to provide robust preliminary estimates when properly calibrated (Neuner, Schreter, Gamnitzer, & Hofstetter, 2020; Svoboda & Masin, 2009).

The effectiveness of pipe umbrella systems in reducing tunnel convergence and ground movements has been widely reported in the literature (Elyasi et al., 2016; Volkmann & Schubert, 2007; Zarei et al., 2019). Still, their representation in simplified numerical models is associated with significant uncertainties, since it is not always clear which simplification is actually the most suitable to reproduce the global behaviour of the problem (Bae, Shin, Sicilia, Choi, & Lim, 2005; Schumacher & Kim, 2013; Zhang et al., 2014):

The goal of this project is not to study the effects of the pipe umbrella system in general, nor to study the behaviour of a single pipe, but to identify a reliable solution able to account for the presence of the system without the need to perform computationally expensive 3D numerical models.

With the necessary limitations, simplifications and assumptions, this thesis therefore evaluates the possibility of simplifying the problem through the modelling of the pipe umbrella in 2D numerical models based on an axisymmetric framework.

The specific objectives of this thesis are:

- To develop an analytical reference workflow in Python, based on the CCM concepts, in order to understand the development of tunnel convergence and stress release;
- To develop simplified two-dimensional axisymmetric numerical models in FEM software such as Lagamine and Plaxis 2D;

- To implement and compare different equivalent representations of the pipe umbrella system in a 2D framework;
- To identify common comparison parameters, based on displacement and equivalent deconfinement, in order to evaluate the consistency and limitations of the proposed 2D strategies.

1.3 Research question

The main research question that is being explored in the current thesis is:

Can the effect of a pipe umbrella pre-support system in shallow tunnelling be represented and predicted using simplified 2D approaches?

1.4 Limitations of the thesis

This thesis is based on a simplified reference problem and is not intended to provide a complete design procedure for a real tunnel project. The aim is to investigate how the effect of a pipe umbrella pre-support system can be represented with two-dimensional numerical models.

The main limitations of the work are summarized as follows:

- The two-dimensional numerical models are developed under axisymmetric conditions; plane strain analyses are not considered;
- Gravity and water pressures are neglected in order to study only the effects of excavation, support activation and pipe umbrella representation;
- The ground behaviour is described by a Mohr–Coulomb elastoplastic model, without considering anisotropy or time-dependent effects. Anisotropy is a typical condition in shallow tunnelling, but it is not considered in the present work for simplification;
- The pipe umbrella is introduced through simplified continuous equivalent representations, rather than by modelling the full installation process, grouting and specific pipe and soil interactions;
- The focus is mainly on tunnel convergence and deformation control, while face stability and the detailed structural design of the pipes are not treated.

1.5 Thesis outline

The thesis is organised as follows:

- Chapter 2: Literature review.
  This chapter introduces the problem of deformation control in shallow tunnelling, the mechanical role of pipe umbrella pre-support systems, and the Convergence–Confinement Method as the theoretical framework of the thesis. It also reviews the main modelling strategies adopted in the literature for pipe umbrella systems.
- Chapter 3: Methodology.
  This chapter presents the workflow adopted and a discussion about the analytical and the FEM models. Also the evaluation parameters are introduced.
- Chapter 4: Reference problem and modelling assumptions
  This chapter defines the reference problem used in the thesis, including the geometry, initial stress state, material parameters and common assumptions used in the analytical and numerical models.
- Chapter 5: Analytical reference model.

This chapter presents the analytical model developed in Python and based on the Convergence–Confinement Method.

- Chapter 6: Two-dimensional numerical models.
  This chapter describes the axisymmetric numerical models developed in Lagamine and Plaxis 2D, including the excavation sequence, support activation and simplified representations of the pipe umbrella system. The limitations of the proposed 2D approaches are also presented.
- Chapter 7: Results.
  This chapter presents the analytical and two-dimensional results in terms of tunnel convergence, stress redistribution, support response and effectiveness of the pipe umbrella representation.
- Chapter 8: Comparison and discussion.
  This chapter compares and analyses critically the results obtained in the different modelling strategies using common indicators, such as radial displacement and equivalent deconfinement.
- Chapter 9: Conclusions and perspectives.
  This chapter summarises the main conclusions of the thesis and proposes possible developments for future work.

1.6 Chapter conclusion

In this chapter, the context in which this research is framed has been introduced. The motivation behind the need and relevance of this thesis has been identified by highlighting the research gap it aims to address. Since the scope of the present project is not to investigate the problem globally, its limitations have also been introduced and explicitly discussed within the chapter. Finally, in order to provide an overview of the thesis structure, the content of each chapter has been summarized.

2 Literature review

2.1 Shallow tunnelling and deformation control

In shallow tunnels, the control of deformation is often one of the main design issues, especially when the excavation is carried out in weak ground or below urban areas. In these situations, the tunnel response cannot be evaluated only in terms of collapse or global stability. The development of convergence, face movements and surface settlements may also govern the design, because even moderate ground movements can become critical for surrounding structures and buried services (Elyasi et al., 2016; Zarei et al., 2019).

As a result, pre-support systems are frequently adopted to improve the ground response during tunnel advance and to limit the deformation that develops before the primary support installation (Volkmann & Schubert, 2007; Zarei et al., 2019).

From a modelling point of view, this problem remains difficult because it is essentially three-dimensional. Full three-dimensional models can reproduce the excavation sequence more directly, but they are often too expensive. This explains the interest in simplified analytical and two-dimensional approaches, provided that their limitations are clearly understood (Neuner et al., 2020; Panet & Sulem, 2022; Svoboda & Masin, 2009).

2.2 Pipe umbrella pre-support: mechanisms, performance and governing parameters

A pipe umbrella is formed by a series of steel pipes installed ahead of the tunnel face, generally along the upper part of the excavation face. The pipes are arranged in the longitudinal direction of advance. Depending on the project, the system may also include grout inside the pipes or in the space between the pipe and the ground, so as to enhance even more the mechanical properties of the soil (Volkmann & Schubert, 2007; Zarei et al., 2019).

The role of the pipe umbrella is not limited to a simple increase of stiffness. It also modifies the way loads are transferred around the face and towards the already supported part of the tunnel. The system can also reduce the demand on the primary support (Zarei et al., 2019; Zhang et al., 2014).

The efficiency of the system depends on several aspects, such as the pipe–soil interaction, the type of contact between pipes and ground and the excavation sequence. These aspects explain why the behaviour of a pipe umbrella is difficult to represent with a single simplified parameter (Elyasi et al., 2016; Volkmann & Schubert, 2007; Zarei et al., 2019).

2.2.1 Key influencing parameters

The response of the pipe umbrella system is influenced by geometric, mechanical, and construction-related parameters, which are often analyzed through parametric studies (Elyasi et al., 2016; Morovatdar, Palassi, & Ashtiani, 2020; Zarei et al., 2019). From the geometric viewpoint, the most important parameters are the pipe length, the diameter, the thickness, the number of pipes and the spacing in the transversal direction (Figure 2.1). These are the main elements affecting the density and stiffness of the pre-reinforced zone. The inclination angle with respect to the tunnel axis and the fraction of the tunnel perimeter covered by the pipes are also important (Morovatdar et al., 2020; Volkmann & Schubert, 2007).

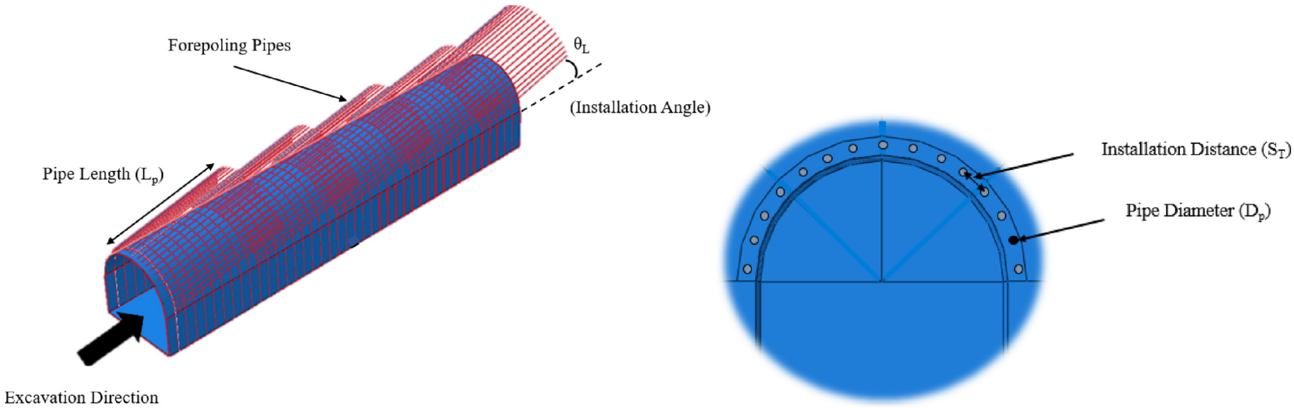

Figure 2.1: Main design variables in the umbrella method: pipe length, installation angle, transverse installation distance, and pipe diameter. Source: adapted from (Morovatdar et al., 2020).

From the viewpoint of the construction process, the response of the pipe umbrella system is also influenced by the excavation step, the distance from the face at which the umbrella is constructed, and the overlap between successive umbrellas (Elyasi et al., 2016; Ranjbarnia, Fakher, & Sayyah, 2018).

Finally, the possible grouting and the interaction between the soil and the pipe have an important influence on the effective stiffness of the system. Even if the geometry of the pipes is the same, different results can be obtained by considering different interaction conditions or different pipe stiffness (Schumacher & Kim, 2013; Volkmann & Schubert, 2007; Zhang et al., 2014). It is thus necessary to highlight these parameters and keep them constant while comparing different approaches.

2.2.2 Performance indicators in the literature (settlement, convergence)

In the literature, the performance of pipe umbrella systems is generally assessed through deformation indicators, since their main purpose is to reduce ground movements during excavation (Elyasi et al., 2016; Zarei et al., 2019), as they are also useful for comparing different pipe umbrella configurations (Morovatdar et al., 2020; Zarei et al., 2019).

At the tunnel level, the most frequently reported results include the crown displacement and the tunnel convergence and the deconfinement level. These results often help in understanding the impact of the pre-support in terms of deformation as well as the stage at which the pre-support is effective before or after the primary support (Ranjbarnia et al., 2018; Zarei et al., 2019).

2.3 Convergence–Confinement Method as theoretical basis

The Convergence–Confinement Method (CCM) is a design-oriented approach used to describe the interaction between the ground and the support during tunnel excavation. The method provides a simplified representation of the three-dimensional excavation process by replacing the effect of the advancing face with a progressive release of confinement at the tunnel boundary (Panet & Sulem, 2022).

In its classical formulation, the CCM is developed for an axisymmetric reference problem. However, the same concept is also commonly used in two-dimensional numerical modelling by imposing an equivalent deconfinement level for reproducing the effect of tunnel advance. In both cases, the main objective is to describe how the ground progressively deforms as the confinement is lost and how the support reacts after its installation (Panet & Sulem, 2022).

2.3.1 Main assumptions of the CCM

According to Panet and Sulem (2022), the classical formulation of the Convergence–Confinement Method is based on a simplified reference problem defined by the following assumptions:

- the tunnel has a circular cross-section;
- the ground is homogeneous and isotropic;
- the initial stress state is isotropic;
- the tunnel is sufficiently deep, which is to say that the tunnel radius is small compared with the tunnel depth;
- the influence of the advancing face is represented through a progressive reduction of the confinement acting at the tunnel boundary;
- the stress release is described by the deconfinement ratio λ, which varies from 0 to 1.

For $\lambda = 0$, the ground remains in its initial confined state, whereas for $\lambda = 1$, the tunnel boundary is fully deconfined. These assumptions enable interpretation of the three-dimensional excavation process using a simplified ground–support interaction model.

2.3.2 Ground–support interaction framework

Within this framework, the behaviour of the ground along the tunnel boundary is described by a ground convergence law, which expresses the relationship between the pressure at the boundary and the radial displacement:

$$f_m(p, u_R) = 0, \tag{2.1}$$

where $u_R = u_r(R)$ is the wall displacement and $p = \sigma_r(R)$ is the stress at the tunnel boundary. The support behaviour is described by a support confinement law:

$$f_s(p,\, u_R - u_{R,d}) = 0, \qquad u_{R,d} = u_R(d), \tag{2.2}$$

where d is the distance of installation of the support from the tunnel face and $u_{R,d}$ is the displacement that has already occurred before support activation.

The equilibrium condition of the supported tunnel section is reached when the confinement provided by the support equals the confinement required by the ground response. In practice, this condition is obtained at the intersection between two characteristic curves, the Ground Reaction Curve (GRC) and the Support Reaction Curve (SRC) (Panet & Sulem, 2022), as illustrated in Figure 2.2.

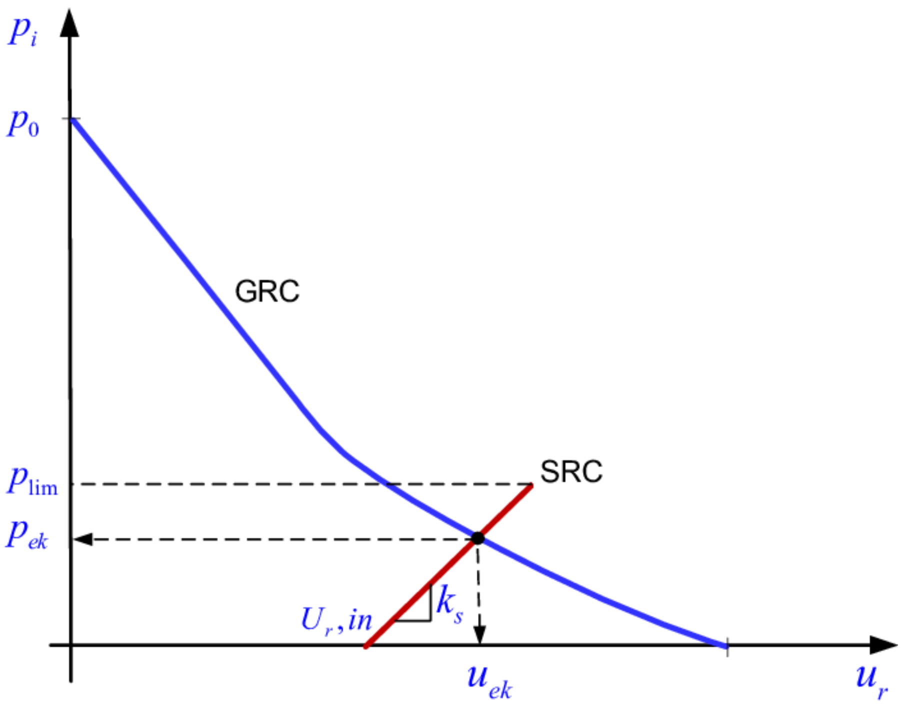

Figure 2.2: Example of Convergence–Confinement Method interaction diagram between GRC and SRC. Source: adapted from (Barla, 2010).

The GRC defines the relationship between the radial displacement of the tunnel wall and the stresses, while the SRC defines the relationship between the support pressure and the displacement of the support system (Panet & Sulem, 2022). The final equilibrium state provides the final convergence and the corresponding support pressure.

From a practical point of view, the CCM shows that part of the tunnel convergence occurs before the support becomes active. The method therefore provides a consistent way to describe the effect of support installation distance and to compute the final ground–support equilibrium (Panet & Sulem, 2022). Even in problems involving pre-support systems, such as umbrella arches, CCM-based formulations have been used to analyze the effect of pre-support in controlling tunnel deformation (Ranjbarnia et al., 2018).

2.3.3 Ground Reaction Curve (GRC)

The Ground Reaction Curve analytical expression depends on the constitutive model adopted for the ground and on the assumptions used to represent stress release.

The expressions reported in the following subsections follow the formulation presented by Panet and Sulem (2022).

2.3.3.1 Elastic, isotropic case

In the case of an isotropic elastic ground, the radial displacement field due to excavation can be written as

$$u_r(r) = \lambda \frac{R^2}{r} \frac{\sigma_0}{2G}, \tag{2.3}$$

where R is the tunnel radius, r is the radius of the considered point, σ_0 is the initial isotropic stress, G is the shear modulus of the ground, and λ is the deconfinement ratio.

The stress field in polar coordinates (Figure 2.3) is defined as

$$\sigma_r(r) = \left(1 - \lambda \frac{R^2}{r^2}\right) \sigma_0, \tag{2.4}$$

$$\sigma_\theta(r) = \left(1 + \lambda \frac{R^2}{r^2}\right) \sigma_0. \tag{2.5}$$

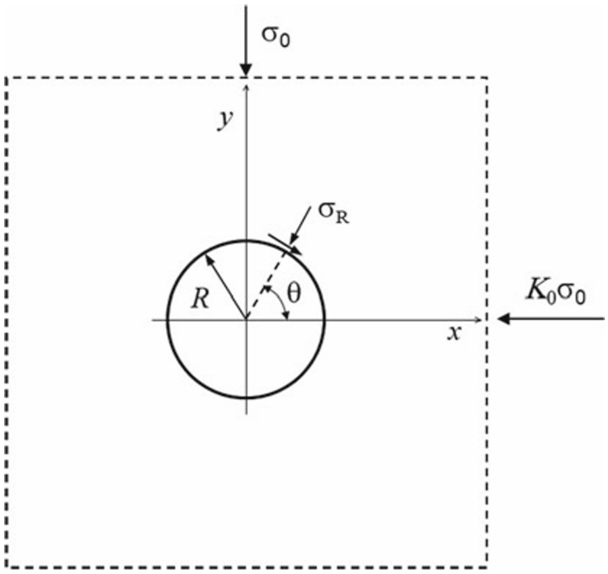

Figure 2.3: Definition of the radial σ_R and orthoradial stresses σ_θ. Source: (Panet & Sulem, 2022).

These expressions show that the stress perturbation decreases with the distance from the tunnel wall. The corresponding radial displacement and stress distributions are illustrated in Figure 2.4.

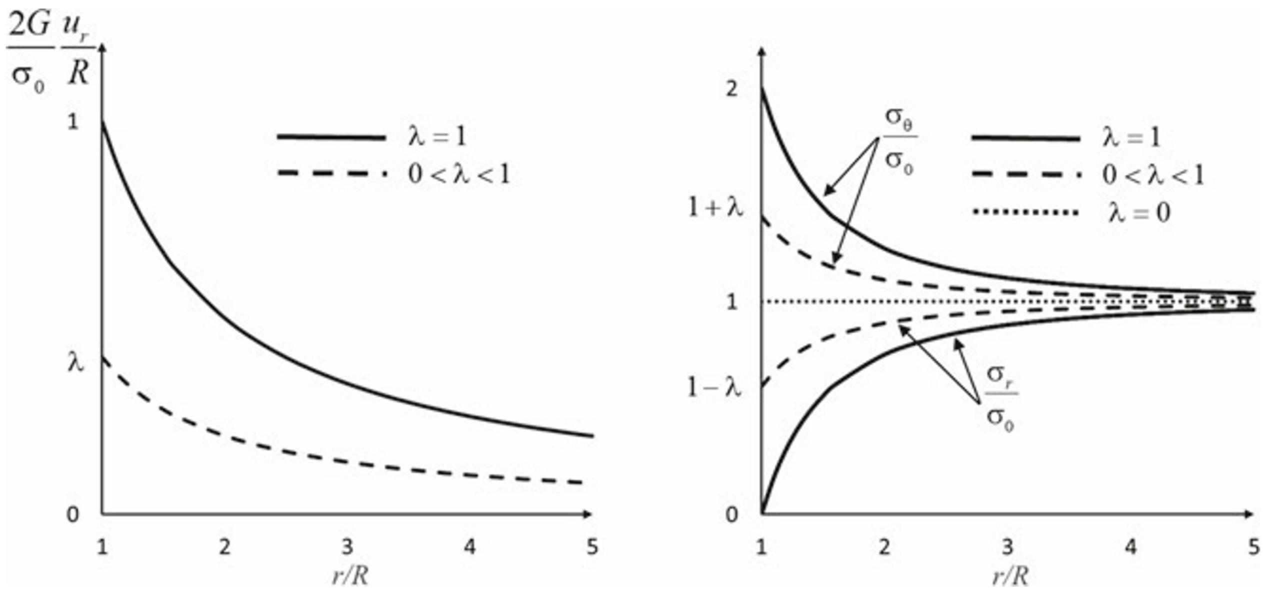

Figure 2.4: Radial displacement and stress distributions around a circular tunnel in an isotropic elastic medium for different values of λ. Source: (Panet & Sulem, 2022).

At the tunnel wall ($r = R$), these expressions become

$$u_R \equiv u_r(R) = \lambda \frac{\sigma_0 R}{2G}, \tag{2.6}$$

$$\sigma_R \equiv \sigma_r(R) = (1-\lambda)\sigma_0, \tag{2.7}$$

$$\sigma_\theta(R) = (1+\lambda)\sigma_0. \tag{2.8}$$

Equations (2.6) and (2.8) lead to the formulation of the elastic soil response curve $\sigma_R(u_R)$ in terms of the deconfinement ratio λ. A schematic representation can be seen in Figure 2.5.

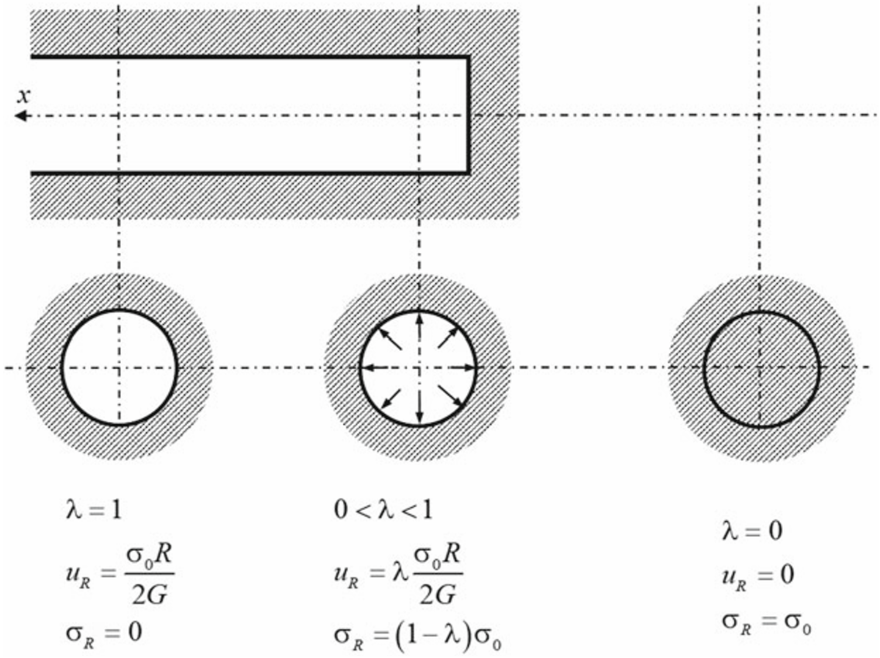

Figure 2.5: Schematic representation of the deconfinement ratio, wall stresses and wall displacements as a function of the distance from the tunnel face. Source: (Panet & Sulem, 2022).

2.3.3.2 Elastic–perfectly plastic case (Mohr–Coulomb)

For the elastoplastic case, an elastic–perfectly plastic material is assumed and yielding is described by a Mohr–Coulomb criterion (Figure 2.6). A convenient form of this criterion is

$$\sigma_1 = K_p\, \sigma_3 + \sigma_c, \tag{2.9}$$

where σ_1 and σ_3 are the major and minor principal stresses, K_p is a frictional parameter, and σ_c is a strength parameter.

The Mohr–Coulomb criterion is defined in terms of major and minor principal stresses as

$$F(\sigma_1, \sigma_3) = \sigma_1 - K_p\, \sigma_3 - \sigma_c = 0, \tag{2.10}$$

The parameter K_p and the uniaxial compressive strength σ_c are defined as

$$K_p = \frac{1+\sin\varphi}{1-\sin\varphi}, \qquad \sigma_c = \frac{2C\cos\varphi}{1-\sin\varphi}. \tag{2.11}$$

where φ is the friction angle and C is the cohesion.

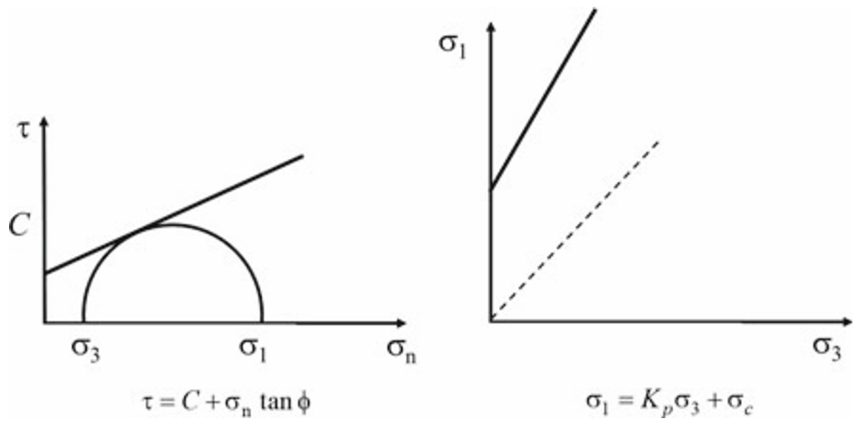

Figure 2.6: Mohr–Coulomb criterion in the τ–σ_n plane and in the principal stress plane. Source: (Panet & Sulem, 2022).

The corresponding dilatancy parameter is defined as (Panet & Sulem, 2022)

$$K_\psi = \frac{1+\sin\psi}{1-\sin\psi}. \tag{2.12}$$

By setting the dilatancy angle $\psi = 0$, then $K_\psi = 1$.

The onset of plasticity is defined by the intersection between the elastic stress path and the Mohr–Coulomb criterion at the tunnel wall. This defines the deconfinement ratio at the onset of plasticity, denoted by λ_e. For an isotropic initial stress state, λ_e is given by

$$\lambda_e = \frac{1}{K_p+1}\left(K_p - 1 + \frac{\sigma_c}{\sigma_0}\right). \tag{2.13}$$

For $\lambda \le \lambda_e$, the material remains elastic and equations (2.6)–(2.8) are valid. For $\lambda > \lambda_e$, a plastic region develops with radius $R_p(\lambda)$, and the wall displacement becomes a nonlinear function of λ through R_p (Figure 2.7). The plastic radius is given by

$$R_p(\lambda) = R\left[\frac{2\lambda_e}{(K_p+1)\lambda_e - (K_p-1)\lambda}\right]^{\frac{1}{K_p-1}}. \tag{2.14}$$

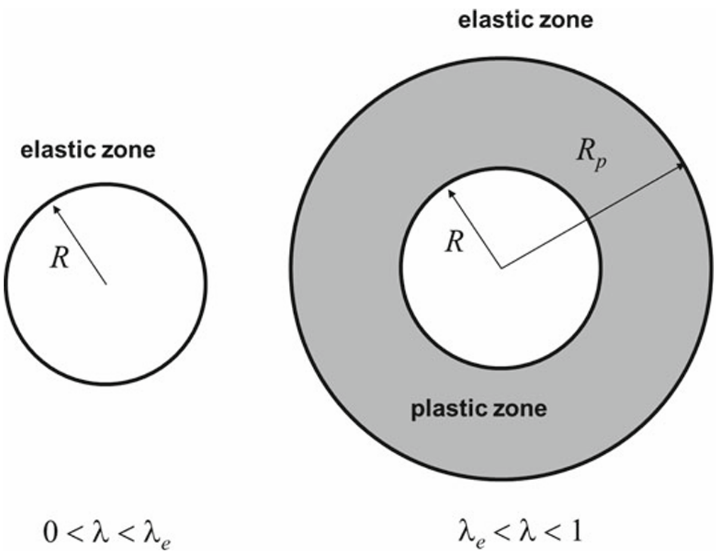

Figure 2.7: Development of a plastic zone around the tunnel for $\lambda > \lambda_e$. Source: (Panet & Sulem, 2022).

In the elastoplastic regime ($\lambda > \lambda_e$), the solution can be expressed first in terms of the radial coordinate r. A plastic zone develops for $R \leq r \leq R_p(\lambda)$, while the region $r > R_p(\lambda)$ is still elastic. The displacement field is

$$u_r(r) = \begin{cases} \lambda_e \dfrac{R_p^2}{r} \dfrac{\sigma_0}{2G}, & r > R_p, \\ \lambda_e \dfrac{\sigma_0 \, r}{2G} \left[F_1 + F_2 \left(\dfrac{r}{R_p} \right)^{K_p - 1} + F_3 \left(\dfrac{R_p}{r} \right)^{K_\psi + 1} \right], & r \leq R_p, \end{cases} \tag{2.15}$$

where F_1, F_2, and F_3 are constants:

$$F_1 = -(1 - 2\nu) \, \frac{K_p + 1}{K_p - 1}, \tag{2.16}$$

$$F_2 = 2 \, \frac{1 + K_\psi K_p - \nu \, (K_p + 1)(K_\psi + 1)}{(K_p - 1)(K_p + K_\psi)}, \tag{2.17}$$

$$F_3 = 2(1 - \nu) \, \frac{K_p + 1}{K_p + K_\psi}. \tag{2.18}$$

The stress field in polar coordinates is

$$\sigma_r(r) = \begin{cases} \left(1 - \lambda_e \dfrac{R_p^2}{r^2} \right) \sigma_0, & r > R_p, \\ \dfrac{\sigma_0}{K_p - 1} \left[2\lambda_e \left(\dfrac{r}{R_p} \right)^{K_p - 1} - \dfrac{\sigma_c}{\sigma_0} \right], & r \leq R_p, \end{cases} \tag{2.19}$$

and

$$\sigma_\theta(r) = \begin{cases} \left(1 + \lambda_e \dfrac{R_p^2}{r^2} \right) \sigma_0, & r > R_p, \\ \sigma_c + K_p \, \sigma_r(r), & r \leq R_p. \end{cases} \tag{2.20}$$

The stress redistribution associated with the development of the plastic zone is illustrated in Figure 2.8.

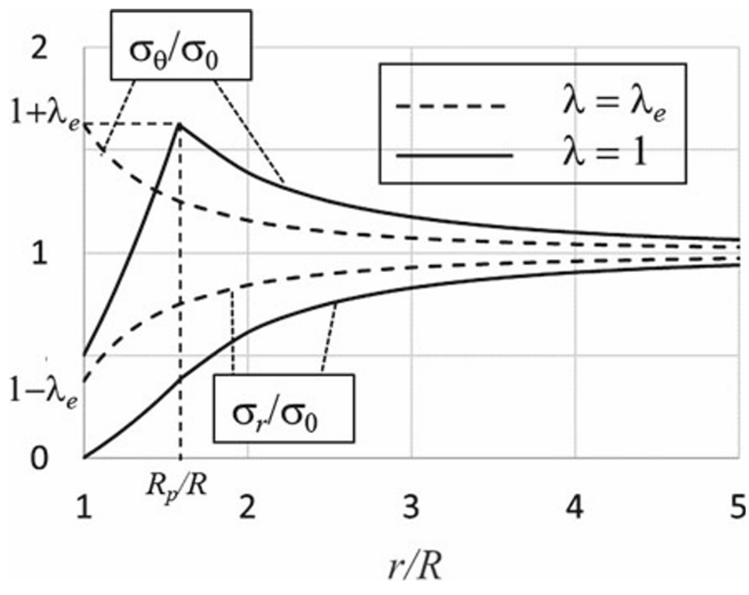

Figure 2.8: Radial and orthoradial stress distributions in an elastic–perfectly plastic ground with Mohr–Coulomb criterion. Source: (Panet & Sulem, 2022).

At the tunnel wall ($r = R$), the above expressions lead to

$$u_R(\lambda) = u_r(R) = \begin{cases} \lambda \, \dfrac{\sigma_0 R}{2G}, & \lambda \leq \lambda_e, \\ \lambda_e \, \dfrac{\sigma_0 R}{2G} \left[F_1 + F_2 \left(\dfrac{R}{R_p} \right)^{K_p - 1} + F_3 \left(\dfrac{R_p}{R} \right)^{K_\psi + 1} \right], & \lambda > \lambda_e, \end{cases} \tag{2.21}$$

$$\sigma_r(R) = \begin{cases} (1-\lambda)\sigma_0, & \lambda \leq \lambda_e, \\ \dfrac{\sigma_0}{K_p - 1} \left[2\lambda_e \left(\dfrac{R}{R_p} \right)^{K_p - 1} - \dfrac{\sigma_c}{\sigma_0} \right], & \lambda > \lambda_e, \end{cases} \tag{2.22}$$

$$\sigma_\theta(R) = \begin{cases} (1+\lambda)\sigma_0, & \lambda \leq \lambda_e, \\ \sigma_c + K_p \, \sigma_r(R), & \lambda > \lambda_e. \end{cases} \tag{2.23}$$

2.3.4 Support Reaction Curve (SRC)

In the CCM, the support response is governed by the relationship between the confinement provided by the lining and the radial displacement (Panet & Sulem, 2022).

2.3.4.1 SRC in terms of displacement increment after installation

The support is installed at a distance d behind the face, meaning that it only reacts to the additional displacement that occurs after its installation. The general equation for a linear SRC is

$$p_s = \begin{cases} 0, & \text{before installation}, \\ \dfrac{K_{sn}}{R} \left(u_R - u_{R,d} \right), & \text{after installation}, \end{cases} \tag{2.24}$$

where $u_R = u_r(R)$ is the wall displacement and $u_{R,d}$ is the wall displacement at support installation.

The meaning of $u_{R,d}$, p_s, and the final equilibrium displacement is illustrated in Figure 2.9. The support does not act from the beginning of the excavation process, but only after part of the convergence has already developed.

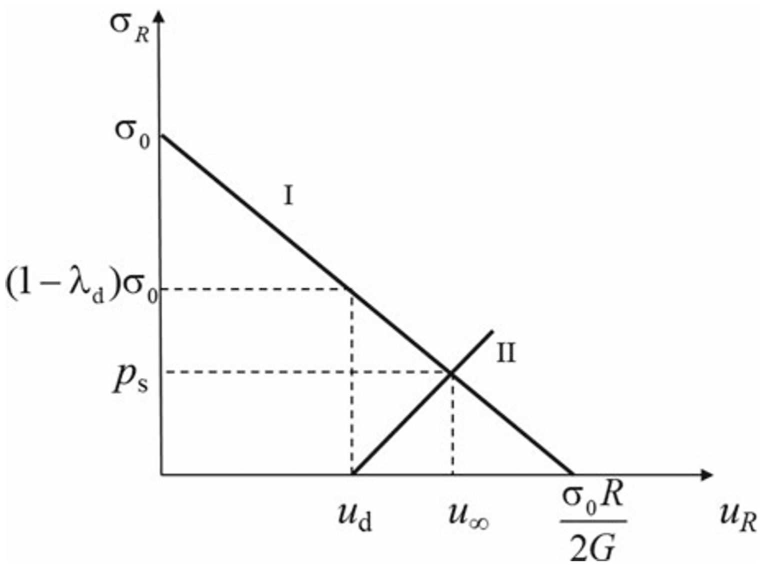

Figure 2.9: Schematic interaction between GRC and SRC. Source: (Panet & Sulem, 2022).

2.3.4.2 Normal stiffness modulus K_{sn}

For a circular lining of thickness e_b, Young's modulus E_b, and Poisson ratio ν_b, the normal stiffness modulus is expressed as

$$K_{sn} = \begin{cases} \dfrac{E_b}{1-\nu_b^2}\dfrac{e_b}{R}, & \dfrac{R}{e_b} > 10 \quad \text{(thin lining)}, \\ \dfrac{E_b\,(R^2-(R-e_b)^2)}{(1+\nu_b)[(1-2\nu_b)R^2+(R-e_b)^2]}, & \dfrac{R}{e_b} \le 10 \quad \text{(thick lining)}. \end{cases} \tag{2.25}$$

2.3.5 Longitudinal Displacement Profile (LDP)

The Longitudinal Displacement Profile (LDP) is one of the components of the Convergence–Confinement Method. It describes how the radial displacement at the tunnel wall evolves along the tunnel axis as a function of the distance x from the tunnel face. While the GRC and SRC describe the ground–support equilibrium in a given section, the LDP introduces the longitudinal effect of the tunnel face and makes it possible to estimate how much convergence has already occurred before support installation (Panet & Sulem, 2022).

The usual assumption is that the wall displacement is zero ahead of the face, reaches its ultimate value far behind the face, and varies between these two conditions:

$$u_R(x) = \begin{cases} 0, & x < -2R, \\ \alpha(x)\, u_R(\infty), & -2R \le x \le 4R, \\ u_R(\infty), & x > 4R, \end{cases} \tag{2.26}$$

where $\alpha(x)$ is a dimensionless shape function:

$$\alpha(x) = \alpha_0 + (1-\alpha_0)\, a(x), \tag{2.27}$$

with

$$a(x) = 1 - \left(\frac{mR}{mR+x}\right)^2. \tag{2.28}$$

Typical values are $\alpha_0 = 0.25$ and $m = 0.75$ (Panet & Sulem, 2022).

The LDP provides the displacement that has already occurred before support installation. If the support is installed at a distance d behind the tunnel face, the corresponding displacement is

$$u_{R,d} = u_R(d). \tag{2.29}$$

This value represents the convergence that has developed before the support starts to react.

In the elastic case, the wall displacement is proportional to the deconfinement ratio. The LDP can also be used to define the deconfinement level at the support installation distance:

$$\lambda_d = \frac{u_R(d)}{u_R(\infty)}. \tag{2.30}$$

Since

$$u_R(d) = \alpha(d)\, u_R(\infty), \tag{2.31}$$

then

$$\lambda_d = \alpha(d). \tag{2.32}$$

This relation is exact in the elastic case. In the elastoplastic case, the LDP shape is corrected through the factor $1/\xi$.

2.3.5.1 Elastic case

In the purely elastic case, the ultimate wall displacement for $\lambda = 1$ is

$$u_R(\infty) = \frac{\sigma_0 R}{2G}. \tag{2.33}$$

2.3.5.2 Elastoplastic case and scaling factor ξ

In the elastoplastic regime, the LDP keeps the same general form; however, its magnitude is scaled by $1/\xi$ and the axial development is slightly affected through the term $x\,\xi$ in $a(x)$, which is now defined as

$$a(x) = 1 - \left(\frac{mR}{mR + x\,\xi}\right)^2. \tag{2.34}$$

The ultimate wall displacement $u_R(\infty)$ does not take the elastic value of $\sigma_0 R/(2G)$ anymore because of the development of the plastic zone for $\lambda > \lambda_e$. For this case, the ultimate displacement is written as

$$u_R(\infty) = \frac{1}{\xi}\,\frac{\sigma_0 R}{2G}, \tag{2.35}$$

where the scaling factor $1/\xi$ ensures consistency between the LDP and the elastoplastic GRC. In other words, $\alpha(x)$ controls the displacement development along the axis, while $1/\xi$ controls the actual magnitude of the final displacement in the elastoplastic regime.

Accordingly, Eq. (2.26) can be written explicitly as

$$u_R(x) = \begin{cases} 0, & x < -2R, \\ \dfrac{1}{\xi}\,\alpha(x)\,\dfrac{\sigma_0 R}{2G}, & -2R \le x \le 4R, \\ \dfrac{1}{\xi}\,\dfrac{\sigma_0 R}{2G}, & x > 4R. \end{cases} \tag{2.36}$$

The scaling factor $1/\xi$ is defined as

$$\frac{1}{\xi} = \frac{u_R(\infty)_{\mathrm{ep}}}{u_R(\infty)_{\mathrm{el}}}, \tag{2.37}$$

and it can be evaluated from

$$\frac{1}{\xi} = \lambda_e \left[F_1 + F_2 \left(\frac{R}{R_p}\right)^{K_p - 1} + F_3 \left(\frac{R_p}{R}\right)^{K_\psi + 1}\right]. \tag{2.38}$$

2.3.6 Coupling of LDP and SRC

In order to follow the evolution of support confinement along the tunnel axis, the SRC can be combined with the longitudinal displacement profile $u_R(x)$. This gives

$$p_s(x) = \begin{cases} 0, & x < d, \\ \dfrac{K_{sn}}{R}\left(u_R(x) - u_R(d)\right), & x \ge d. \end{cases} \tag{2.39}$$

Equation (2.39) is referred to as the support confinement law along the tunnel axis.

2.4 Modelling approaches of the pipe umbrella systems

Reduced-order analytical and two-dimensional models are still widely used, especially at preliminary or not too complex design stages. In these models, the three-dimensional effects of tunnel advance are introduced indirectly, for example through a deconfinement level, a new longitudinal displacement profile or equivalent material properties. When a pipe umbrella is present, an additional simplification is required, since the reinforcement consists of discrete longitudinal elements installed ahead of the face.

The following subsections summarise the main strategies used in the literature to represent pipe umbrella systems, ranging from explicit three-dimensional modelling to simplified equivalent representations.

2.4.1 Explicit three-dimensional modelling

The most direct way to represent a pipe umbrella system is to use an explicit three-dimensional numerical model. In this approach, the excavation sequence, the advancing face, the primary support and the individual pipes can be represented directly. The main advantage is that the real geometry of the system can be included, together with parameters such as pipe length, diameter, spacing, inclination, overlap between consecutive umbrellas and installation sequence (Elyasi et al., 2016; Zarei et al., 2019).

In several studies, the pipes are introduced as structural or beam elements embedded in the soil. This makes it possible to evaluate not only the reduction movements, but also the internal forces developed in the pipes and in the primary support (Schumacher & Kim, 2013; Zarei et al., 2019). Three-dimensional models are therefore particularly useful for studying the load transfer mechanism of the pipe umbrella and the interaction between the reinforcement, the surrounding ground and the support system (Wu, Liu, Lin, Zhang, & Yao, 2024; Zhang et al., 2014).

Nonetheless, three-dimensional modelling requires a higher modelling effort and a larger computational cost than simplified two-dimensional approaches. Consequently, simplified approaches remain preferred for preliminary design and parametric studies (Neuner et al., 2020; Svoboda & Masin, 2009).

An example of explicit three-dimensional representation is shown in Figure 2.10.

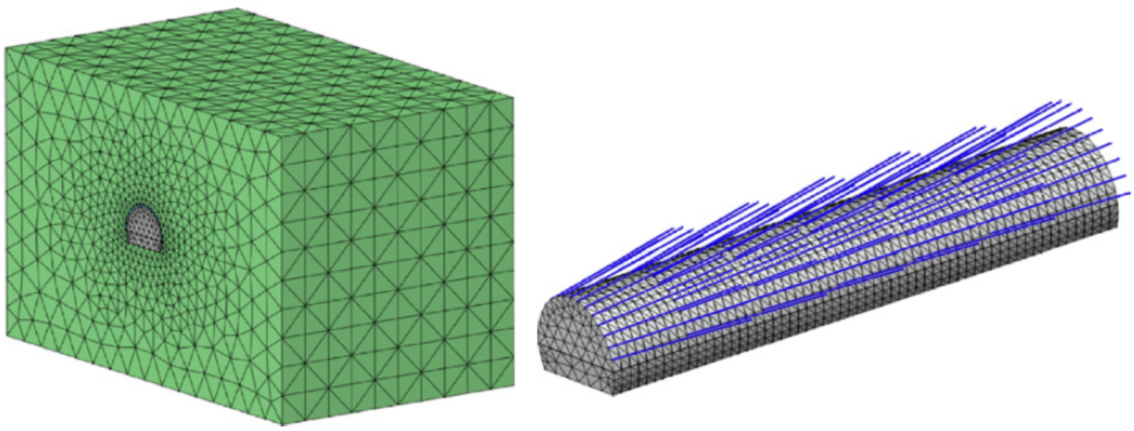

Figure 2.10: Example of full three-dimensional modelling of a pipe umbrella system. Source: adapted from (Song et al., 2013).

2.4.2 Analytical approaches

Analytical approaches provide a simplified way to interpret the mechanical behaviour of pipe umbrella systems. In these methods, the pipes are often represented as beams interacting with the surrounding soil, such as elastic foundation models or beam–spring systems (Song et al., 2013; Wu et al., 2024; Zhang et al., 2014).

These approaches are useful because they provide a clearer and simpler mechanical interpretation of the pipe umbrella action. In particular, they allow the effect of bending stiffness, pipe spacing, ground stiffness and support stiffness to be assessed with relatively simple calculations. Beam-based models have been used to study the deflection of umbrella pipes, the bending moments and shear forces along the pipes, and the transfer of loads towards the already supported region and the ground ahead of the tunnel face (Wu et al., 2024; Zhang et al., 2014).

Other simplified formulations are based on the Convergence–Confinement Method. In this case, the effect of the umbrella system is introduced through a modified support reaction curve. For example, Ranjbarnia et al. (2018) proposed a CCM-based analytical approach in which the longitudinal displacement profile of the unsupported tunnel is used to estimate the activation of the umbrella elements and their contribution to the supported tunnel response.

Although analytical and structural methods cannot reproduce the full three-dimensional interaction between discrete pipes and the surrounding ground, they are valuable for understanding the governing mechanisms and for performing preliminary evaluations. They also provide a useful intermediate level between full three-dimensional numerical models and simplified two-dimensional equivalent representations.

A simplified analytical representation of a single umbrella element is shown in Figure 2.11.

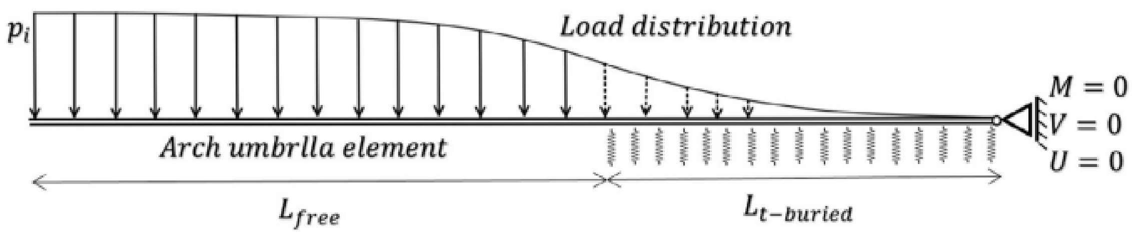

Figure 2.11: Simplified analytical representation of an arch umbrella element as a hinged beam element on springs. Source: adapted from (Ranjbarnia et al., 2018).

2.4.3 Homogenization and equivalent anisotropic material approaches

Bae et al. (2005) proposed a homogenization approach to represent pipe reinforced ground as an equivalent continuous material for a three-dimensional model. Instead of modelling each pipe and the surrounding ground, the reinforced zone is replaced by an equivalent anisotropic material. The equivalent properties such as the Young's moduli and Poisson's ratios in all the directions are obtained from new constitutive equations which are based on the ratio of volume occupied by the ground, the steel pipes and, when present, the grout.

The homogenization procedure leads to an equivalent anisotropic elastic material, in which the pipe axis represents one of the axes of the local Cartesian reference system, while the other two are perpendicular to it. So, the stiffness along the pipe direction is generally higher than the stiffness in the transverse directions. In addition to the Young's moduli and Poisson's ratios, the method also provides the equivalent shear moduli required to describe the complete elastic response of the homogenized material.

The concept of the homogenization procedure is schematically shown in Figure 2.12.

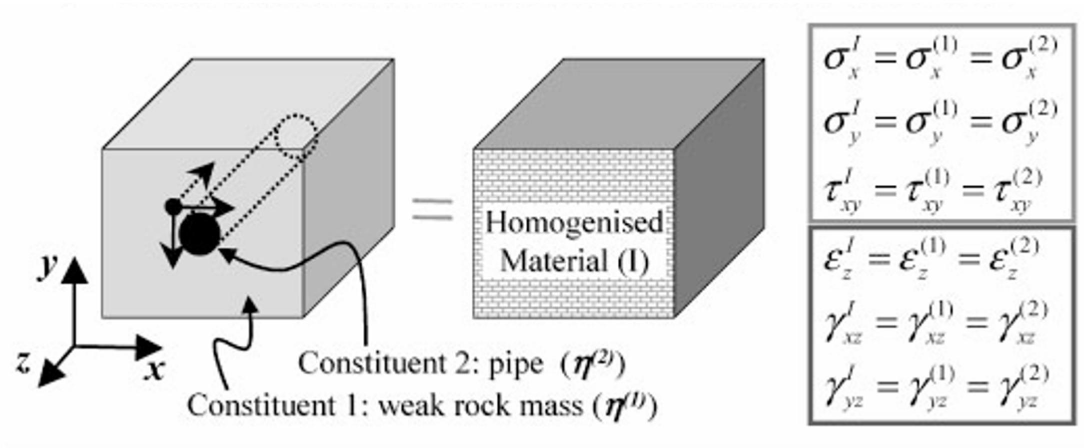

Figure 2.12: Schematic representation of the local homogenization procedure for pipe reinforced ground. Source: adapted from (Bae et al., 2005).

The method is based on the assumption of perfect bonding between the soil and the pipe. As a consequence, compatibility and equilibrium conditions can be imposed between the different elements.

This method is developed for implementation in a three-dimensional finite element model; indeed, the equivalent properties are first obtained in the local reference system of the reinforcement. This local system is then related to the global reference system of the tunnel through the orientation angles of the pipes, as shown in Figure 2.13.In this way, the position of the pipes along the installation arch can be taken into account.

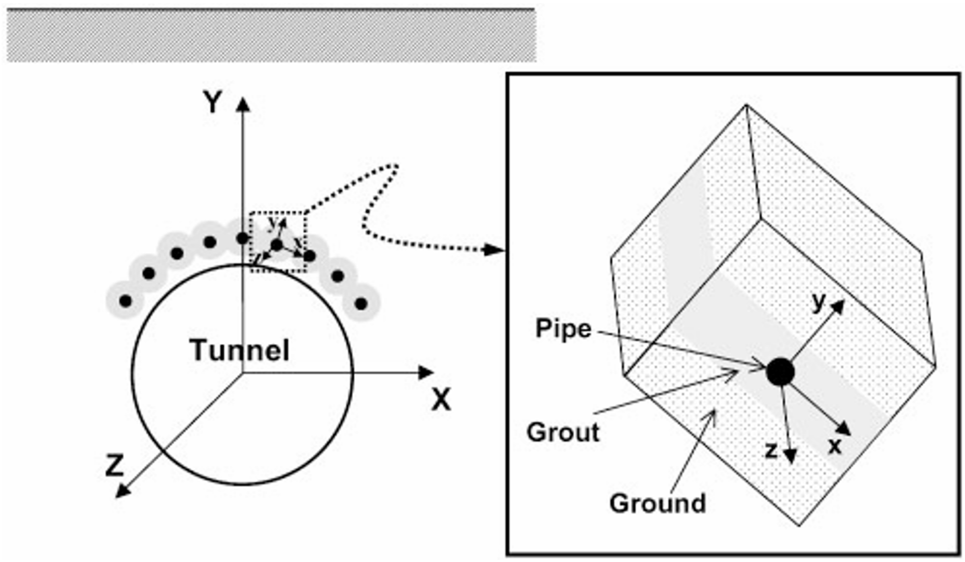

Figure 2.13: Local and global reference systems used for the homogenized ground reinforced with pipes. Source: adapted from (Bae et al., 2005).

Nevertheless, the formulation might be useful to derive equivalent elastic properties for simplified numerical models. In that case, the equivalent reinforced zone must be defined consistently with the volume fraction adopted in the homogenization process. Moreover, it must be noted that the correspondence between the homogenized material axes and the numerical material model must be defined carefully when the method is adapted to a two-dimensional model.

2.4.4 Linear elastic equivalent volume approaches

Equivalent section approach can be also used. In this type of method, the steel pipes and the surrounding tributary soil are replaced by a homogeneous linear elastic equivalent volume. The equivalent properties are usually obtained by imposing the equivalence of axial and bending stiffness. This approach is conceptually related to the equivalent section method commonly used for composite tunnel supports (Carranza-Torres & Diederichs, 2009). In the context of pipe umbrella modelling, this idea can be adapted by replacing the pipe–soil system with an equivalent continuous volume introduced around the tunnel crown.

2.4.5 Enhanced soil approaches

Another possibility is to represent the reinforced zone as an equivalent improved soil. As the pipes are not introduced as structural elements, their effect is included through modified Mohr–Coulomb parameters, such as increased cohesion and Young's modulus. This type of approach allows the pipe umbrella effect to be represented directly into the material properties.

Having said that, the results depend strongly on the assumed influence zone, on the way the pipe contribution is distributed, and on the adopted rules used to derive the equivalent strength and stiffness parameters (Grasso, Mahtab, Ferrero, & Pelizza, 1991; Grasso, Mahtab, Pelizza, & Rabajoli, 1993; Panet, 1995).

2.5 Chapter conclusion

Throughout this chapter, the pipe umbrella system has been analysed in greater detail with the support of the existing literature. First, its working principles, parameters, and the physical and mechanical aspects that most strongly influence its performance were introduced, also explaining how the performance is assessed through common indicators. The convergence-confinement method was then presented in detail together with its main formulations, as it represents the theoretical basis on which this work is founded. Subsequently, some of the most common methods adopted to model and study the effects of the pipe umbrella system were presented, with particular attention given to the approaches that are implemented later in this document, namely the anisotropic material approach, the linear elastic equivalent volume approach, and the enhanced soil approach.

3 Methodology

Defining the methodology adopted to address the problem represents a fundamental conceptual step. Through this chapter, the reader is provided with an overall understanding of the general logical process followed, before moving into the more specific treatment of the topic. The methodology introduces the main aspects of the project, the workflow adopted, and the tools employed. Moreover, it is hereby explained in more detail how the analytical and 2D modelling were carried out, and finally the main parameters considered for the performance assessment are defined.

3.1 Overview and used tools

The workflow helps to visualize schematically the global logical flow followed for the thesis. Since every part of this process is accurately explained in its relative chapter, only a schematic bullet list of it is presented:

⇒ Mathematical understanding of the soil behaviour based on the CCM;

⇒ Development of the same calculations through a code;

⇒ Interpretation of the results to better understand the phenomena and the most important parameters involved;

⇒ Sensitivity analysis of the results, for the purpose of defining a common reference problem for all the following stages, with fixed data and common assumptions;

⇒ Recalibration of the analytical model and implementation of the problem in the FEM software, referring to the previously defined assumptions;

⇒ Literature review to study the methods commonly used for modelling the pipe umbrella system;

⇒ Identification of possible new methods based on known bibliographic references;

⇒ Implementation of the new methods in the numerical models;

⇒ Comparison of the obtained results and identification of the main parameters;

⇒ Definition of the future perspectives.

The tools adopted to develop this thesis are:

- Excel for data analysis and simple calculations;
- Python for the analytical part and for solving more complex mathematical problems;
- Lagamine for the 2D axisymmetric model;
- Plaxis 2D for the 2D axisymmetric model;
- AI tools as coding, translation and linguistic assistant.

3.2 Analytical workflow

The analytical workflow follows the structure of the Convergence–Confinement Method. The problem is implemented both in elastic and elastoplastic environment. Starting from the reference geometry and material parameters defined in Chapter 4, the Python code is organised according to the following steps:

- first of all, it was necessary to study the behaviour of the soil by introducing the required parameters. From this, it was then possible to build the Ground Reaction Curve of the soil, able to describe the relationship between wall convergence and confinement loss;

- the next step was focusing on the construction of the Support Reaction Curve, based on the stiffness of the lining and on the displacement already developed before support activation, computed through the Longitudinal Displacement Profile formulations;
- from the two previous passages, the ground–support equilibrium point can be identified. Visually it represents the intersection between the GRC and the SRC;
- after that, the focus is on the Longitudinal Displacement Profile, which was already used for the SRC calculation. Nonetheless, its utility is not reduced to that, indeed, the free response of the soil can be studied along the tunnel axis, giving an overall understanding of the evolution of convergence. In this sense the wall displacement is calculated as function of the distance from the advancing face;
- afterwards, a sensitivity analysis of all the involved parameters is performed to better understand the physical problem and the influence of each geotechnical parameter on the results;
- the last part of the code is dedicated to the outputs and the extraction of the results and reference quantities used for comparison with the numerical models, namely wall convergence, radial stress, support pressure and deconfinement level.

This workflow provides a consistent analytical reference for the unsupported and supported tunnel cases only. The pipe umbrella is not introduced directly in this analytical formulation, but the results are later used to interpret the two-dimensional numerical models and to check the order of magnitude of results.

3.3 Numerical modelling workflow: Lagamine and Plaxis 2D

At first, the 2D models for the free soil and lining only cases are compared with the analytical solution, for a verification of the robustness and correctness of both implementations.

The same initial reference problem was built both in Plaxis 2D and in Lagamine, with some important differences. In the first Lagamine implementation, the support was not directly connected to the ground. Instead, a gap was defined between the lining surface and the soil, and between the lining and the excavation face. This approach makes it possible to study the soil behaviour during progressive deconfinement and to capture the interaction between the materials without modelling actual excavation steps. This is why the lining only models in Lagamine and Plaxis 2D have different initial configurations and were not directly compared.

Subsequently, different FEM methods were developed to predict the soil behaviour and the convergence when a pipe-type reinforcement is present. Three different strategies were adopted to model the pipe umbrella in a simplified axisymmetric model. All three are based on the idea of modifying and numerically modelling a homogenized influenced region parallel to the tunnel axis and characterised by a certain thickness, located between the tunnel wall and a certain radius defined according to the method used.

Considering that, as already mentioned, the initial Lagamine model was not comparable with Plaxis 2D due to the different initial layout of the lining, another Lagamine model equal to the Plaxis 2D one was created, in order to obtain a real comparison of the outputs. However, considering the greater modelling flexibility of Plaxis 2D, only the first of the three adopted methods could be developed in parallel in both software packages.

The three models are briefly explained below; more detailed explanations are provided in the next chapters:

- The first one is defined as linear elastic equivalent volume approach. In this model, the pipes and the soil located within the influenced region are replaced by an equivalent continuous volume with homogenized stiffness properties. This strategy is used both in Plaxis 2D and in Lagamine.
- The second strategy is based on Bae et al. (2005) and aims to create an anisotropic homogenized material through the mathematical homogenization of the constitutive equations of the pipe–soil system within a given tributary volume. This approach generates a homogenized material with anisotropic properties, which was introduced in Plaxis 2D through the Jointed Rock model. This model allows different material properties to be defined depending on the considered direction.
- The third strategy is defined as the enhanced soil approach. Here, the reinforced region is replaced by a soil zone with improved stiffness and, in one of the tested configurations, improved cohesion. Two variants of this approach are considered: one in which only the Young's modulus is increased while the cohesion is kept equal to that of the original soil, and one in which both Young's modulus and cohesion are increased.

After the results are obtained, it is possible to proceed with the comparison of the outputs, identifying the most reliable parameters to establish a solid comparison between the developed 2D methods.

3.4 Parameters used for comparison of the results

The main parameter used for the comparison of results is the radial displacement of the tunnel wall but, to compare the different two-dimensional models using a common indicator, an equivalent deconfinement ratio was also introduced. The idea is first to define the Ground Reaction Curve of the unsupported ground. This curve gives the relation between the radial displacement at the tunnel wall and the radial pressure acting on the excavation boundary.

In the convergence–confinement theory (Panet & Sulem, 2022), the deconfinement ratio is defined as

$$\lambda = 1 - \frac{\sigma_R}{\sigma_0}. \tag{3.1}$$

Here σ_R represents the radial stress at the tunnel boundary, and σ_0 denotes the initial isotropic stress. Thus, $\lambda = 0$ indicates the initial stress state, whereas $\lambda = 1$ signifies complete deconfinement.

Once the Ground Reaction Curve is known, each value of radial displacement can be associated with a corresponding radial pressure and, through the previous equation, with a deconfinement ratio. In numerical analyses, this relation can be obtained directly from the free-ground response by progressively releasing the radial stress at the tunnel boundary.

For supported and reinforced configurations, the GRC of the soil is used as a reference curve to identify an equivalent deconfinement ratio λ_{eq} that takes into consideration the presence of the pipe umbrella. In that sense, the pipe umbrella affects the deformation of the soil, which can then be related back to an equivalent deconfinement ratio. This ratio can be interpreted as an enhanced deconfinement condition, since the pipe umbrella reduces the deformation for the same stress release level. The equivalent ratio is therefore used as a comparison parameter between the different 2D models.

This step is particularly interesting considering that several softwares, including Plaxis 2D, may require a deconfinement ratio in two-dimensional analyses to reproduce a condition associated with a target displacement or a given loading state. Of course, the deconfinement ratio associated with the maximum displacement is not representative of the global behaviour of the ground reinforced by the pipe umbrella, but from a general and parametric point of view, it provides a numerical indicator of the effect of the pre-support, and allows the different simplified models to be compared through the same parameter.

A second possible interpretation is based on the stress state rather than on the maximum displacement. In this case, a new Ground Reaction Curve is obtained by considering the soil reinforced by the pipe umbrella, without activating the lining. The reinforced region is left free to deform while the internal confinement is progressively reduced.The behaviour of the soil can be plotted to create a new reinforced GRC, and the stress obtained at the tunnel wall can then be used to define an equivalent deconfinement ratio based on the stress level. In the present work, this second approach was tested only for the linear elastic equivalent volume method, and is therefore used only as an additional interpretation tool for this specific case.

3.5 Chapter conclusion

This chapter aims to provide the reader with the main information and concepts necessary to understand and interpret the problem addressed in the following chapters. The methodological choices, particularly in terms of the parameters adopted for comparing the results, represent a central aspect of this project, as they clearly define how the different models are assessed and why a specific modelling strategy was followed. Thus, this chapter represents a link between the general understanding of the problem and its specific analytical and numerical investigation.

4 Reference problem and modelling assumptions

This chapter defines the assumptions considered for this thesis. The objective is to present the geometrical data, material parameters and general modelling assumptions that are common to the analytical model and to the numerical simulations.

The same reference problem is used in the analytical formulation, in Lagamine and in Plaxis 2D, so that the results obtained from the different approaches can be compared consistently. The differences between the models can be associated with the modelling strategy, the excavation sequence, the way support is represented, or how the pipe umbrella is idealized, rather than with differences in input parameters.

This chapter only reports the common assumptions and quantities used. Details about the geometry, boundary conditions, mesh characteristics, and staged construction procedures are explained in separate chapters for each modelling environment: Chapter 5 for the analytical model and Chapter 6 for the two-dimensional models.

In this work, the two-dimensional numerical models are developed under axisymmetric conditions only. Plane strain analyses are not considered. Therefore, the term "2D model" refers here to an axisymmetric model and not to a plane strain transverse section. This choice allows a direct comparison with the analytical Convergence–Confinement formulation, which is also based on an axisymmetric reference problem (Panet & Sulem, 2022).

4.1 Geometry

The reference tunnel is idealized as a circular excavation with radius

$$R = 2.5 \text{ m}.$$

The detailed geometry of each numerical model is defined directly in the corresponding modelling chapter, since the representation of the domain, the boundaries and the excavation sequence depend on the software and on the type of analysis considered.

The general scope of the thesis is related to deformation control in shallow tunnel conditions, although the reference problem is intentionally idealized as a deep circular tunnel in both the analytical and numerical models. In the numerical models, the tunnel is placed sufficiently far from the boundaries, about $30R$. This choice limits the influence of the boundaries and allows the response to be interpreted mainly in terms of excavation-induced stress release and support interaction (Figure 4.1). It is important to note that this distance does not aim to reproduce the actual depth of a shallow tunnel, as it is only adopted to define an idealized enviroment consistent with the CCM assumptions.

Gravity is not included in the analytical model nor in the numerical models. This assumption is introduced to keep the reference problem simple and directly comparable between the different approaches. Furthermore, the unit weight of the soil is not used to generate the stress field. Consequently, the shallow tunnel condition is not introduced through the tunnel depth or by introducing gravity, but by directly assigning an initial stress state compatible with shallow tunnel conditions, as described in the following section.

These assumptions, in accordance with the CCM hypothesis, make the problem easier to tackle and understand.

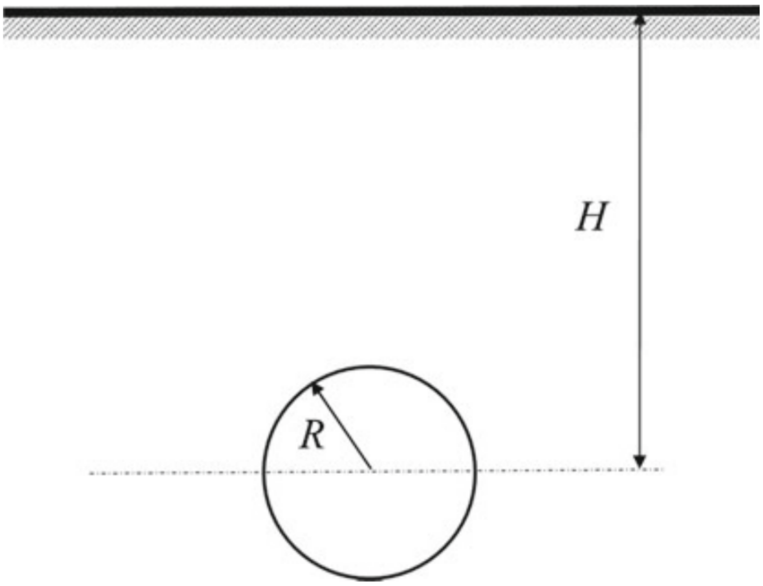

Figure 4.1: Scheme of the idealized geometry of the problem: R is 2.5 and H is 30 times the radius. Source: (Panet & Sulem, 2022)

4.2 Stress state and soil idealisation

4.2.1 Initial stress state

The initial stress state is assumed to be isotropic and uniform over the soil. The reference stress is taken equal to

$$\sigma_0 = 200 \text{ kPa}, \qquad K_0 = 1.$$

The same stress level is adopted in the analytical model and reproduced in the numerical models according to the specific implementation used in each software.

Considering that gravity is not taken into account, the initial stress state is defined directly and not generated by the unit weight of the soil γ, which was always taken equal to zero in each simulation. Nevertheless, as already explicitly stated in the previous section, the chosen value of initial stresses is intended to represent a stress level consistent with a shallow tunnel conditions.

4.2.2 Hydraulic conditions and effective stresses

Water pressure is not included in the reference analyses, and so, no pore pressure field is defined. Under these assumptions, the total stresses coincide with the effective stresses:

$$\sigma = \sigma'.$$

Consequently, the strength parameters of the Mohr–Coulomb model are used directly in terms of effective stresses.

4.2.3 Ground parameters

The Mohr–Coulomb model is the one used to characterize the soil behaviour. The same ground parameters are adopted in the analytical model and in the numerical simulations, maintaining consistency between the different approaches. The dilatancy angle is taken equal to zero.

The adopted ground parameters are reported in Table 4.1.

Table 4.1: Ground parameters adopted for the Mohr–Coulomb model.

Parameter	Symbol	Value
Young's modulus	E	50 MPa
Poisson's ratio	ν	0.25
Friction angle	φ'	20°
Cohesion	c'	30 kPa
Dilatancy angle	ψ	0°

4.3 Lining parameters

The lining is always modelled as a linear elastic material. A full concrete lining is considered, with a Young's modulus equal to 30 GPa. The lining thickness adopted in the reference numerical models is

$$e_b = 0.20 \text{ m}.$$

In Lagamine, the lining is introduced as a continuum volume, whereas in Plaxis 2D it is represented by a plate element with equivalent axial and bending stiffness.

The adopted support parameters are summarized in Table 4.2. Since gravity is not included in the reference analyses, the specific mass is not considered.

Table 4.2: Lining parameters adopted.

Parameter	Symbol	Value
Young's modulus	E_b	30 GPa
Poisson's ratio	ν_b	0.20
Lining thickness	e_b	0.20 m
Specific mass	ρ_b	0

4.4 Pipe umbrella geometry

The pipe umbrella considered in this work is composed of hollow steel pipes. In the pipe umbrella system it is common that grouting is adopted and that the pipes are inclined and overlapped, but none of these conditions are considered in this thesis. Only in the enhanced soil method the pipe inclination was taken into account for the cross section identification.

It is assumed that the pipes are arranged with a transverse spacing of

$$s_t = 0.50 \text{ m}.$$

The same pipe geometry is used as the basis for the equivalent representations introduced later in the numerical models. For now, only the real geometrical and mechanical properties of the pipes are reported, while the way in which the pipe umbrella is simplified and introduced in the two-dimensional models is described in Chapter 6.

The pipes have an external diameter equal to

$$D_e = 88.9 \text{ mm},$$

and a wall thickness equal to

$$t_p = 5 \text{ mm}.$$

The steel is modelled as a linear elastic material with Young's modulus $E_s = 210$ GPa and Poisson's ratio $\nu_s = 0.30$.

The main pipe parameters are reported in Table 4.3.

Table 4.3: Steel pipe parameters adopted for the pipe umbrella.

Parameter	Symbol	Value
External diameter	D_e	88.9 mm
Wall thickness	t_p	5 mm
Steel Young's modulus	E_s	210 GPa
Steel Poisson's ratio	ν_s	0.30

These properties are used later to derive the equivalent mechanical parameters of the reinforced zone, but the installation sequence and the overlapping of the pipes are not reproduced.

4.5 Chapter conclusion

This chapter aims to define the assumptions and modelling choices that are common to all the approaches presented in this thesis. By collecting these aspects in a dedicated section, the framework within which the analyses are carried out is clearly established, while avoiding unnecessary repetitions in the following modelling chapters. The adopted choices are based on the literature review, which provided typical values, characteristic parameters, and relevant modelling assumptions associated with the pipe umbrella system. Therefore, this chapter represents a common reference for the subsequent analytical and numerical models.

5 Analytical reference model

The theoretical background of the Convergence–Confinement Method was explained in Chapter 2, Section 2.3. The present chapter describes how this formulation is applied in the thesis.

The model is based on geometry, initial stress state and material parameters defined in Chapter 4. The calculations are performed for an axisymmetric circular tunnel, considering both elastic and elastic–perfectly plastic ground responses.

5.1 Role of the analytical model

In this study, the Convergence–Confinement Method is used to interpret the development of tunnel convergence, confinement loss and ground–support interaction (Panet & Sulem, 2022). The objective is not to reproduce the pipe umbrella system directly, but to obtain a reference response for the unsupported and supported tunnel case, which is useful for checking the order of magnitude of the numerical results.

The analytical approach played a fundamental initial role in understanding the mathematical behavior of tunnels. Thanks to its implementation in code, it was possible to analyze the behavior of the ground in different conditions, and its interaction with the lining.

5.2 Specific assumptions adopted

The tunnel is represented by an axisymmetric circular excavation. The elastic–perfectly plastic response is described with the Mohr–Coulomb criterion, consistently with the model assumptions.

The unsupported distance between the tunnel face and the support installation is taken equal to

$$d = 1 \text{ m}.$$

The same unsupported distance is used in the numerical models, in order to keep the analytical and FEM comparisons consistent. The influence of this parameter can be observed from the elastic analytical response reported in Figure 5.1. The figure shows how the support reaction curve changes as a function of the unsupported distance from the tunnel face.

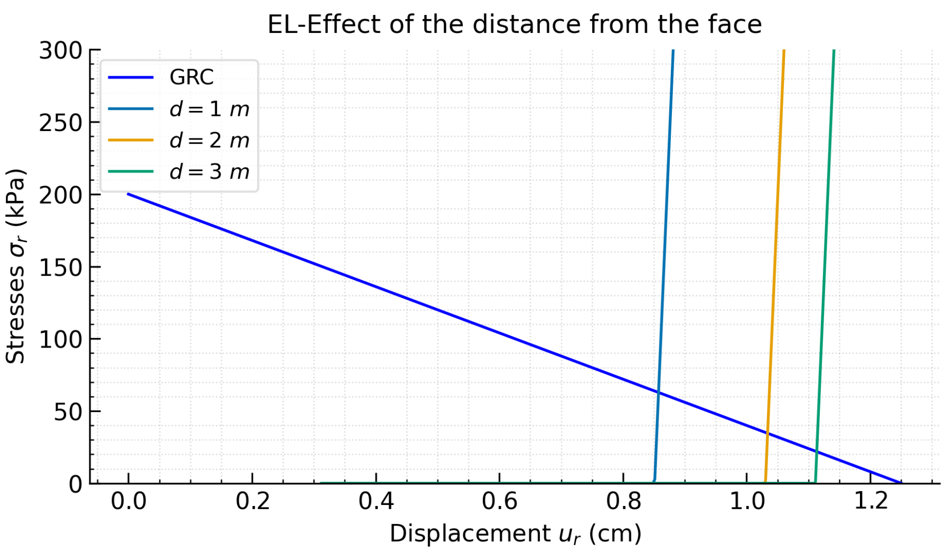

Figure 5.1: Effect of the unsupported distance from the face on the GRC–SRC interaction for elastic soil.

5.3 Python implementation

The analytical model was implemented in Python using a Jupyter notebook. The workflow is already introduced in the methodology chapter (Chapter 3). The complete notebook is not reported in the thesis text, since the analytical equations used in the code have already been introduced in Chapter 2, Section 2.3.

The input parameters are introduced as scalar variables, so that sensitivity analyses can be performed easily and, by changing their values, it was possible to graphically and numerically assess the difference in the outputs.

The first results obtained from the Python implementation refer to the elastic analytical case. Hereby, are presented as examples the radial and orthoradial stresses and the radial displacement profile (Figure 5.2).

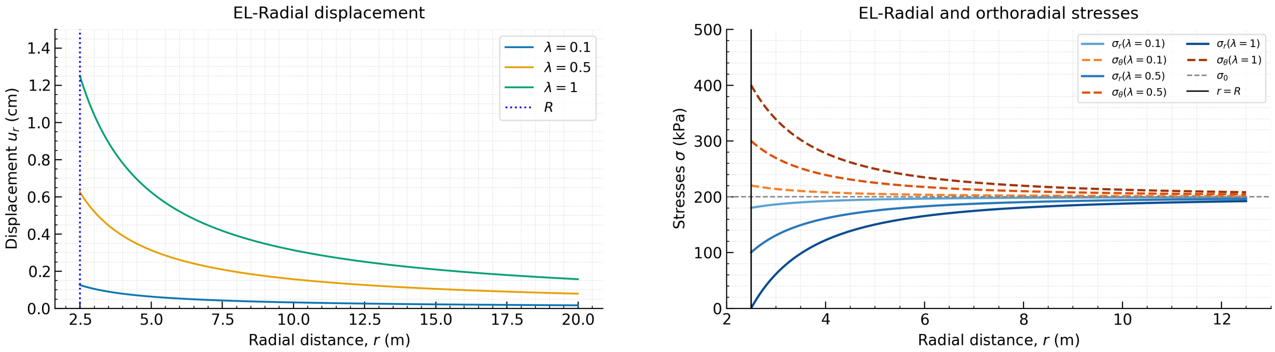

(a) Radial displacement. **(b)** Radial and orthoradial stresses.

Figure 5.2: Elastic analytical results: radial displacement profile and radial and orthoradial stress distributions.

The elastic–perfectly plastic response was then investigated through a sensitivity analysis on the main mechanical parameters. As an interesting example, it is reported the influence of the effective cohesion on the Ground Reaction Curve in Figure 5.3.

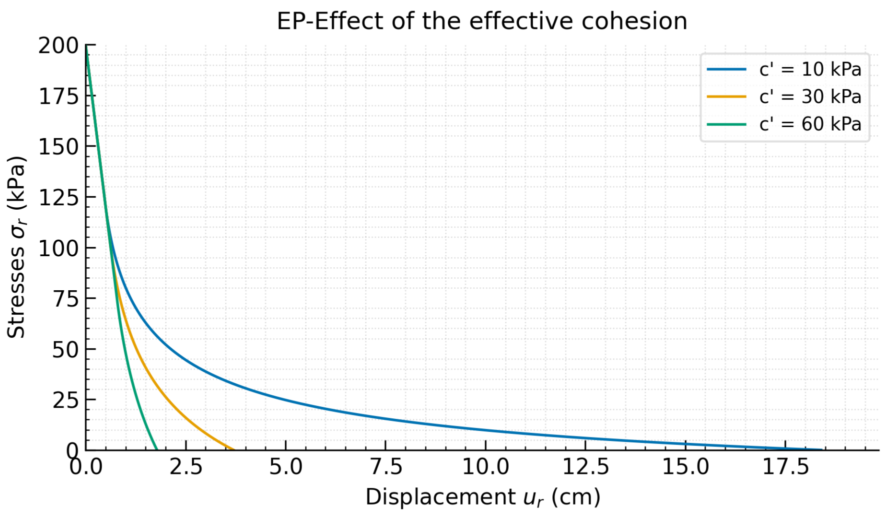

Figure 5.3: Effect of the effective cohesion on the GRC with elastic–perfectly plastic soil.

Another interesting parameter to study is the friction angle, whose influence on the GRC is shown in Figure 5.4.

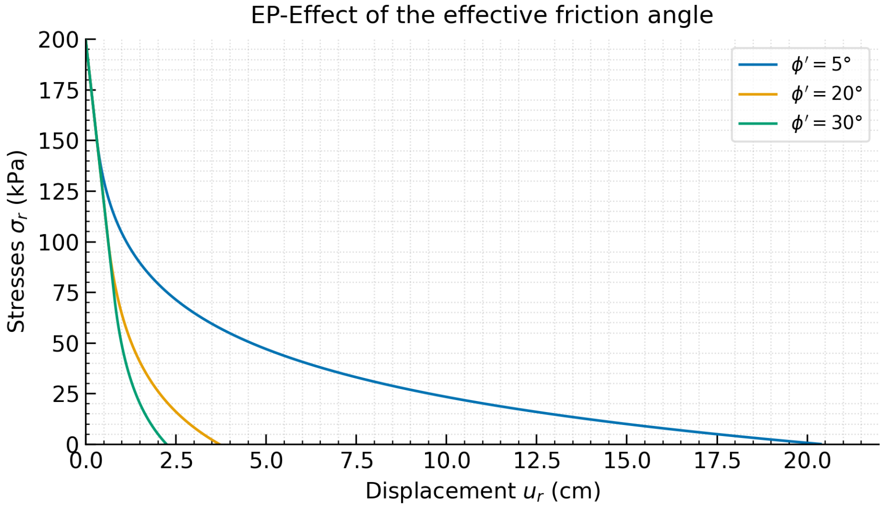

Figure 5.4: Effect of the effective friction angle on the GRC with elastic–perfectly plastic soil.

5.4 Discussion on applicability and limitations

The analytical reference model is based on the classical assumptions of the Convergence–Confinement Method (Panet & Sulem, 2022). These assumptions make the formulation useful for interpretation and preliminary comparison, but they also limit its direct applicability to the complete shallow tunnel problem considered in this thesis.

Hence, the analytical solution is not used as a direct prediction tool for the pipe umbrella system. The pre-support effect is instead evaluated through the numerical models and through the equivalent mechanical representations described in the following chapters.

5.5 Chapter conclusion

In this chapter, the scope and limitations of the analytical model have been explicitly defined. Some specific assumptions of this model have also been introduced, together with the main aspects related to its Python implementation. For greater clarity, selected graphical outputs obtained directly from the code have been presented, in order to show how the analytical solution behaves in different conditions. Overall, this chapter defines the analytical model as a reference for the following comparison with the numerical results.

6 2D numerical models

This chapter describes the two-dimensional numerical models implemented in Lagamine and Plaxis 2D. The model is based on the assumptions defined in Chapter 4. The objective is to reproduce the excavation response under simplified and controlled conditions, and to provide new numerical strategies for pipe implementation. The same problem is implemented in both numerical environments, but the modelling assumptions are not exactly the same.

The chapter is organised as follows. First, the base models without pipe umbrella are described for both Lagamine and Plaxis 2D, with particular attention to the geometry, boundary conditions, mesh and lining representation. Then, the simplified strategies adopted to represent the pipe umbrella are presented. These include the linear elastic equivalent volume approach, the homogenized anisotropic material approach and the enhanced soil approach. Finally, the excavation and support sequence used in the numerical analyses is described, since it defines the staged construction process from which the comparison results are extracted.

6.1 Lagamine base model: geometry, boundary conditions and mesh

The Lagamine model is an axisymmetric model representing a longitudinal section of the tunnel along the excavation axis. In this representation, the half tunnel is described as a longitudinal void inside the ground mass. The boundary of the void represents the tunnel wall and the tunnel face.

The model dimensions are chosen so as to limit boundary effects. The external boundaries are placed at a distance of approximately $30R$ from the tunnel wall and from the excavation face. Considering that the radius is equal to 2.5 m, then the quantity

$$30R = 75 \text{ m}.$$

This distance is large enough to prevent the constraints from affecting too much the stress and displacement fields in the proximity of the tunnel, while the shallow tunnel condition required is introduced through the stress value.

In Lagamine, the stress state is inserted through a combination of initial stresses and `LICHA` boundary-condition laws. The initial stress field inside the soil is defined as equal to $-\sigma_0$. To ensure the initial equilibrium of the model, boundary pressures with the same magnitude and opposite sign are applied on two boundaries specifically.

Two different `LICHA` laws are used. The first one is set on the upper boundary located above the tunnel. This pressure represents the far-field confinement and is kept constant during the analysis. The second `LICHA` law is applied on the internal boundary of the tunnel, which is to say along the excavation wall. This internal pressure is initially equal to σ_0, so that the tunnel boundary is also in equilibrium with the initial stress state.

Only the internal pressure acting on the tunnel boundary is progressively modified. This reduction is not used to reproduce the excavation sequence itself, but to obtain the Ground Reaction Curve in the absence of the lining. The internal pressure is decreased step by step down to zero, and the corresponding tunnel convergence is recorded.

The model is constrained to avoid rigid body motion. Roller conditions were considered as the best fitting option since they allow the movements along specific directions and they influence very few the output of the simulations in that sense. Thus, roller constraints are applied along the external boundaries where no `LICHA` elements are present:

- horizontal displacements are fixed on the lateral boundaries, $u_y = 0$;
- vertical displacements are fixed at the bottom boundary, $u_x = 0$.

Since these constraints are located far from the excavation, they are expected to have a limited influence on the tunnel response.

The general geometry and the adopted modelling scheme are shown in Figure 6.1 and Figure 6.2.

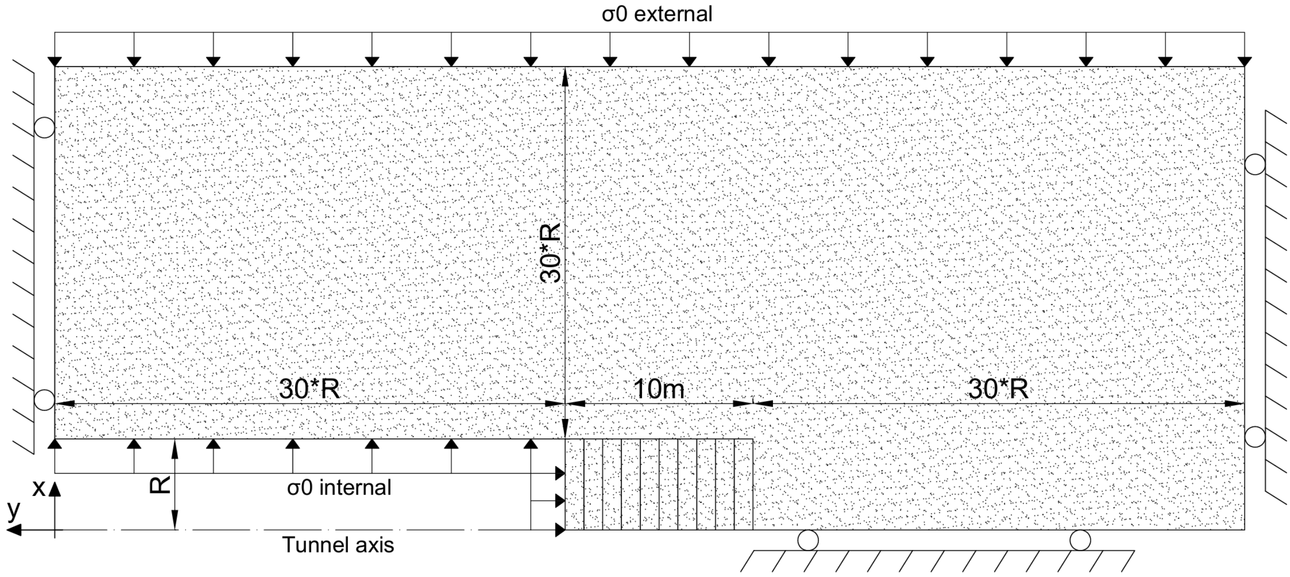

Figure 6.1: Simplified scheme of the 2D axisymmetric model.

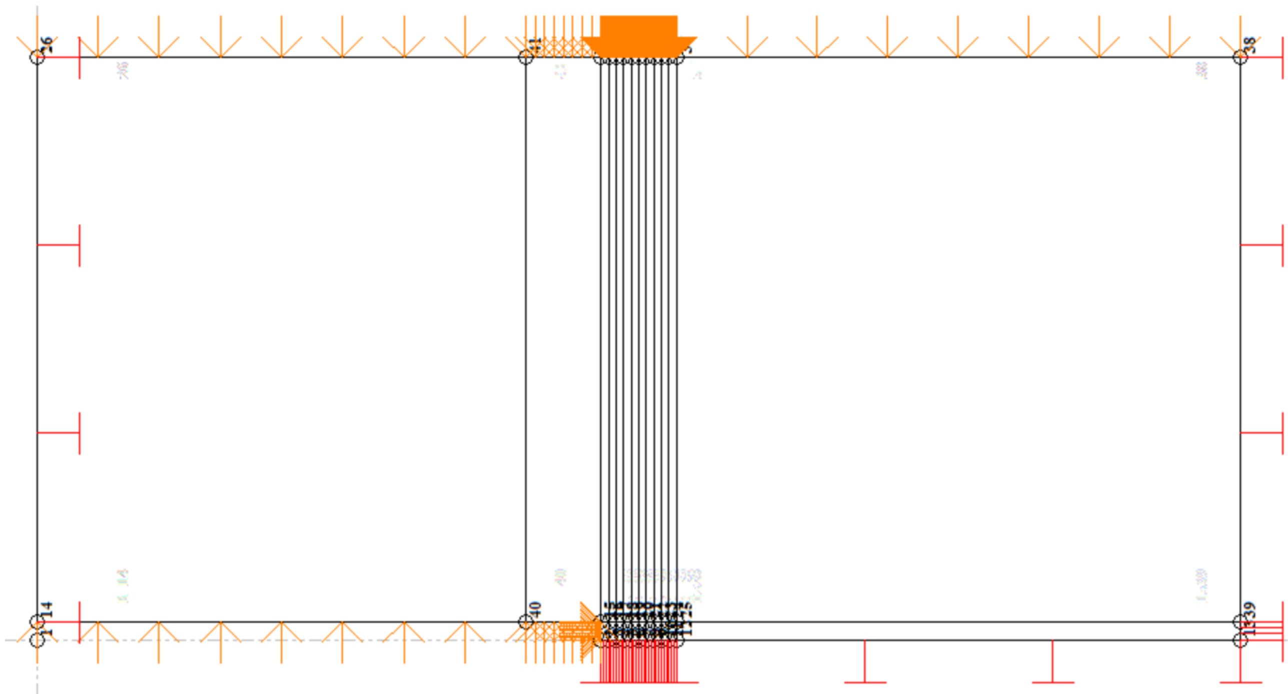

Figure 6.2: Geometry of the 2D axisymmetric model in Lagamine.

A graded mesh is used in the Lagamine model. The mesh is refined near the excavation boundary and around the tunnel face, where the largest stress changes and displacements are expected. The element size then progressively increases with the distance from the tunnel, in order to reduce the computational cost while maintaining a smooth transition in mesh density in order also to avoid oscillations and instability issues. The mesh adopted in the Lagamine model is shown in Figure 6.3 and Figure 6.4.

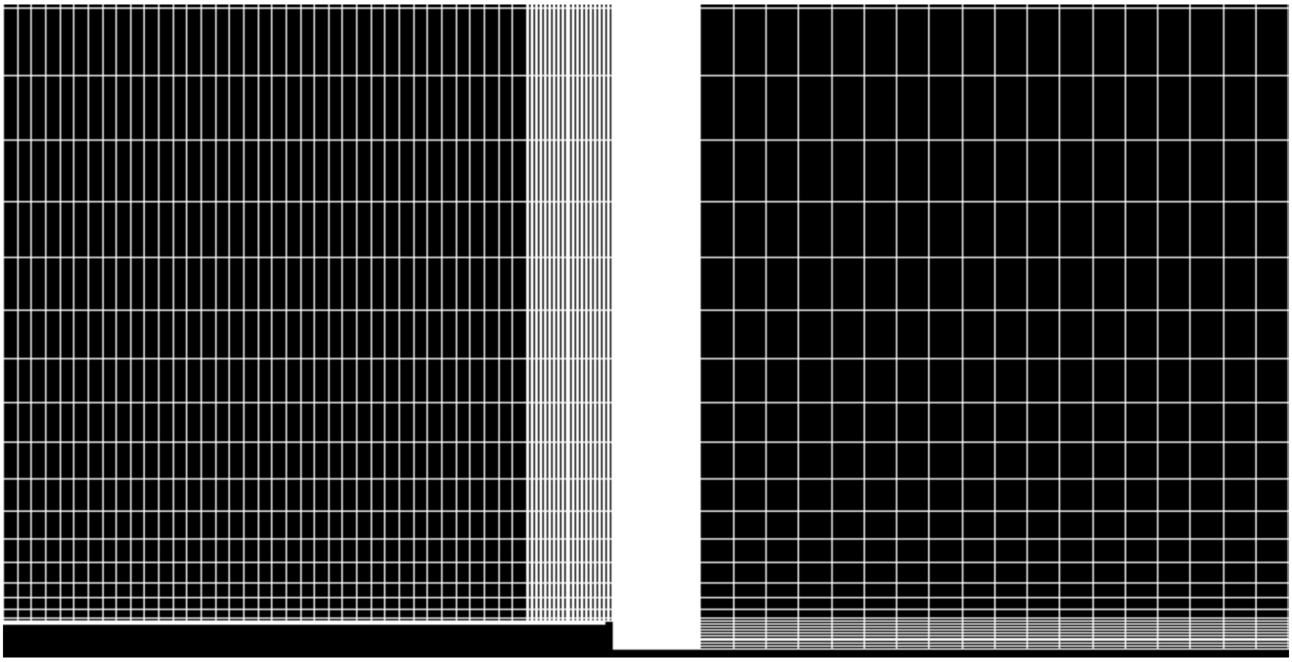

Figure 6.3: Mesh of the Lagamine model. The far-field boundary is located approximately $30R$ from the tunnel.

The lining is modelled in Lagamine as a continuum equivalent volume placed along the tunnel boundary. A lining thickness of

$$t_l = 0.20 \text{ m}$$

is adopted. This means that the support occupies a finite region in the mesh and it is assigned with the elastic material properties reported in Table 4.2.

For the base model of Lagamine the support was initially modelled with a gap of $2cm$ from the tunnel walls and a gap of $1m$ from tunnel face. This approach was useful for the comparison with the analytical part in terms of sensitive analysis of the geotechnical parameters (Figure 6.4).

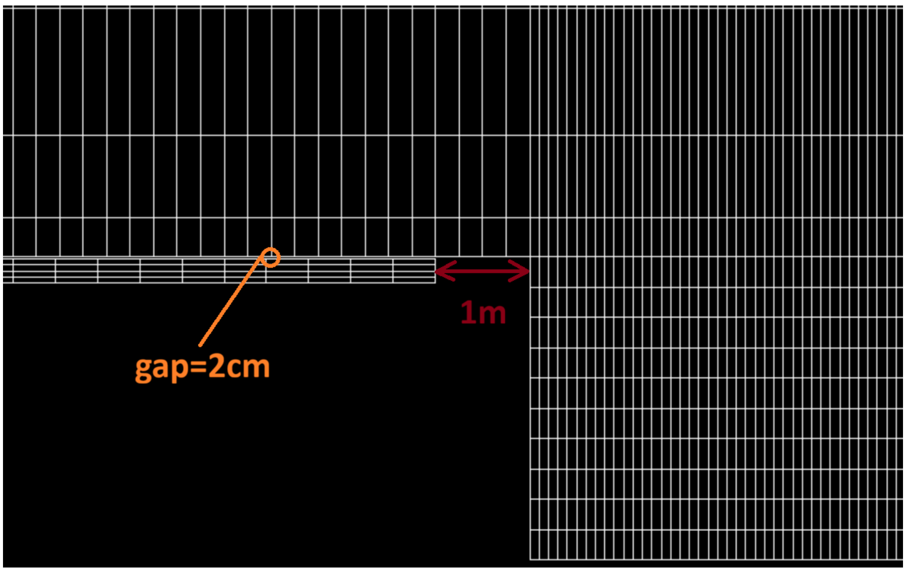

Figure 6.4: Mesh refinement close to the excavation boundary in the Lagamine model.

6.2 Plaxis 2D base model: geometry, boundary conditions and mesh

The exact same problem was also implemented in Plaxis 2D. The Plaxis 2D model has the same global dimensions as the Lagamine one, as well as same tunnel geometry, soil parameters and support properties. The objective is not to introduce a different physical problem, but to reproduce the same simplified excavation process in a second FEM environment.

The geometry of the Plaxis 2D model is shown in Figure 6.5. As in the Lagamine model, the external boundaries are located sufficiently far from the excavation as to reduce boundary effects ($30R$). Roller boundary conditions are also used, but for this case, they are applied all over the boundaries since no external pressures are applied.

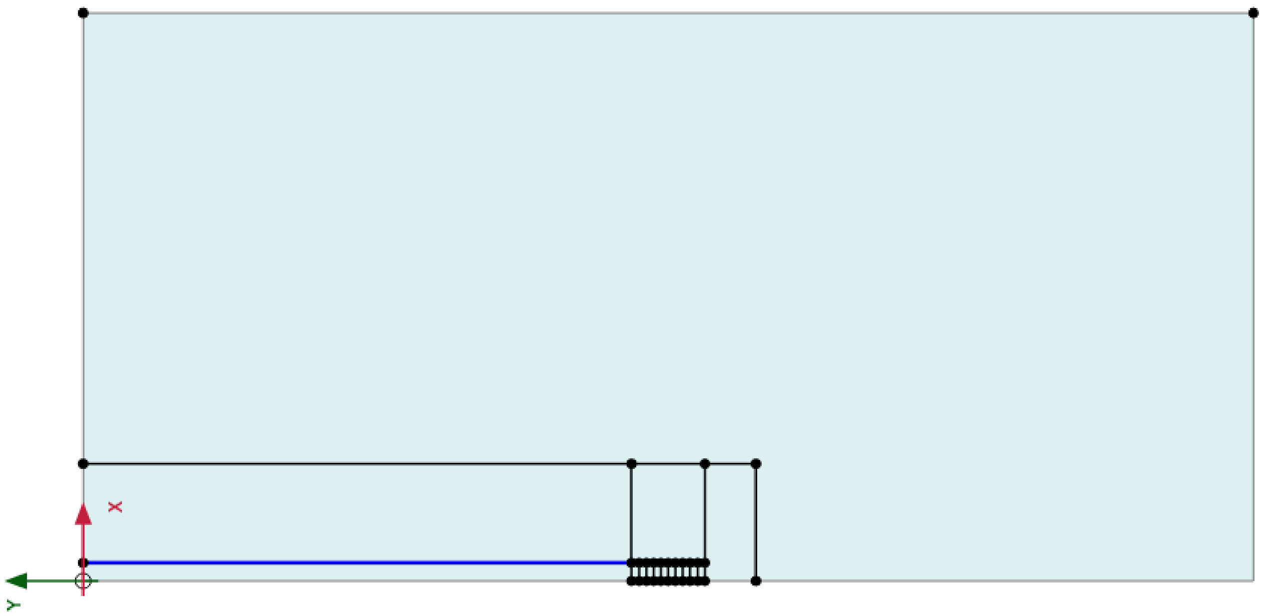

Figure 6.5: Geometry of the Plaxis 2D axisymmetric model. The same dimensions adopted in the Lagamine model are used.

The main difference between the two implementations concerns the way in which the initial stress state is introduced. In Plaxis 2D, no external pressures are applied at the model boundaries. Instead, a uniform initial stress of -200 kPa is assigned to the soil. This value corresponds to the isotropic pressure adopted in the reference problem, with the sign convention used in Plaxis 2D. Therefore, the initial stress state is kept consistent with the Lagamine model.

Another difference is about the numerical representation of the lining. In Lagamine, the lining is modelled as an equivalent continuum volume with a finite thickness. In Plaxis 2D, the lining is instead modelled using a plate element, and no rectangular element is required to represent the support thickness. The plate is directly connected to the ground and is introduced through its axial and bending stiffnesses, EA and EI. These stiffnesses correspond to the same lining thickness adopted in Lagamine; which is

$$t_l = 0.20 \text{ m}.$$

For a linear elastic lining, the equivalent axial and bending stiffnesses per unit width are

$$EA = E_b t_l, \qquad EI = \frac{E_b t_l^3}{12}. \tag{6.1}$$

Then, Plaxis 2D can associate an equivalent structural thickness to the plate from the ratio between EA and EI.

The Plaxis 2D mesh is shown in Figure 6.6. Differently from the Lagamine mesh, Plaxis 2D uses triangular finite elements. The mesh is refined in the vicinity of the tunnel and of the pre-support region, while larger elements are used far from the excavation, where the gradients of stress and displacement are smaller.

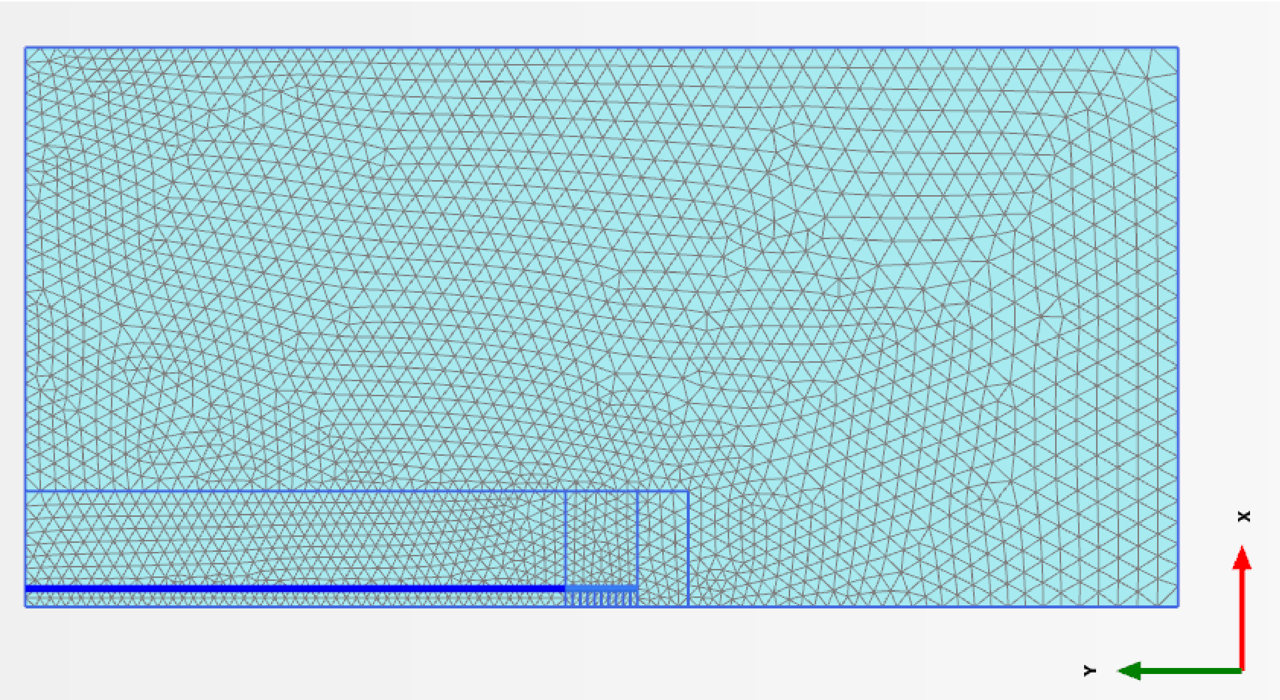

Figure 6.6: Finite element mesh adopted in Plaxis 2D. A triangular mesh is used, with refinement near the excavation region.

The same excavation and support sequence, which is described later, is performed in Plaxis 2D and in Lagamine. In Plaxis 2D, the part of the tunnel already excavated in the initial condition is realized by deactivating the corresponding soil elements and activating the support in this region. In Lagamine, the same initial configuration is represented directly in the mesh by leaving the already excavated region empty.

6.3 Pipe umbrella representation in the axisymmetric models

As introduced in Chapter 3, three simplified strategies were considered to represent the pipe umbrella system in the two-dimensional models. These are:

- the linear elastic equivalent volume method based on an equivalent section;
- the homogenized anisotropic material method;
- the enhanced soil method.

6.3.1 Linear elastic equivalent volume approach based on equivalent section

The first simplified strategy consists in representing the pipe umbrella as an equivalent continuous volume. This approach is based on the idea that the steel pipes and the soil located between adjacent pipes can be replaced by a homogeneous material with equivalent axial and bending stiffness. The equivalent volume is modelled in FEM environments in the portion of soil characterized by the presence of the pipes as a straight zone parallel to the tunnel axis. In this approach, the equivalent mechanical properties are obtained from a representative section. This approach is implemented both in Lagamine and Plaxis 2D.

The procedure is based on the equivalent section approach (Carranza-Torres & Diederichs, 2009). In the present work, this method is adapted to a section composed of steel pipes and soil. The objective is to define a homogeneous equivalent section having the same global stiffness as the original pipe–soil system. A simplified scheme is presented in Figure 6.7.

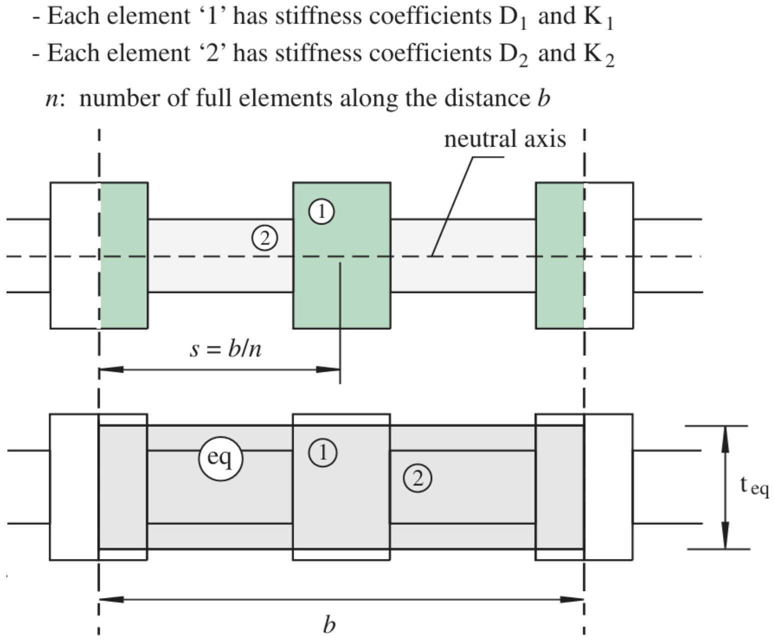

Figure 6.7: Simplified illustration of the equivalent section approach. Source: adapted from (Carranza-Torres & Diederichs, 2009).

The axial and bending stiffness coefficients of each component are defined as

$$D_j = \frac{E_j A_j}{1-\nu_j^2}, \tag{6.2}$$

$$K_j = \frac{E_j I_j}{1-\nu_j^2}, \tag{6.3}$$

where E_j, ν_j, A_j, and I_j are respectively the Young's modulus, Poisson's ratio, cross-sectional area, and second moment of area of component j. The steel pipe is denoted as component 1, while the soil portion associated with each pipe is denoted as component 2.

The pipe spacing is fixed equal to

$$s_t = 0.50 \text{ m}.$$

For a reference width $b = 1$ m, the number of pipes contained in this width is

$$n = \frac{b}{s_t}. \tag{6.4}$$

The steel pipe has an external diameter $D_e = 88.9$ mm and a wall thickness $t_p = 5$ mm. No grout contribution is considered in this simplified calculation. Since the pipe is hollow, the inner void of the pipe is assumed to be occupied by soil and is therefore included in the soil component of the representative section.

The steel area and second moment of area of the pipe are denoted by A_1 and I_1, respectively. These quantities are evaluated from the real hollow steel section and are reported in Table 6.1.

The soil portion associated with each pipe is then defined from the tributary width s_t. In this simplified equivalent section calculation, the thickness of the soil portion is taken equal to the external diameter of the pipe in order to reduce the rigidity of the system, which is expected to be already enough rigid, considering that it is modelled as a linear elastic plate. The following value represents the thickness of the soil layer only, not the final equivalent thickness:

$$t_{\text{soil}} = D_e.$$

Thus, the pipe and the surrounding tributary soil are homogenized over the same representative section. Since the internal part of the pipe is assumed to be filled with soil, only the steel contribution is subtracted from the full tributary section. The area and second moment of area of the soil component are thus computed as

$$A_2 = s_t t_{\text{soil}} - A_1, \tag{6.5}$$

$$I_2 = \frac{s_t t_{\text{soil}}^3}{12} - I_1. \tag{6.6}$$

The equivalent axial and bending stiffnesses over the reference width are then

$$D_{\text{eq}} = n(D_1 + D_2), \tag{6.7}$$

$$K_{\text{eq}} = n(K_1 + K_2). \tag{6.8}$$

The equivalent thickness of the layer is obtained by imposing the equivalence between axial and bending stiffness:

$$t_{\text{eq}} = \sqrt{12\frac{K_1 + K_2}{D_1 + D_2}}. \tag{6.9}$$

The corresponding equivalent Young's modulus is then calculated as

$$E_{\text{eq}} = \frac{n(D_1 + D_2)}{b\, t_{\text{eq}}}. \tag{6.10}$$

The main input data, section properties and equivalent values obtained from the calculation are summarized in Table 6.1. The Poisson's ratio of the equivalent material is taken equal to that of the soil.

Table 6.1: Input data and equivalent material properties adopted for the linear elastic equivalent volume approach.

Parameter	Symbol	Value
Input data		
Steel Young's modulus	E_1	210000 MPa
Steel Poisson's ratio	ν_1	0.30
Soil Young's modulus	E_2	50 MPa
Soil Poisson's ratio	ν_2	0.25
Section properties		
Steel area	A_1	1.318×10^{-3} m^2
Steel second moment of area	I_1	1.164×10^{-6} m^4
Soil area	A_2	4.313×10^{-2} m^2
Soil second moment of area	I_2	2.811×10^{-5} m^4
Equivalent values		
Equivalent axial stiffness	D_{eq}	612861 kN
Equivalent bending stiffness	K_{eq}	540.1 kNm^2
Equivalent thickness	t_{eq}	0.103 m
Equivalent Young's modulus	E_{eq}	5960 MPa
Equivalent Poisson's ratio	ν_{eq}	0.25

These properties are introduced in the numerical models as a continuous straight volume parallel to the tunnel axis.

The equivalent volume element introduced in Plaxis 2D is shown in green in Figure 6.8.

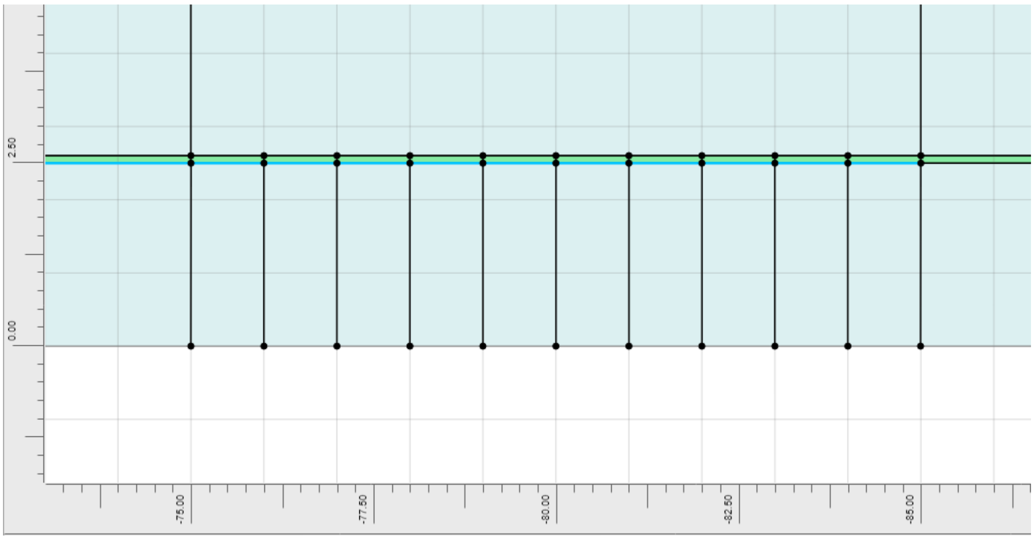

Figure 6.8: Simplified illustration of the linear elastic equivalent volume approach in Plaxis 2D.

For Lagamine, the same problem is developed. However in Lagamine, as mentioned before, both the lining and the area reinforced by the pipes are modelled as equivalent volumes. Apart from this difference, the analysis conditions remain the same. The wider strip represents the lining, while the smaller strip adjacent to it represents the pipe umbrella. A zoom of the Lagamine model is provided in Figure 6.9.

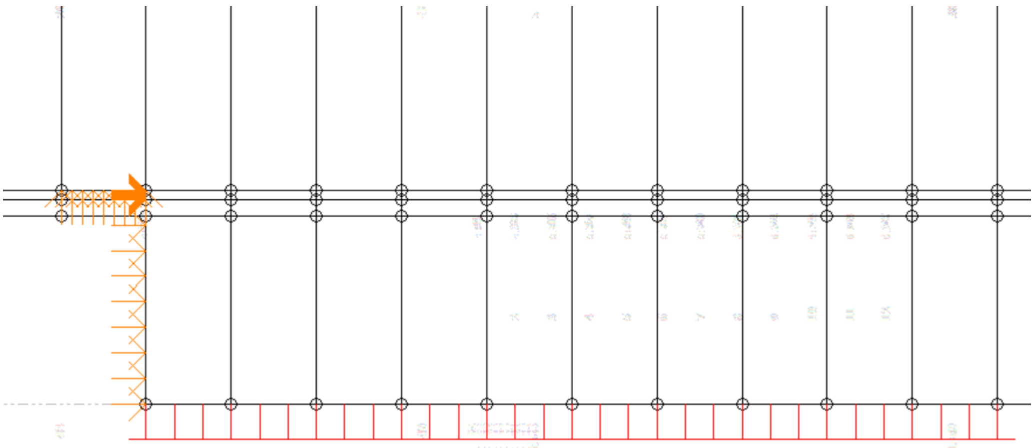

Figure 6.9: Linear elastic equivalent volume scheme implemented in the Lagamine model.

6.3.2 Homogenized anisotropic material method

A second equivalent volume approach was tested following the homogenization approach proposed by Bae et al. (2005). As discussed in the literature review (Section 2.4.3), this method replaces the reinforced ground, composed of soil and steel pipes, with an equivalent anisotropic material. The main advantage of this formulation is that it provides equivalent elastic properties along different directions, allowing the enhanced longitudinal stiffness introduced by the pipes to be represented. In order to apply it, the method was adapted to the Plaxis 2D model only.

The equivalent properties are assigned to a continuous straight layer located in the region affected by the pipe umbrella. The equivalent layer is shown in Figure 6.10. Its thickness was taken equal to the transverse spacing between the pipes,

$$t_{\text{eq,layer}} = s_t = 0.50 \text{ m}.$$

This choice is consistent with the idea of distributing the mechanical contribution of each pipe over its tributary area/volume.

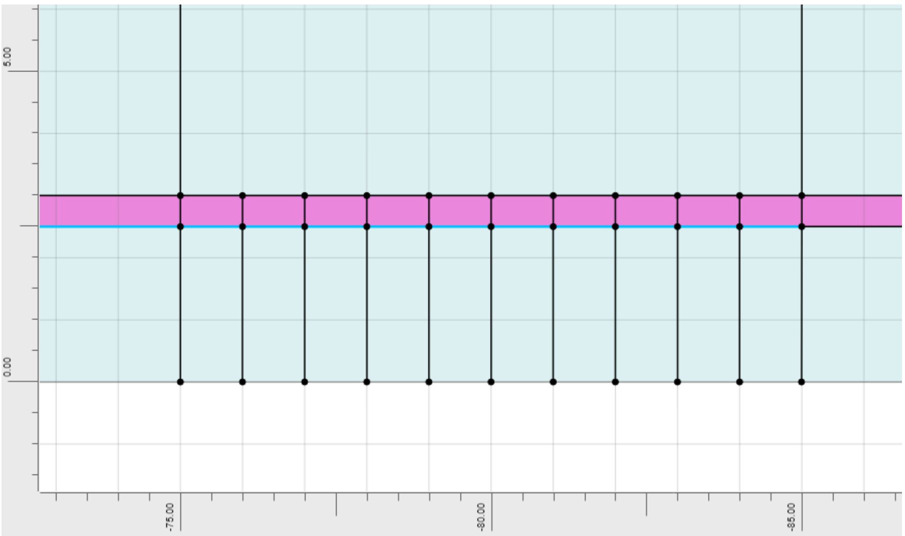

Figure 6.10: Anisotropic material layer introduced in Plaxis 2D for the homogenized pipe umbrella representation.

The elastic homogenization matrices were solved using a simple Python script, following the procedure proposed in the document by Bae et al. (2005). No grout contribution was considered in the calculation; the equivalent material is obtained only from the soil and the steel pipes. In the local reference system used for the homogenization, the z direction is parallel to the pipe axis, while the x and y directions are transverse to the pipes.

The main mathematical steps of the homogenization procedure adopted for this thesis are summarized in the next steps.

Each constituent of the reinforced medium is first described by its own elastic constitutive relationship,

$$\boldsymbol{\sigma}^{(i)} = [D^{(i)}]\boldsymbol{\varepsilon}^{(i)}, \tag{6.11}$$

where $[D^{(i)}]$ is the elastic stiffness matrix and i denotes the considered element, which is to say soil and steel pipes. The contribution of each material is then introduced by its volume fraction, whose depth along z axis is considered unitary,

$$\eta_i = \frac{V_i}{V_{\text{tot}}}, \qquad \sum_i \eta_i = 1. \tag{6.12}$$

Due to the perfect bonding assumption, the strain field of each constituent can be related to the strain of the equivalent material through a structural matrix $[S^{(i)}]$,

$$\boldsymbol{\varepsilon}^{(i)} = [S^{(i)}]\boldsymbol{\varepsilon}^{\text{eq}}. \tag{6.13}$$

The average stress in the homogenized medium is then obtained by summing the stress contribution of all the constituents,

$$\boldsymbol{\sigma}^{\text{eq}} = \sum_i \eta_i \boldsymbol{\sigma}^{(i)}. \tag{6.14}$$

Combining the previous relationships, the equivalent stiffness matrix of the homogenized material can be written as

$$[D^{\mathrm{eq}}] = \sum_i \eta_i [D^{(i)}][S^{(i)}]. \tag{6.15}$$

The equivalent constitutive relationship is therefore

$$\boldsymbol{\sigma}^{\mathrm{eq}} = [D^{\mathrm{eq}}]\boldsymbol{\varepsilon}^{\mathrm{eq}}. \tag{6.16}$$

The elastic constants of the equivalent anisotropic material, such as E_x, E_y, E_z, the shear moduli and the Poisson's ratios, can then be obtained from the compliance matrix,

$$[C^{\mathrm{eq}}] = [D^{\mathrm{eq}}]^{-1}. \tag{6.17}$$

The equivalent elastic constants obtained from the homogenization calculation are summarized in Table 6.2. The highest Young's modulus is obtained in the z direction, as expected, since this is the direction parallel to the steel pipes. The shear modulus involving the pipe direction is also significantly larger than the transverse shear modulus. Due to the two-dimensional nature of the model, no transformation into the global reference system was performed. Instead, the equivalent properties obtained in the local reference system of the representative pipe–soil cell were directly adapted and introduced into the Plaxis 2D model.

Table 6.2: Elastic constants obtained from the homogenization procedure in the local x, y, z system, with z parallel to the pipe axis.

Parameter	Value
$E_x = E_y$	53.46 MPa
E_z	1156.77 MPa
G_{xy}	20.11 MPa
$G_{xz} = G_{yz}$	445.68 MPa
$\nu_{xy} = \nu_{yx}$	0.3295
$\nu_{xz} = \nu_{yz}$	0.01157
$\nu_{zx} = \nu_{zy}$	0.2503

In Plaxis 2D, this elastic anisotropy is modelled through the Jointed Rock model, which is not used to represent an actual jointed rock mass, but as a numerical tool to assign different stiffness values in different directions. According to the Plaxis 2D formulation, the Jointed Rock model is defined by five parameters, which are E_t, E_n, ν_{nt}, ν_{ts}, and G_{nt}, together with the orientation of Plane 1 whose inclination depends on the angle α (Bentley Systems, 2025).

The interpretation of these parameters requires some attention, because the nomenclature used in Plaxis 2D is not the same as the one used in the homogenization calculation. In the Jointed Rock model, E_t is the Young's modulus tangent to Plane 1, while E_n is the Young's modulus normal to Plane 1. The shear modulus G_{nt} is the shear modulus in normal direction to Plane 1. The parameter ν_{ts} is also associated with the direction perpendicular to Plane 1.

For this reason, Plane 1 was oriented so that its normal direction coincides with the pipe direction. In the present modelled Plaxis 2D axisymmetric model, the pipes are aligned with the longitudinal y-axis, which makes Plane 1 perpendicular to the y-axis with $\alpha_1 = 0°$, so that its normal direction is aligned with the pipe axis (Figure 6.11). This orientation is important because it allows the highest stiffness to be assigned normally to Plane 1 and so, along the pipe direction.

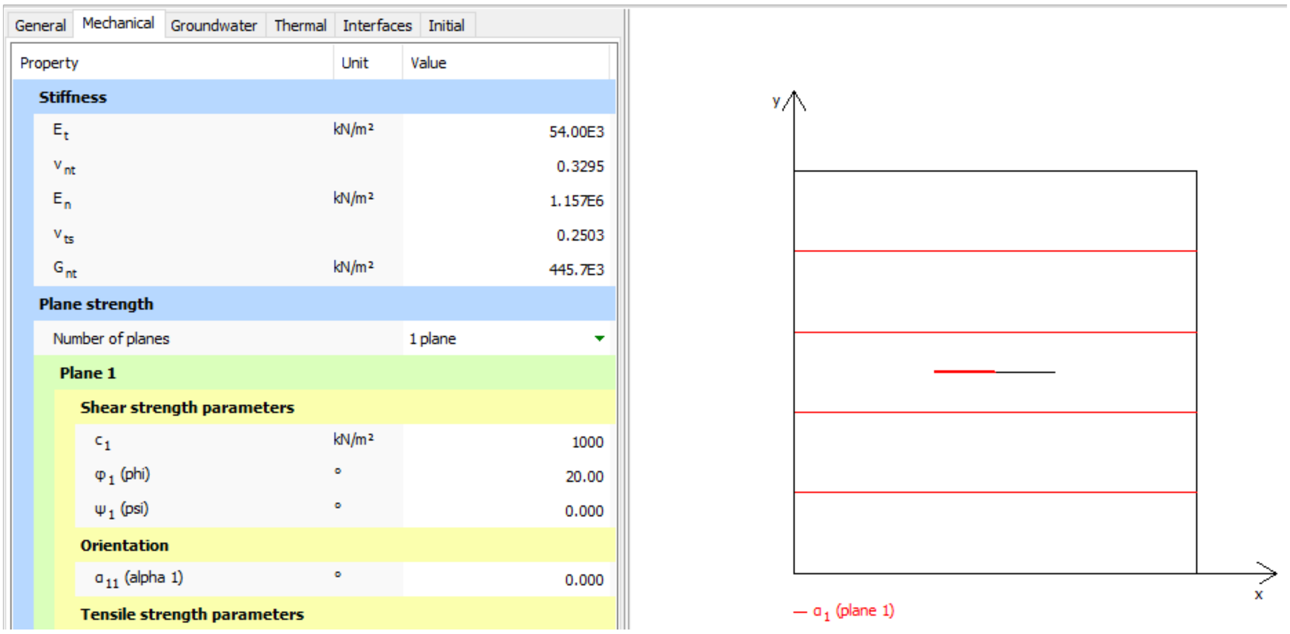

Figure 6.11: Jointed Rock material definition used in Plaxis 2D to introduce the equivalent anisotropic stiffness.

From now on, the apex "Bae" will represent the value in the same reference system used in the paper.

With this convention, the longitudinal stiffness obtained from the homogenization procedure is assigned to the normal direction of Plane 1:

$$E_n = E_z^{\text{Bae}},$$

while the transverse stiffness is assigned to the tangential direction:

$$E_t = E_x^{\text{Bae}} = E_y^{\text{Bae}}.$$

The same interpretation was used for the shear modulus:

$$G_{nt} = G_{xz}^{\text{Bae}} = G_{yz}^{\text{Bae}}.$$

The Poisson's ratios were also taken from the homogenization result. The value ν_{nt} was associated with the tangential response, while ν_{ts} acts perpendicular to the Plane 1:

$$\nu_{nt} = \nu_{xy}^{\text{Bae}},$$

$$\nu_{ts} = \nu_{zx}^{\text{Bae}} = \nu_{zy}^{\text{Bae}}.$$

It is important to highlight that the homogenization procedure used here is purely elastic, and so, the equivalent material parameters obtained from the method only define the stiffness of the reinforced zone. However, the Plaxis 2D Jointed Rock model also requires strength parameters associated with Plane 1. In the present application, these parameters do not represent the real strength of physical joints, since the material is not intended to model a jointed rock.

As a result, the cohesion assigned to Plane 1 was chosen sufficiently high to avoid plastic yielding of the homogenized layer and to keep the response mainly governed by anisotropic elasticity.

The adopted parameters are summarized in Table 6.3.

Table 6.3: Parameters adopted for the homogenized anisotropic equivalent layer in Plaxis 2D.

Parameter	Symbol	Value
Transverse Young's modulus, tangent to Plane 1	E_t	53.46 MPa
Longitudinal Young's modulus, normal to Plane 1	E_n	1156.77 MPa
Shear modulus normal–tangential to Plane 1	G_{nt}	445.68 MPa
Poisson's ratio in the tangential plane	ν_{nt}	0.3295
Poisson's ratio normal–tangential to Plane 1	ν_{ts}	0.2503
Cohesion assigned to Plane 1	c_1	1.0 MPa
Friction angle	φ_1	20°
Dilatancy angle	ψ_1	0°
Plane orientation	α_1	0°

It should be noted that there is no direct correspondence of the physical quantities, but everything comes from an adaptation of the homogenized constants to the reduced set of parameters required by the Plaxis 2D Jointed Rock model.

6.3.3 Enhanced soil method

The third simplified strategy consists in replacing the ground reinforced by the pipe umbrella with an equivalent soil material having improved cohesion and Young's modulus.

This approach is mainly intended to provide a simplified representation of the pipe umbrella in terms of equivalent Mohr–Coulomb parameters. The reinforced cohesion is estimated using the formulation proposed by Grasso et al. (1991, 1993), whereas it was considered to derive the improved Young's modulus again from the section homogenization approach proposed by Carranza-Torres and Diederichs (2009). It should be noted that the improved cohesion procedure was originally developed for tunnel bolting, but the concept is adapted to the pipe umbrella by considering the steel pipes as distributed reinforcement elements within an equivalent improved soil zone. The reinforced region is once again represented as a straight layer parallel to the tunnel axis, located above the tunnel (Figure 6.12).

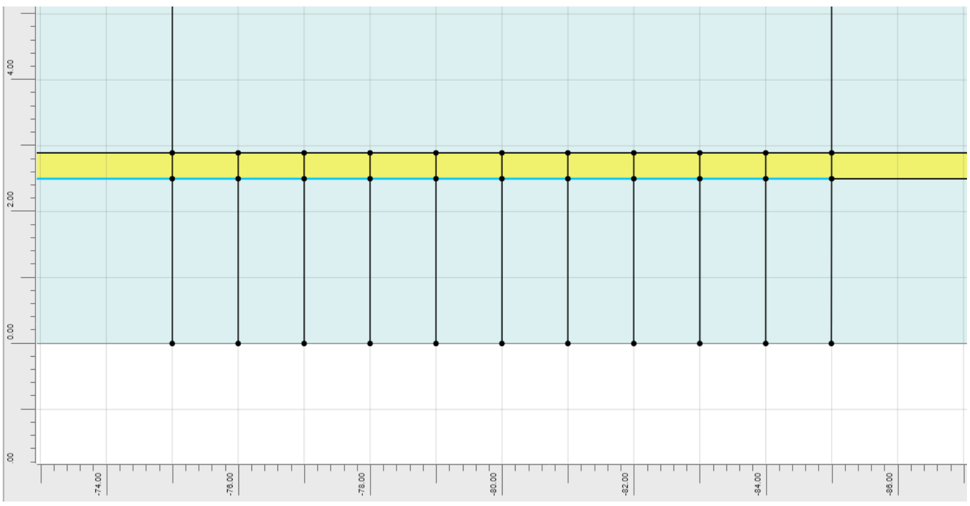

Figure 6.12: Simplified illustration of the enhanced soil approach in Plaxis 2D.

6.3.3.1 Equivalent Young's modulus

The calculation method used to derive the equivalent Young's modulus is based, as previously mentioned, on the procedure presented in Section 6.3.1, but an additional assumption was considered for this specific case. Since the pipes are usually inclined with respect to the tunnel axis, the soil thickness considered in the equivalent section was taken as the projection of the inclined pipe length in the direction perpendicular to the tunnel axis.

Assuming a typical inclination angle θ of 7° and a pipe length equal to 10 m, the soil thickness is

$$t_{\text{soil}} = L_{\text{pipe}} \sin\theta = 10 \sin(7°) = 1.22 \text{ m}. \tag{6.18}$$

This parameter defines only the height of the soil area of the equivalent section. It should not be confused with the equivalent thickness gained from the equivalent section approach.

The parameters used for the calculation, together with the resulting equivalent values, are reported in Table 6.4.

Table 6.4: Parameters used in enhanced soil approach based on equivalent section approach.

Parameter	Symbol	Value
Input data		
Steel Young's modulus	E_1	210000 MPa
Steel Poisson's ratio	ν_1	0.30
Soil Young's modulus	E_2	50 MPa
Soil Poisson's ratio	ν_2	0.25
Section properties		
Steel area	A_1	1.318×10^{-3} m^2
Steel second moment of area	I_1	1.164×10^{-6} m^4
Soil area	A_2	6.087×10^{-1} m^2
Soil second moment of area	I_2	7.566×10^{-2} m^4
Equivalent values		
Equivalent axial stiffness	D_{eq}	673186.761 kN
Equivalent bending stiffness	K_{eq}	8607.42156 kN m^2
Equivalent thickness	t_{eq}	0.392 m
Equivalent Young's modulus	E_{eq}	1718.6055 MPa
Equivalent Poisson's ratio	ν_{eq}	0.25

6.3.3.2 Equivalent cohesion

The reinforced cohesion is calculated using the formulation proposed by Grasso et al. (1991, 1993), where the equivalent cohesion is written as

$$c'_{\text{renf}} = c' + \frac{nT_s}{2S} \tan\left(\frac{\pi}{4} + \frac{\varphi'}{2}\right). \tag{6.19}$$

where c' and φ' are the initial effective cohesion and friction angle of the soil, n is the number of pipes, T_s is the force mobilized by one pipe, and S is the surface over which the reinforcement effect is distributed.

The pipe is treated as a sort of pile foundation and the mobilized force T_s is obtained from the unit shaft resistance along the external surface of the pipe:

$$T_s = \pi D_e L_s q_s. \tag{6.20}$$

Since no grout contribution is considered, the shaft resistance is assumed to develop directly along the steel–soil interface, which requires the external diameter of the pipe to be used in the calculation of the contact surface.

The unit shaft resistance q_s is estimated through an effective stress approach derived from pile design practice. Following Viggiani (1993), the shaft resistance in drained conditions may be expressed as

$$q_s = \mu\sigma'_v. \tag{6.21}$$

where $\sigma'_v = 200kPa$ is the vertical stress and μ is an interface coefficient. Since soil taken as reference for this work is not defined in terms of common nomenclature, to define the value of μ, it was used the table proposed by Viggiani (1993), where $\mu = \tan\phi$. So, for this case, $\mu = 0.36$, giving

$$q_s = 72.79 \text{ kPa}.$$

The corresponding mobilized force is

$$T_s = 203.3 \text{ kN}.$$

In contrast with the other two approaches, the number of pipes is explicitly defined from the adopted spacing along the reinforced arc. The pipe umbrella is assumed to cover a half circumference, and the spacing between adjacent pipes is equal to 0.50 m. The resulting number of pipes is rounded to

$$n = 17.$$

Two possible definitions of the distribution surface S are considered. The first one is the transverse surface of the improved zone:

$$S_{\text{trans}} = \frac{\theta}{2}\left[(R + b_{\text{soil}})^2 - R^2\right]. \tag{6.22}$$

where $\theta = \pi$ and b_{soil} is the actual soil transverse height considered as influenced by the inclined pipe umbrella.

The second one is the longitudinal surface:

$$S_{\text{long}} = L_s\theta R. \tag{6.23}$$

This definition distributes the reinforcement effect along the length over which the pipes interact with the ground. The longitudinal surface gives a more conservative value of the equivalent cohesion, whereas the transverse surface leads to a larger cohesion increase because the same total pipe resistance is distributed over a smaller area.

The values obtained from the calculation are

$$c'_{\text{renf,trans}} = 235.5 \text{ kPa}, \qquad c'_{\text{renf,long}} = 61.4 \text{ kPa}.$$

Considering that the pipes act mainly in the longitudinal direction, it can be assumed that the reinforced area to be considered is not the transverse one, but rather the longitudinal one. For this reason, in the model, the reinforced cohesion was set equal to

$$c'_{\text{renf}} = 61.4 \text{ kPa}.$$

In order to study the influence of the cohesion increase, two enhanced soil configurations were considered in the numerical analyses. In the first one, the Young's modulus of the reinforced region is increased, while the cohesion is kept equal to the original soil cohesion. In the second one, both the Young's modulus and the cohesion are increased, using the reinforced cohesion value calculated above. These two cases are later referred to as the low-cohesion and high-cohesion enhanced soil models.

6.3.4 Possible limitations of the 2D modelling approaches

A limitation common to all methods may be related to the choice of the thickness adopted to model the problem in the FEM software. Indeed, each approach required different conditions in order to be properly characterized, and so it was not intrinsically possible to adopt the same thickness values. This generally leads to different mechanical properties, which may affect the reliability of the results. However, sensitivity analyses were carried out for each model with the aim of calibrating them as accurately as possible and reducing, as far as possible, the effects caused by this inconsistency

The linear elastic equivalent volume is characterized by an isotropic and very stiff material. Consequently, it is not possible to define different mechanical properties depending on the considered direction. This represents one of the main limitations of this method, since the pipe umbrella system actually acts mainly along the tunnel axis. Moreover, the adopted procedure is usually used to homogenize two materials composing the main lining, and not to directly combine the contribution of the ground and the pre-support.

The method based on the homogenization of the pipe–soil system into an anisotropic material, presents limitations related to the fact that the approach proposed by Bae et al. was developed for a 3D model. In that context, the response of the pipes can be studied with respect to their local reference system and then transferred into the global reference system of the tunnel according to the position of the pipes along the installation arch. In the axisymmetric model, instead, equivalent properties are assigned in the radial and longitudinal directions. This simplification is mainly consistent in the crown region of the tunnel, where the local reference system of the pipes can be considered closer to the global reference system of the model. Although the longitudinal direction of the pipes is also assumed in the 2D model as the main stiffness direction, and this choice makes it possible to represent the main anisotropic effect of the pipe umbrella, it still remains a simplification with respect to the complete 3D formulation.

The enhanced soil method derives from the application of the linear elastic equivalent volume for the definition of the Young's modulus, and from the use of formulas originally adopted for bolting with regard to the equivalent cohesion. It is therefore a mixed and innovative approach, and for this reason it is associated with several uncertainties. In this case, the limitations are not only those already highlighted for the linear elastic equivalent volume, but also those related to the calculation of the cohesion of the reinforced ground. Indeed, some assumptions were introduced regarding the interaction between pipes and ground, by considering the behaviour of the pipes as partly analogous to that of foundation piles and bolts.

Overall, these limitations show that the 2D methods should not be interpreted as a direct representation of the pipe umbrella system, but rather as equivalent tools to estimate its global effect on the deformational response of the tunnel.

6.4 Excavation and support sequence

The same excavation sequence is used for all the configurations analysed in this work. Only the way in which the pipe umbrella or the reinforced ground is represented changes from one model to another.

When a pipe umbrella is included, it is activated before the excavation steps. Depending on the adopted approach, it is modelled as an equivalent volume, a homogenized anisotropic material, or an enhanced soil region. The sequence is shown using Plaxis 2D (Figure 6.13), because the activation and deactivation stages are easier to visualise. The same excavation logic is also used in Lagamine, even if it is implemented in a different way.

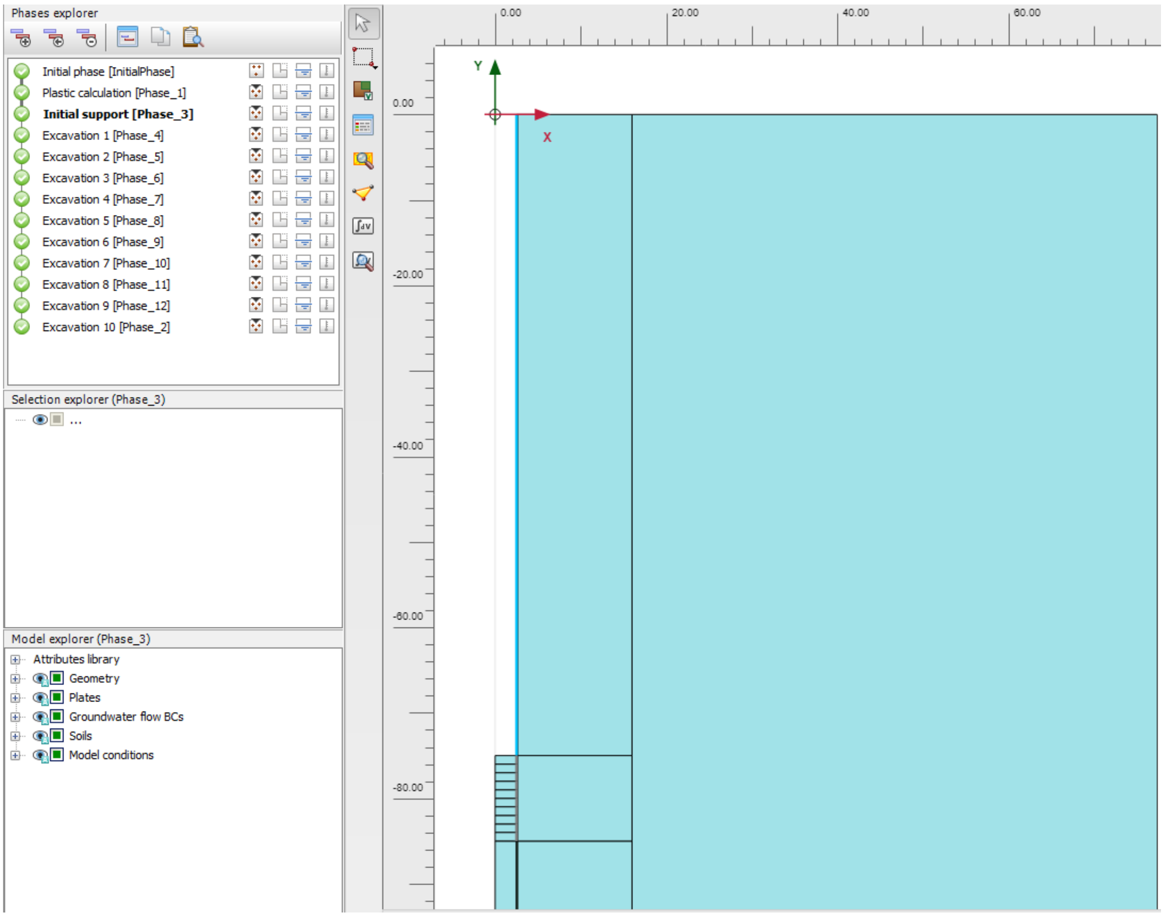

Figure 6.13: Initial large excavation stage in the Plaxis 2D model. The already excavated part of the tunnel is deactivated and the lining (blue line) is activated along the supported region.

In Lagamine, the initial part of the tunnel is directly left empty in the mesh. In Plaxis 2D, the same condition is obtained by deactivating the soil block and activating the lining along the already excavated part. This stage is referred to as the large excavation stage and is used to start the analysis from an already excavated and supported tunnel section.

After this initial stage, the excavation is advanced step by step. The soil below the pipe umbrella is divided into ten soil blocks, each one having a longitudinal length of 1 m. At each calculation phase, one soil block is deactivated to simulate a new excavation step. The lining is then activated along the previously excavated part of the tunnel. In this way, the unsupported length between the tunnel face and the last installed lining section is kept equal to 1 m throughout the whole excavation sequence.

According to the reference system, the first and final excavation stages are shown in Figure 6.14. In the first step, one meter of soil block is deactivated below the pipe umbrella, while the lining is installed up to the previous section. The same procedure is repeated until ten consecutive excavation steps have been performed, corresponding to a total advance of 10 m. The results used for the comparison between the different modelling approaches are extracted from the final excavation stage.

The first excavation step begins at $y = -75$ m, whereas the last excavation is performed at $y = -85$ m. In the plots, the longitudinal distance is shown as positive for easier interpretation, although the tunnel advances along the negative y-direction.

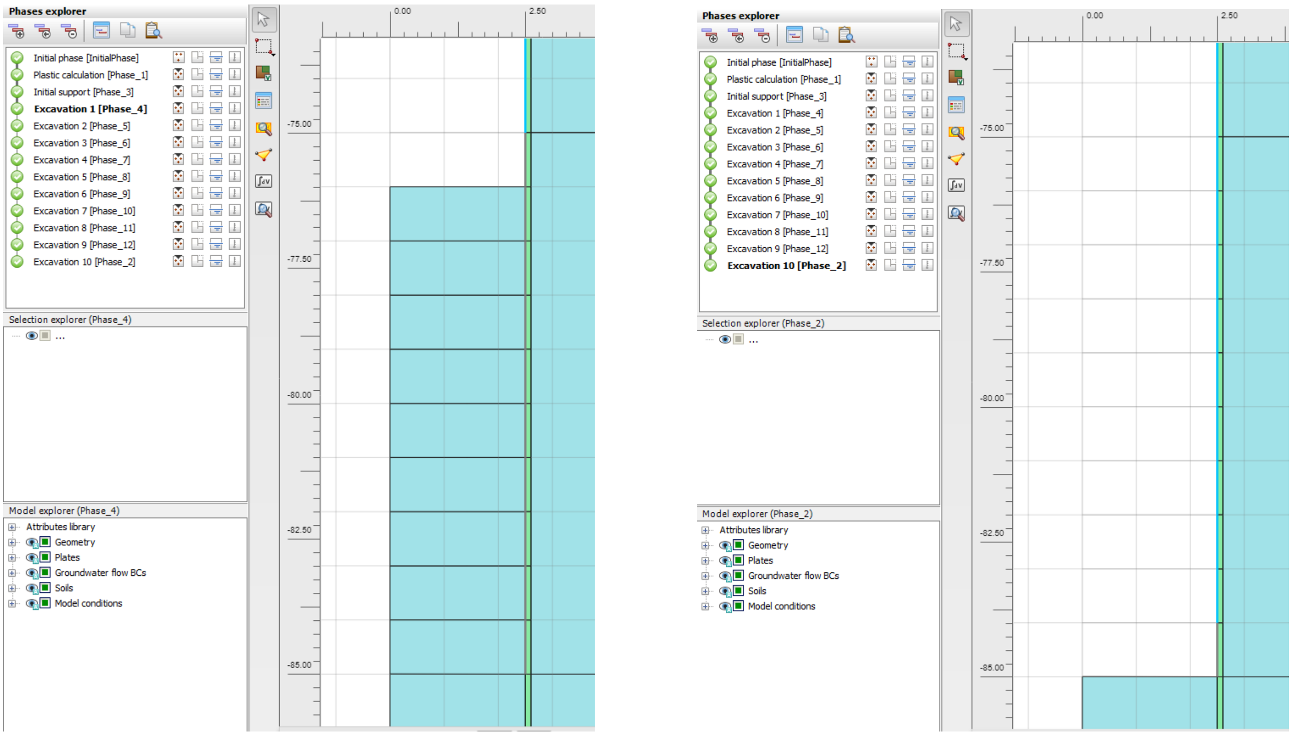

(a) First excavation step.

(b) Last excavation step.

Figure 6.14: Excavation sequence adopted in the Plaxis 2D model. Here, are shown only the first one and the last one

The reason for considering ten excavation steps is to reduce the influence of the initial large excavation stage on the results. In the first excavation phases, the response of the model may still be affected by the initial boundary between the already supported tunnel and the newly excavated part. By advancing the excavation over 10 m, the response becomes more representative of the repeated excavation-support process.

6.5 Chapter conclusion

This chapter deals in detail with the Lagamine and Plaxis 2D numerical models, introducing the additional assumptions specific to each of them, such as mesh, geometry, boundary conditions, and other modelling aspects. Since the simplified representations of the pipe umbrella system are implemented within the FEM models only, their mathematical formulation is also presented in detail. For this reason, this chapter also represents the most appropriate part of the thesis in which to discuss the possible intrinsic limitations of the models, both in general terms and for each approach individually. For greater clarity, all the numerical values obtained for the linear elastic equivalent volume approach, the anisotropic material approach, and the enhanced soil approach are summarized and explicitly reported. Considering that the excavation steps are a fundamental aspect in the study of the tunnel response, the excavation and support sequence is also clarified. Overall, this chapter acts as a bridge between the model setup and modelling assumptions, and the results obtained from the analyses.

7 Results

7.1 Analytical results

The first result is the interaction between the Ground Reaction Curve and the Support Reaction Curve, shown in Figure 7.1. In this calculation, the unsupported distance was taken equal to $d = 1$ m,, which corresponds to the free span adopted throughout this work.

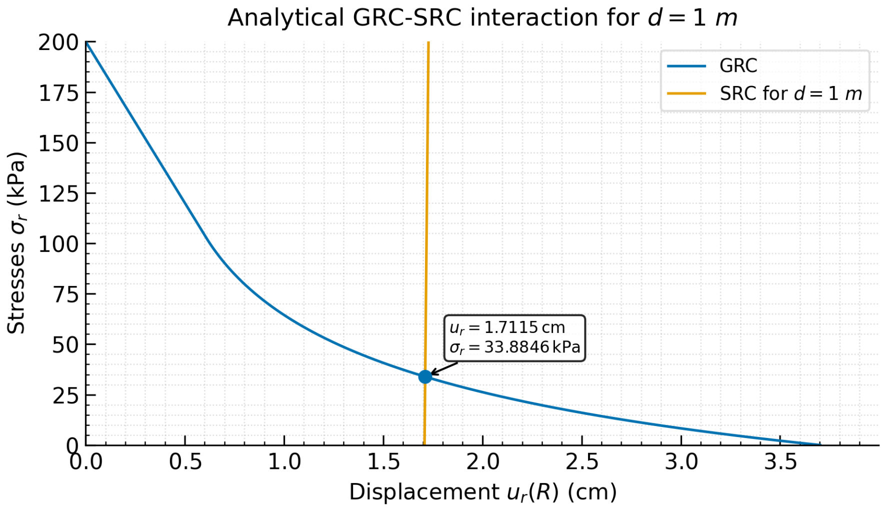

Figure 7.1: Analytical elasto-plastic GRC–SRC interaction for an unsupported distance $d = 1$ m.

The intersection between the two curves gives the final equilibrium condition between the ground and the support. In the present case, the obtained values are

$$u_R = 1.71 \text{ cm}, \qquad \sigma_R = 33.88 \text{ kPa}.$$

The support reaction curve appears almost vertical because the support stiffness is much higher than the ground stiffness. In fact, the Young's modulus of the support is of the order of 30 GPa, whereas the Young's modulus of the ground is 50 MPa.

According to the CCM formulation, the analytical model also allows the radial distribution of displacements and stresses around the tunnel to be evaluated. This is shown in Figure 7.2, where different values of the deconfinement ratio λ are considered. The results follow the expected theoretical trends.

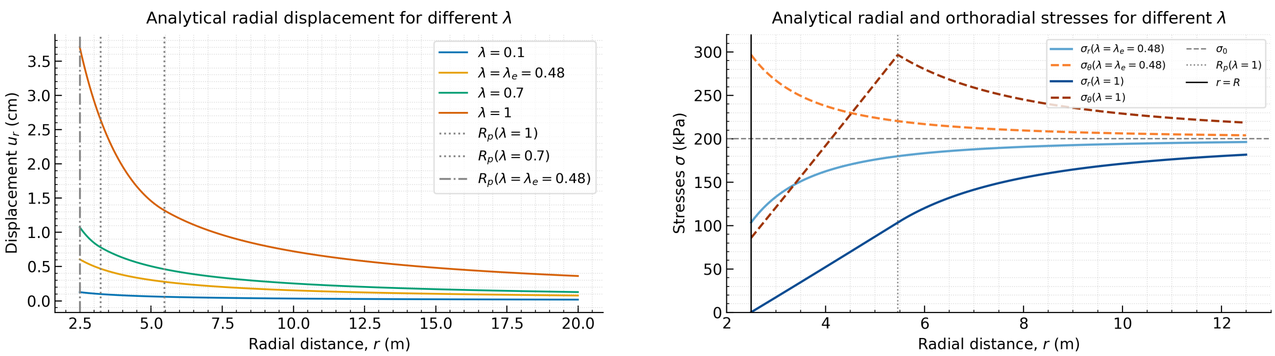

(a) Radial displacement.

(b) Radial and orthoradial stresses.

Figure 7.2: Analytical elasto-plastic radial displacement and stress distributions for different deconfinement ratios.

Finally, the longitudinal displacement profile was obtained using the analytical formulation adopted in Section 2.3.5 for the unsupported case (Figure 7.3). Several approaches were studied during the development of the analytical model, but the selected formulation is based on the Panet–Corbetta approach (Panet & Sulem, 2022). The LDP is necessary because the support reaction depends on the displacement that has already occurred before the support installation. In the LDP plot, a distance x equal to zero corresponds to the tunnel face.

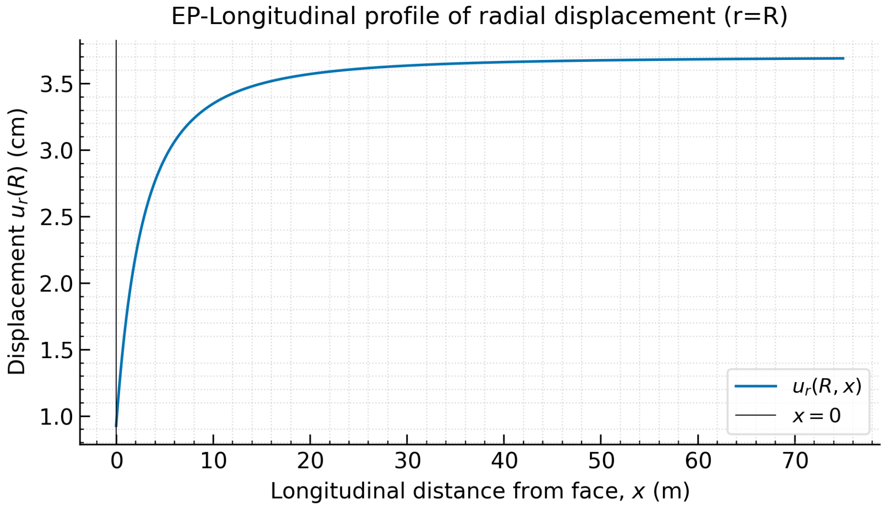

Figure 7.3: Analytical elasto-plastic longitudinal displacement profile at the tunnel wall. x=0 is the tunnel face.

As shown in the figure above, the radial displacement increases rapidly close to the tunnel face and then progressively tends towards an asymptotic value far behind the face. The final radial displacement is approximately

$$u_R(\infty) \simeq 3.7 \text{ cm}.$$

This value represents the fully developed convergence of the unsupported tunnel.

7.2 2D FEM results

7.2.1 Lagamine

7.2.1.1 Unsupported soil case

For this case, no lining was activated, so that the curve represents just the free response of the ground. At first, the GRC is obtained from the model by selecting a point sufficiently far from the excavation face and from the model boundaries, so that the response is representative of the free soil behaviour under progressive stress reduction. The Lagamine GRC and LDP are shown in figure Figure 7.4.

In the longitudinal displacement profile, it is clear that the radial displacement increases rapidly close to the tunnel face and then progressively tends towards an asymptotic value of about

$$u_R(\infty) \simeq 3.7 \text{ cm}.$$

This result is consistent with the physical interpretation of the LDP, where most of the displacement develops close to the tunnel face, while the remaining part progressively develops far from the face. In the LDP, a distance equal to zero corresponds to the tunnel face.

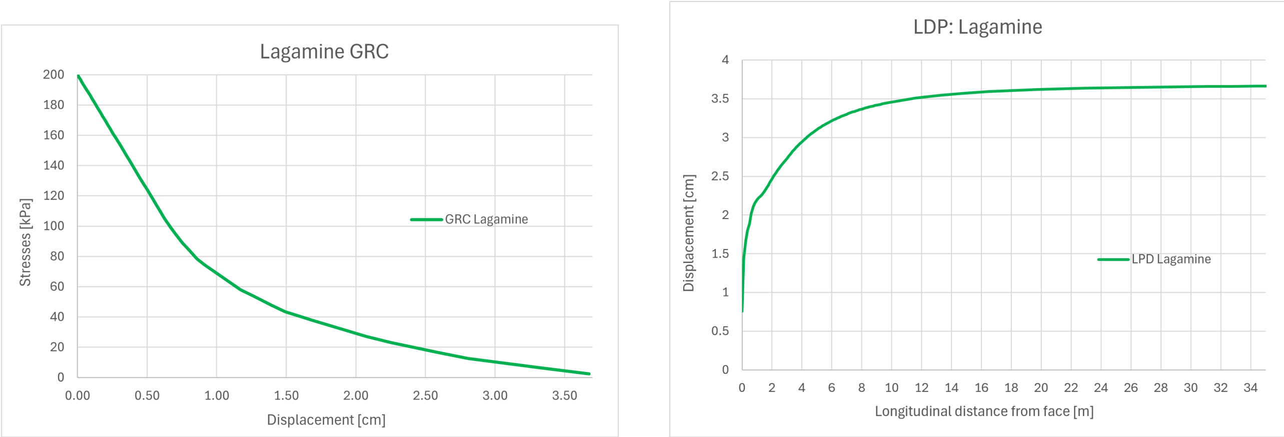

(a) Ground Reaction Curve. (b) Longitudinal displacement profile.

Figure 7.4: Ground Reaction Curve and longitudinal displacement profile at the tunnel wall obtained from the unsupported Lagamine model. Distance=0 represents the tunnel face in LDP.

7.2.1.2 Lining without presupport (support modelled with gap)

The longitudinal contact pressure obtained on the lining is shown in Figure 7.5. In this analysis, an initial gap of 2 cm was introduced between the ground and the support. As a consequence, the lining starts to react only after this amount of convergence is reached. After contact is established, the pressure increases rapidly and progressively tends towards an almost constant value of about

$$u_R = 2.00 \text{ cm}, \qquad \sigma_R \simeq 24 \text{ kPa}.$$

This value corresponds to the support pressure associated with the imposed gap of 2 cm, and therefore with the displacement that occurs before the lining starts to interact with the ground. in the longitudinal profile a distance equal to zero corresponds to the tunnel face.

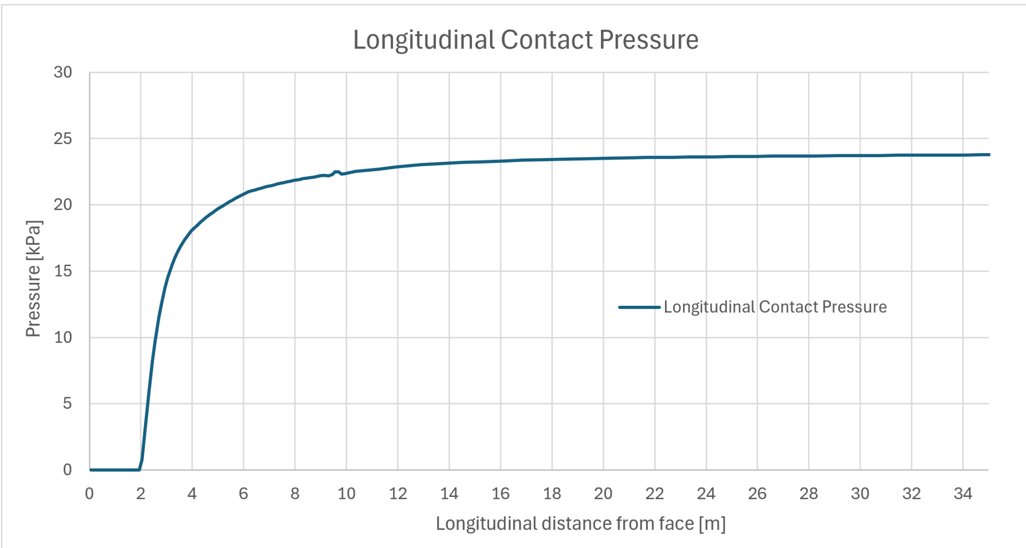

Figure 7.5: Longitudinal evolution of the contact pressure on the lining obtained from the Lagamine model. Distance=0 represents the tunnel face.

A specific effort was required to obtain a sufficiently smooth contact pressure profile. In the preliminary simulations, local oscillations appeared around the transition between the refined mesh close to the excavation and the coarser mesh farther from the tunnel. These oscillations were mainly related to the contact formulation and to the change in mesh size, which required the mesh density, the number of integration points, and the contact penalty parameters to be progressively adjusted until a stable pressure distribution could be visualized.

7.2.1.3 Linear elastic equivalent volume case

The following figure, obtained from the Lagamine results, refers to the tenth excavation step of the linear elastic equivalent volume approach, which is modelled in the same way as Plaxis 2D. From the results presented below, it can be observed that, differently from Plaxis 2D, the soil corresponding to the ten excavation steps is not actually removed from the visualization, but remains represented in the model. However, thanks to the legend shown in the figure, it is still possible to identify and define the magnitude of the results and of the deformations.

In particular, the maximum deformation develops close to the lining and to the linear elastic equivalent volume as shown in Figure 7.6. In this zone, the radial deformation is approximately

$$u_{R,max} \simeq 0.1 \text{ cm},$$

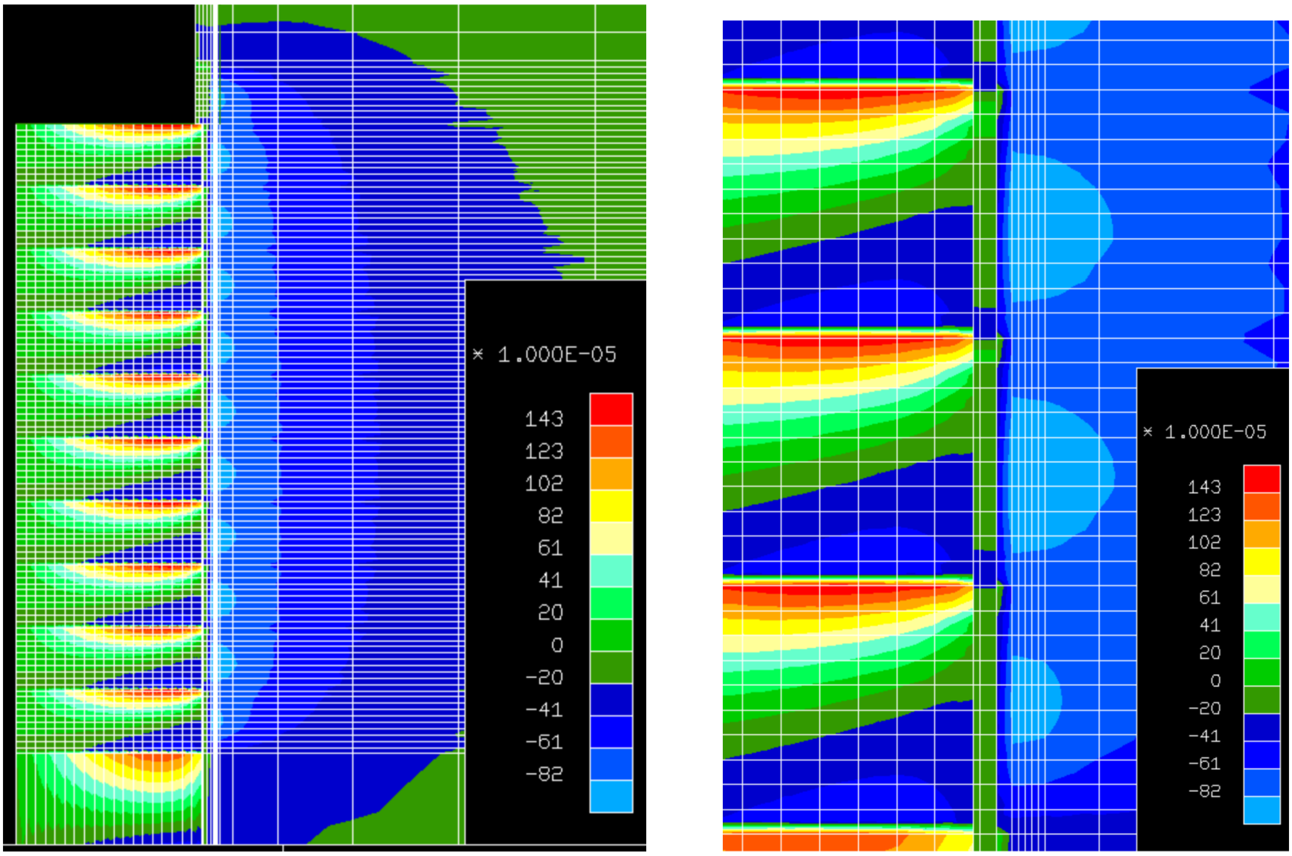

(a) General view. **(b)** Zoom on the reinforced zone.

Figure 7.6: Radial displacements obtained in Lagamine for the linear elastic equivalent volume model at excavation phase 10.

7.2.2 Plaxis 2D

7.2.2.1 Unsupported soil case

The unsupported case represents the free-ground response, without lining and without pre-support. It is used as a reference condition to evaluate the free behaviour of the soil.

The radial displacement and radial stress fields are shown in Figure 7.7. The maximum longitudinal radial displacement reached is

$$u_R(\infty) \simeq 3.7 \text{ cm}.$$

The stress field shows the progressive stress release around the excavation boundary, with the highest stress redistribution concentrated close to the tunnel wall. When the soil reaches its maximum value, the stresses are equal to zero.

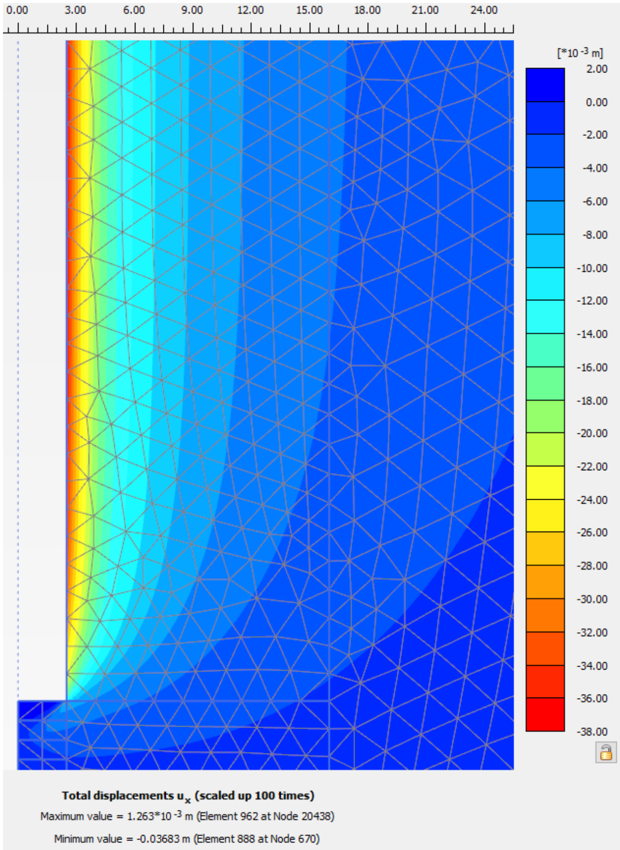

(a) Radial displacement field.

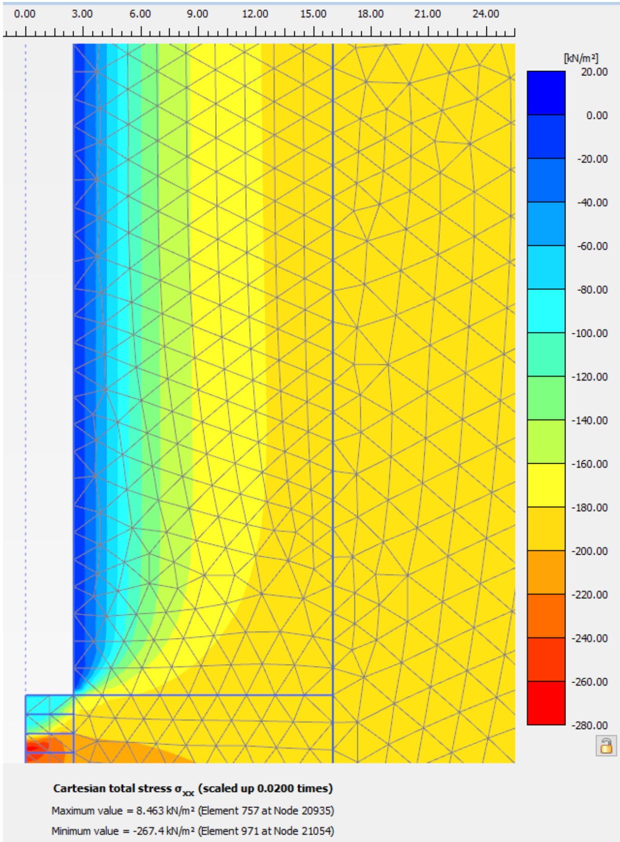

(b) Radial stress field.

Figure 7.7: Plaxis 2D results for the unsupported tunnel case: radial displacement and radial stress field

The same unsupported analysis was used to derive the Plaxis 2D Ground Reaction Curve shown in Figure 7.8. The procedure used to get the curve is the same as the one followed for Lagamine.

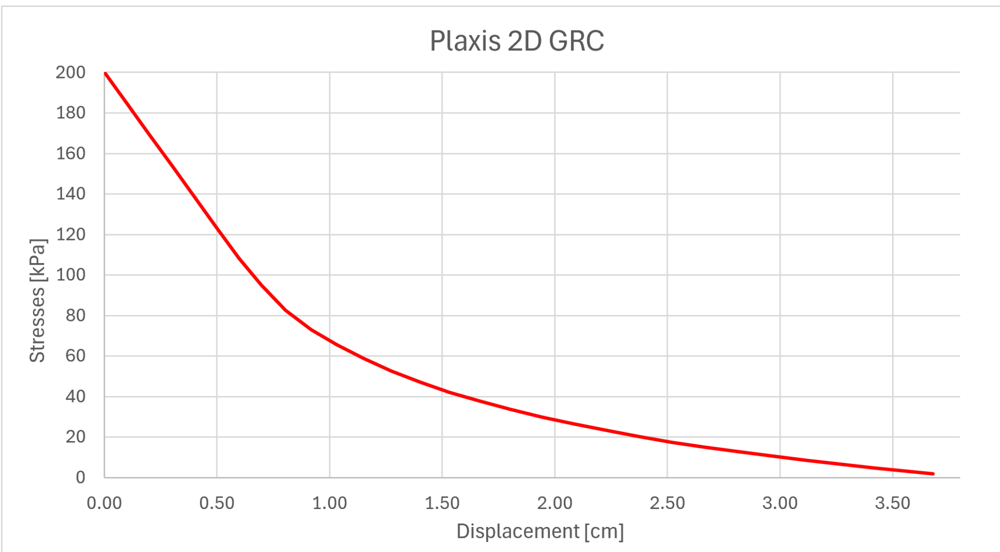

Figure 7.8: Ground Reaction Curve obtained from the unsupported Plaxis 2D model.

The plastic points obtained for the unsupported case are shown in Figure 7.9. In this regard, plasticity develops over a quite wide region around the excavation. The maximum plastic radius is approximately

$$R_p(\infty) \simeq 3 \text{ m}.$$

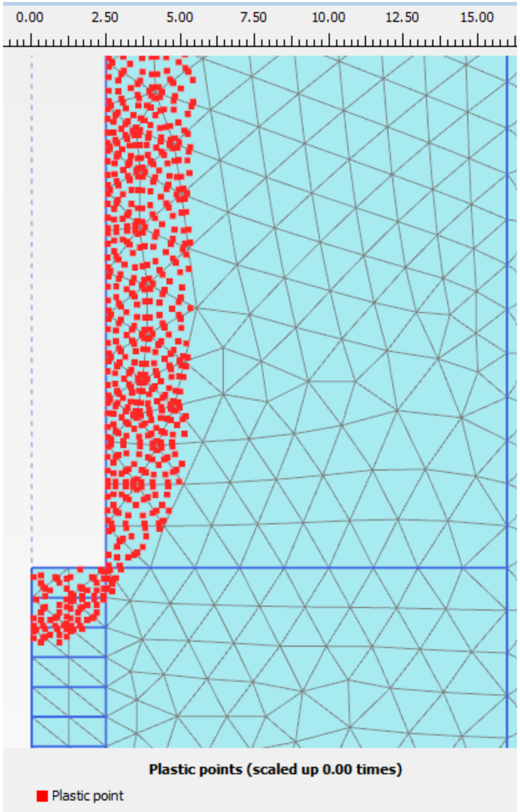

Figure 7.9: Plastic points in Plaxis 2D for the unsupported tunnel case.

7.2.2.2 Lining-only case

The lining-only case represents the reference case for the results comparison in terms of effectiveness of the pipe umbrella system. So, no pipe model is introduced in this step. The lining is activated with an unsupported distance equal to 1 m, as defined in the previous chapters. Only results of the 10th excavation step are provided.

The radial displacement field and the plastic points are shown in Figure 7.10. The maximum radial displacement is

$$u_{R,\max} \simeq 1.0 \text{ cm}.$$

The radial displacement field has a peculiar shape because at each excavation phase, the portion of soil where no lining is active yet is supported half by the soil above the face and half by the lining just installed in the previous step.

The plastic points show that the introduction of the lining reduces the extension of the plastic zone in certain areas, but still, the soil reaches failure in the unsupported part and in the soil and behind the excavation face.

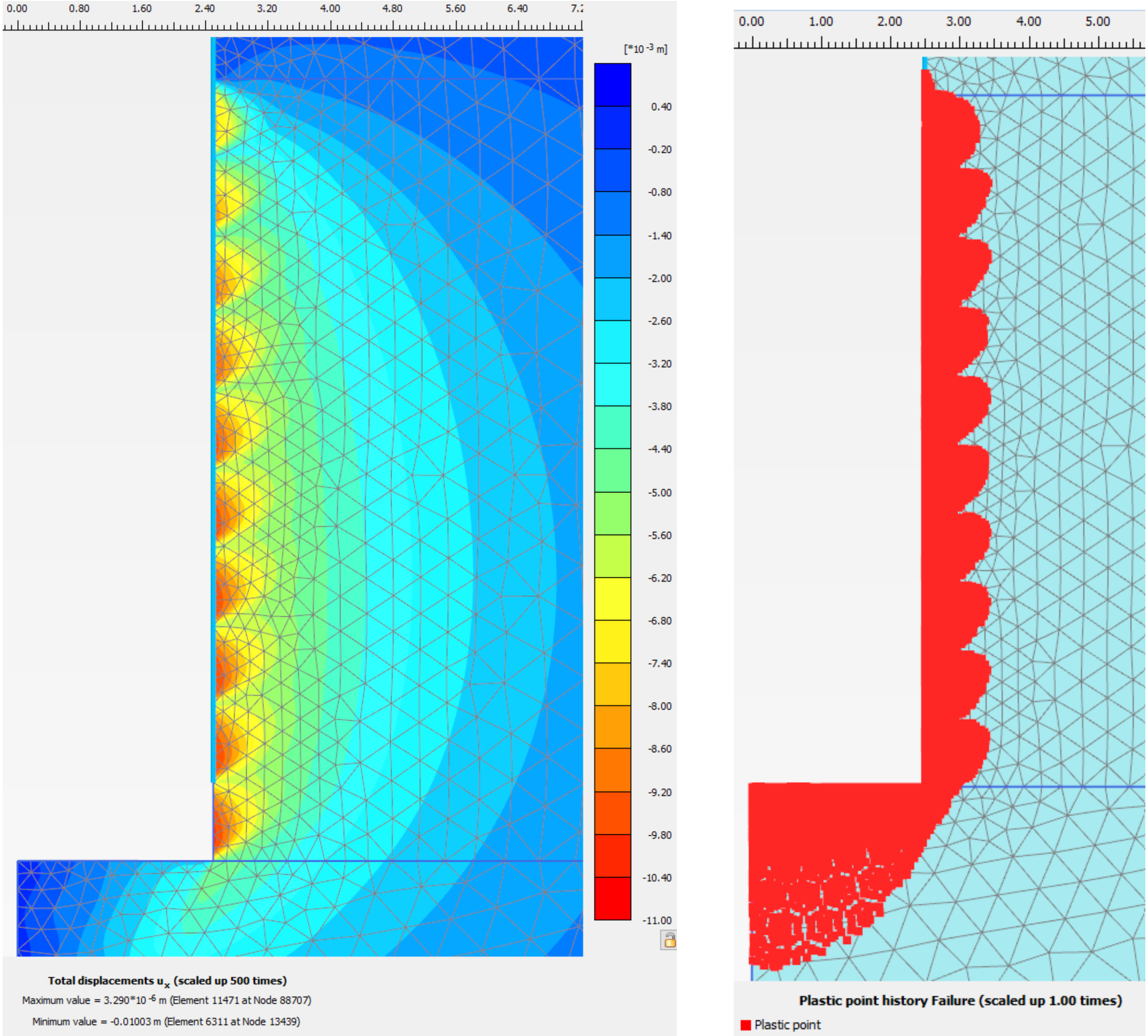

(a) Radial displacement field. **(b)** Plastic points.

Figure 7.10: Plaxis 2D results for the lining-only case at excavation phase 10: radial displacement field and plastic points.

The radial stress field is reported in Figure 7.11. The blue stress zones developing along the lining represent the stress caused by the support–ground interaction. Localized stress concentrations can be observed close to the end of each lining segment, where the support is activated step by step. It is interesting to observe that, before the lining activation, the unsupported soil reaches the highest deconfinement level, shown in dark blue. After the lining is activated, the stress level increases again along the tunnel boundary. This can be interpreted as the contact pressure mobilized between the support and the surrounding soil.

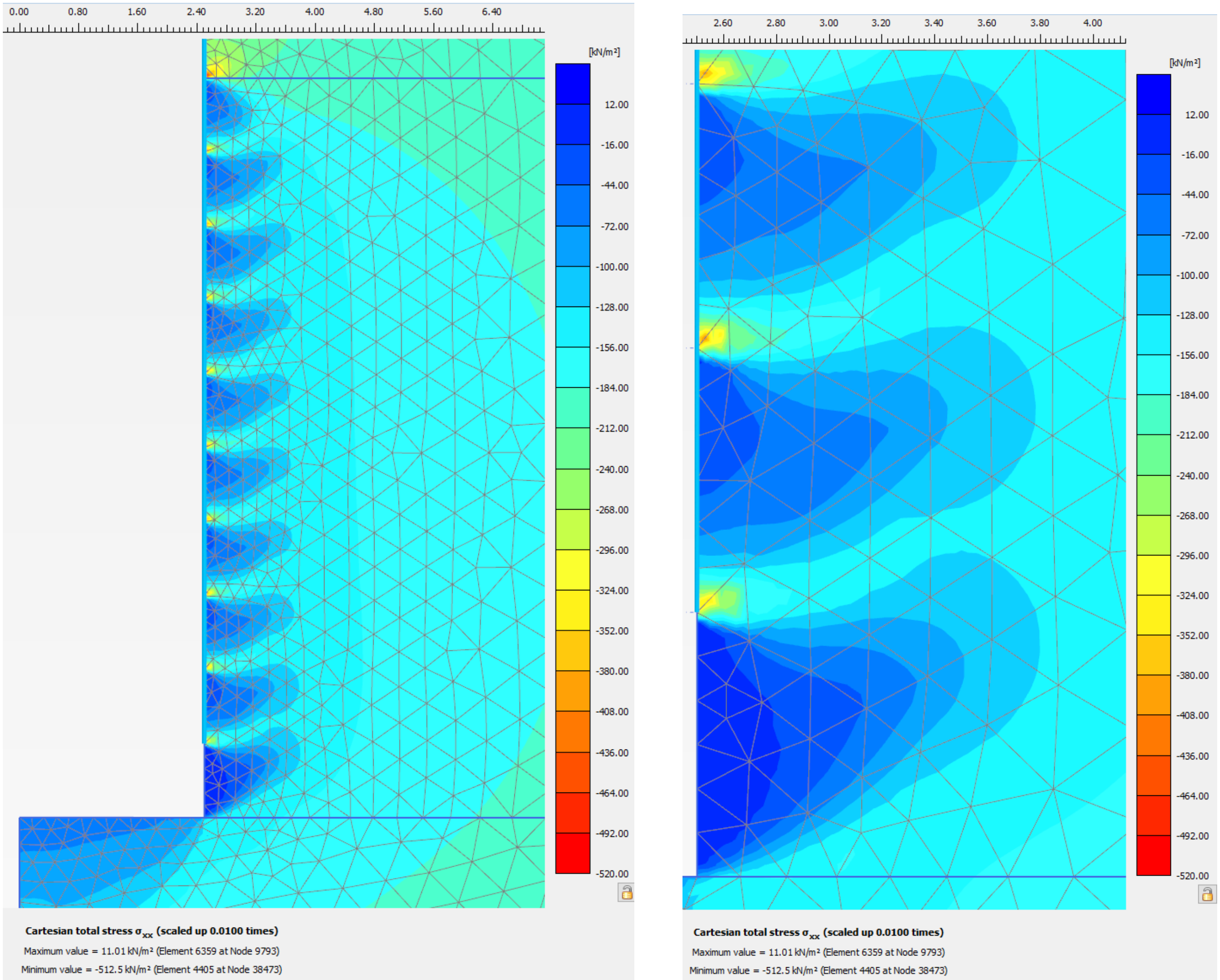

(a) Radial stress field

(b) Zoom near the lining.

Figure 7.11: Radial stress field in Plaxis 2D for the lining-only case, without pre-support, at excavation phase 10.

7.2.2.3 Linear elastic equivalent volume method

The linear elastic equivalent volume method is the first simplified approach used to introduce the effect of the pipe umbrella. In this case, the pre-support is modelled as a continuous equivalent volume, whose stiffness was obtained from the equivalent section procedure described previously.

The displacement field and the plastic points obtained at excavation phase 10 are shown in Figure 7.12. The displacement field shows the same general excavation pattern observed in the supported configurations, but with a reduced displacement magnitude. The maximum radial displacement is about

$$u_{R,\max} \simeq 0.13 \text{ cm}.$$

The plastic points are mainly located close to the tunnel face and behind the face. No clear plastic zone develops along the excavation and lining activation sequence.

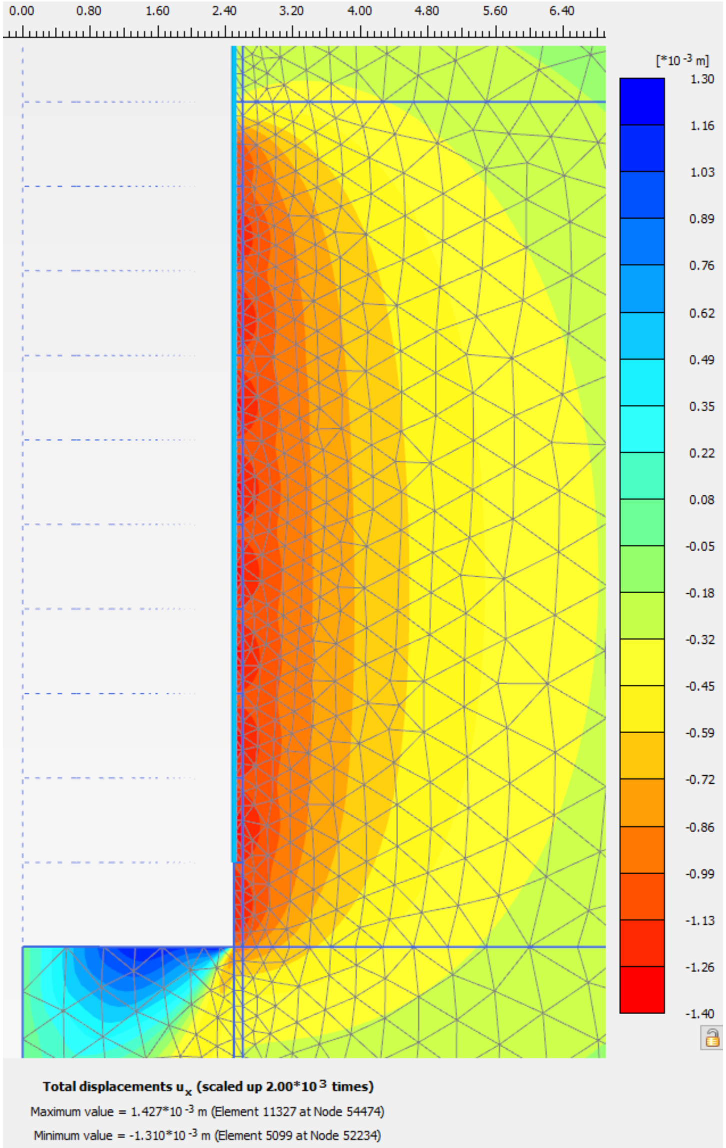

(a) Radial displacement field.

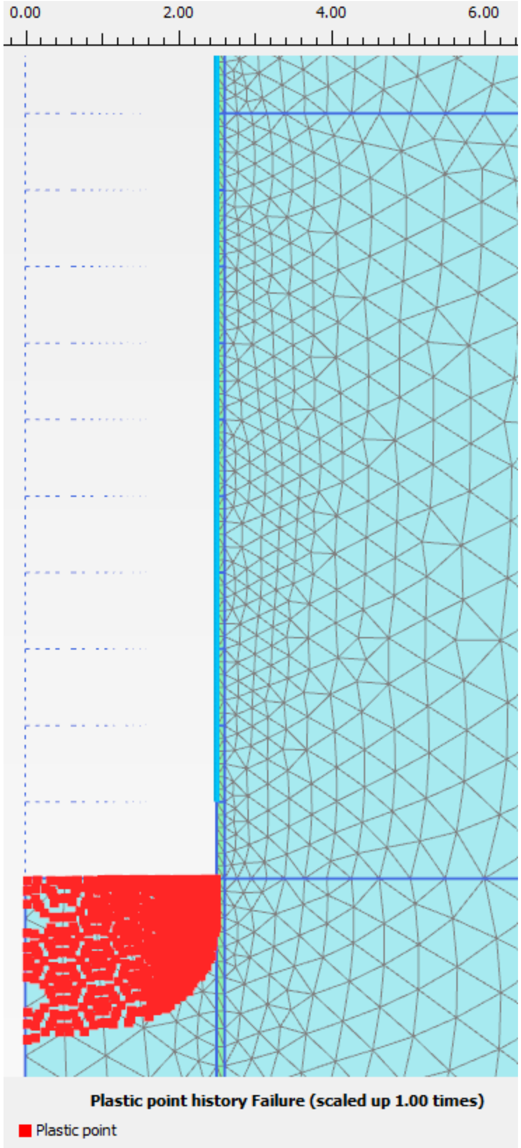

(b) Plastic points.

Figure 7.12: Plaxis 2D results for the linear elastic equivalent volume method at excavation phase 10: radial displacement field and plastic points.

The radial stress field is shown in Figure 7.13. The results point out that the stress redistribution is mainly concentrated near the supported tunnel boundary, inside the equivalent volume. Local stress peaks appear near the edge of the lining. These local concentrations are mainly observed at the lining boundary and are not used as quantitative values of pressure in the reinforced zone.

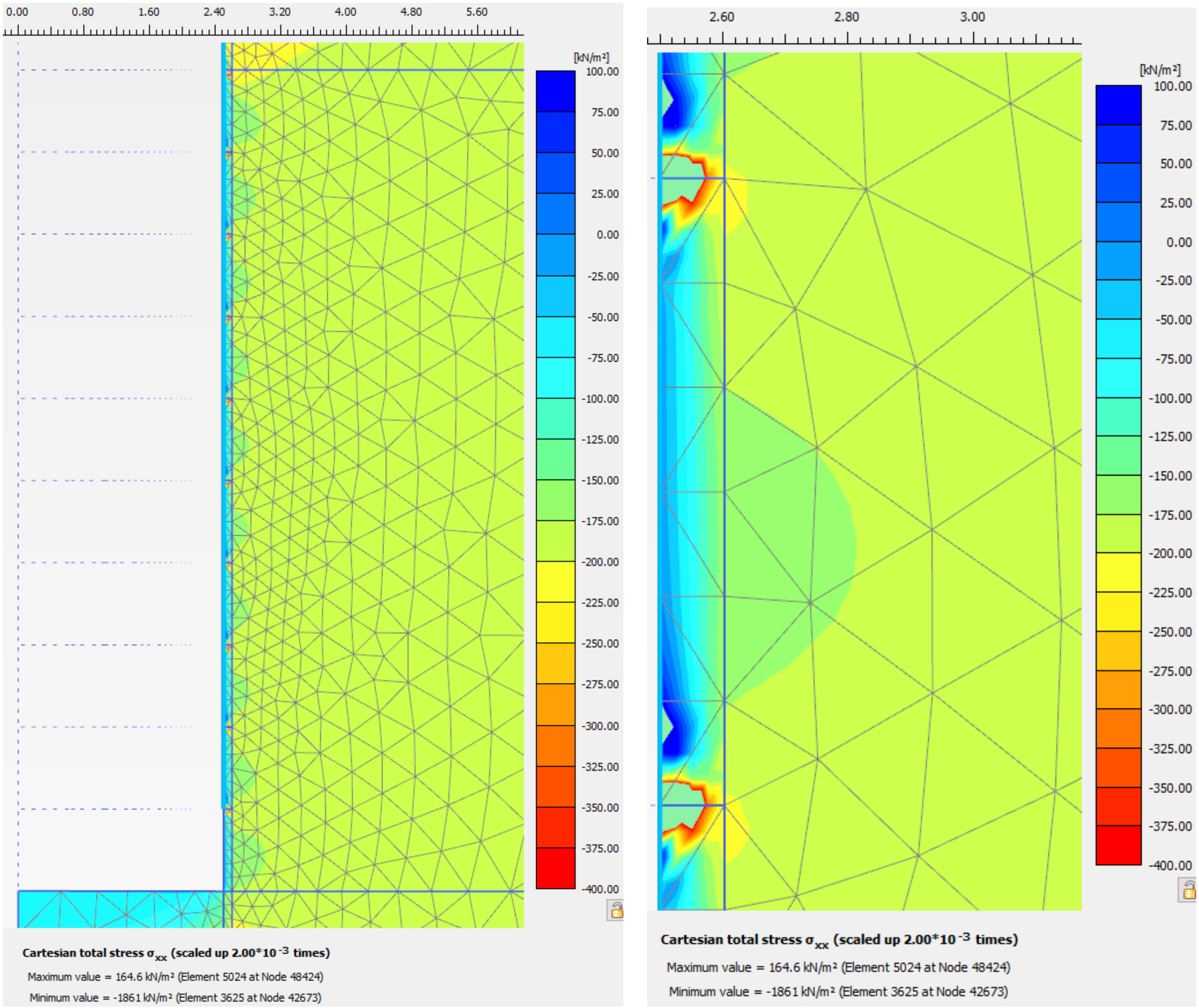

(a) Radial stress field **(b)** Zoom near the equivalent volume.

Figure 7.13: Radial stress field obtained in Plaxis 2D for the linear elastic equivalent volume method at excavation phase 10.

7.2.2.4 Homogenized anisotropic material method

The results attained with the homogenized anisotropic material method are reported in Figure 7.14. The distribution of radial displacements is slightly different from the ones observed so far; relevant displacements seem to start to occur only after about 3 excavation steps. Here the value of maximum radial displacement is approximately

$$u_{R,\max} \simeq 0.5 \text{ cm}.$$

The plastic points are concentrated only in the excavation face region and do not develop inside the homogenized material layer, because the cohesion of the material was set very high for the purpose of avoiding plastification and remaining in elastic domain.

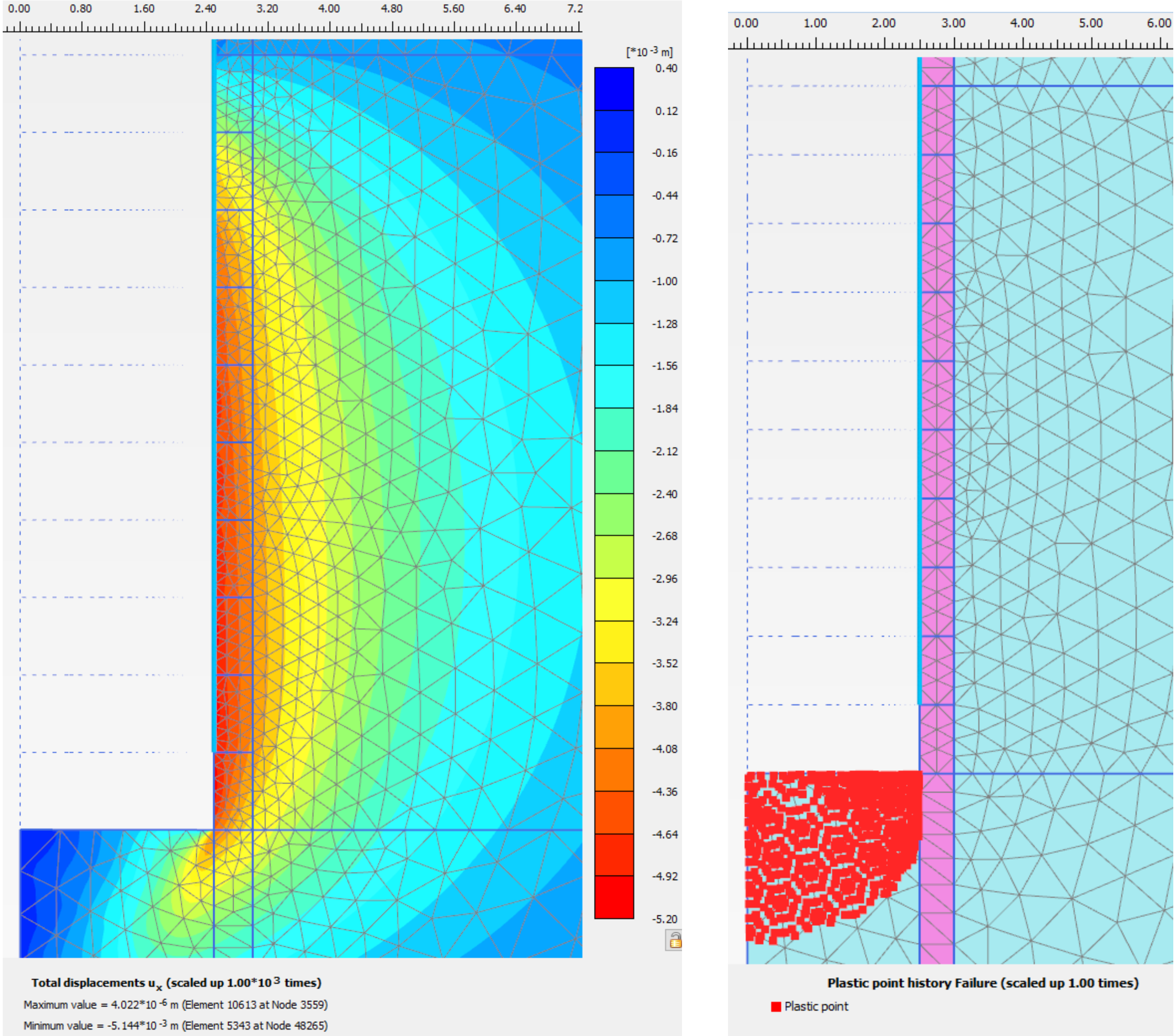

(a) Radial displacement field.

(b) Plastic points.

Figure 7.14: Plaxis 2D results for the homogenized anisotropic material method at excavation phase 10: radial displacement field and plastic points.

The stress field is shown in Figure 7.15. The results indicate that the radial stress redistribution is mainly concentrated near the supported tunnel wall. As in the other supported cases, local stress peaks appear near the edge of the lining and the stresses increase once the lining is activated.

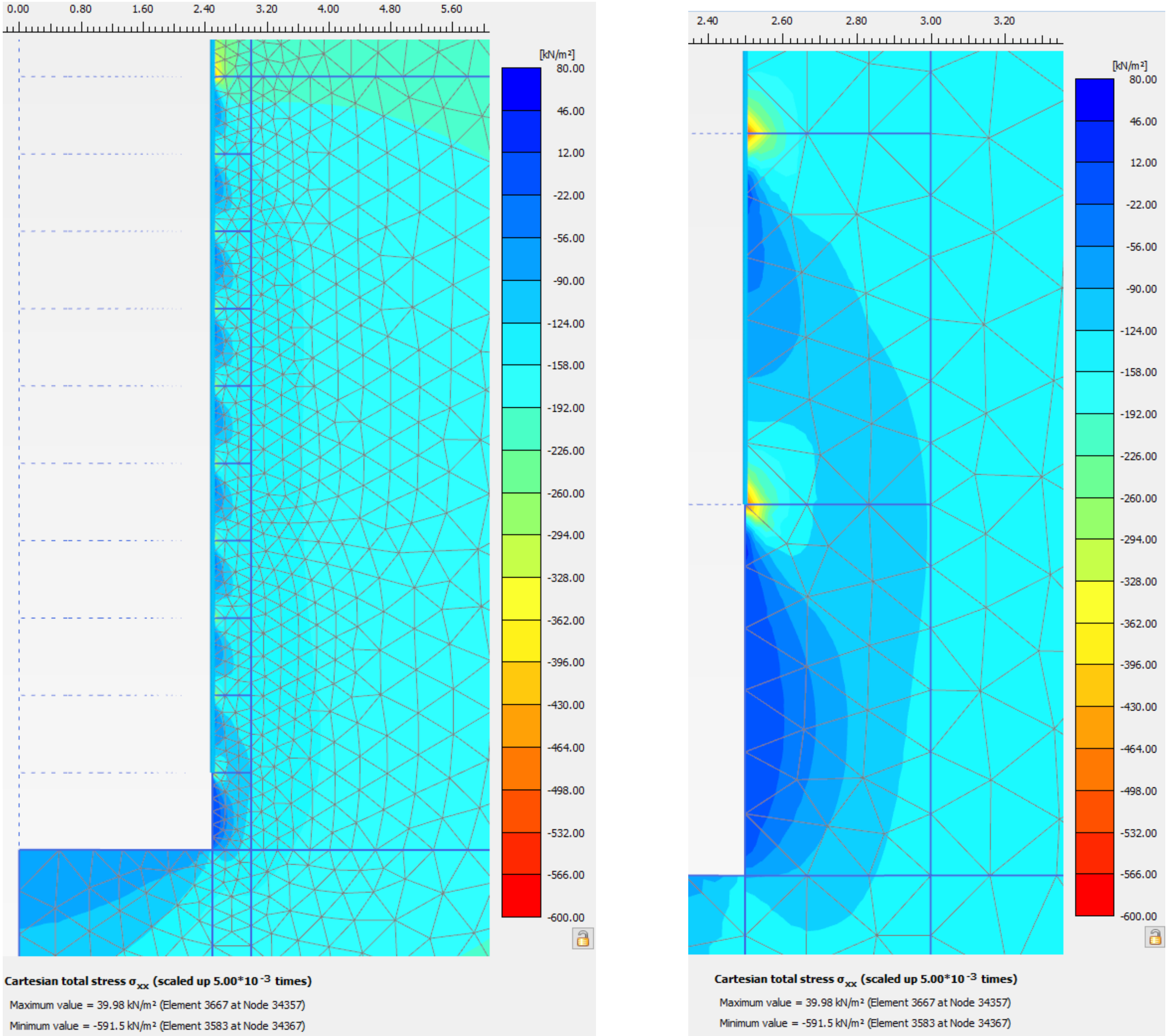

(a) Radial stress field **(b)** Zoom near the lining.

Figure 7.15: Radial stress field obtained in Plaxis 2D for the homogenized anisotropic material method at excavation phase 10.

7.2.2.5 Enhanced soil method

The results obtained with the enhanced soil method are shown in the following figures. Both the cases are presented, the one where the cohesion of the reinforced region is kept equal to the original soil cohesion, and the one where higher cohesion is assigned to the reinforced soil.

The radial displacement fields are shown in Figure 7.16. The maximum radial displacement for the same cohesion case is approximately

$$u_{R,\max} \simeq 0.72 \text{ cm}$$

while for the higher-cohesion case it decreases to approximately

$$u_{R,\max} \simeq 0.44 \text{ cm}$$

In both cases, the shape of the radial displacement field remains similar to the one observed in the lining-only case and in the linear elastic equivalent volume case. The main difference is then mainly related to the magnitude of the displacement. The case of higher cohesion shows less deformations.

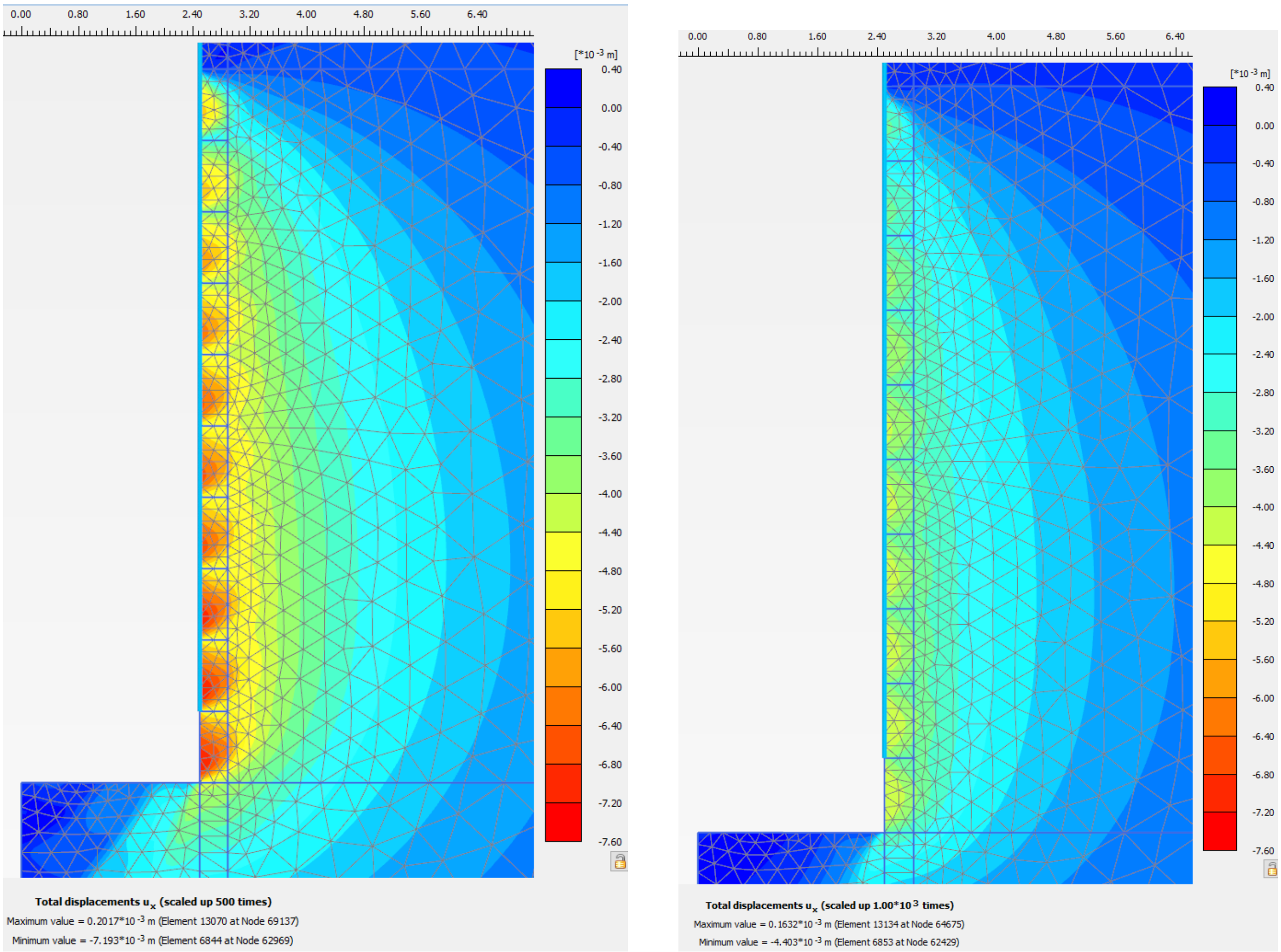

(a) Same cohesion case.

(b) Higher cohesion case.

Figure 7.16: Radial displacement field obtained in Plaxis 2D for the enhanced soil method at excavation phase 10.

The Figure 7.17 shows the results in terms of stresses. The general pattern does not differ too much from the other cases, where the stress redistribution is higher close to the wall. It is clear that in the higher cohesion case the stresses are higher; an expected output considering the reduced displacements. The intensity of stresses is greater where the lining is active, as contact pressure between the lining and the soil is present.

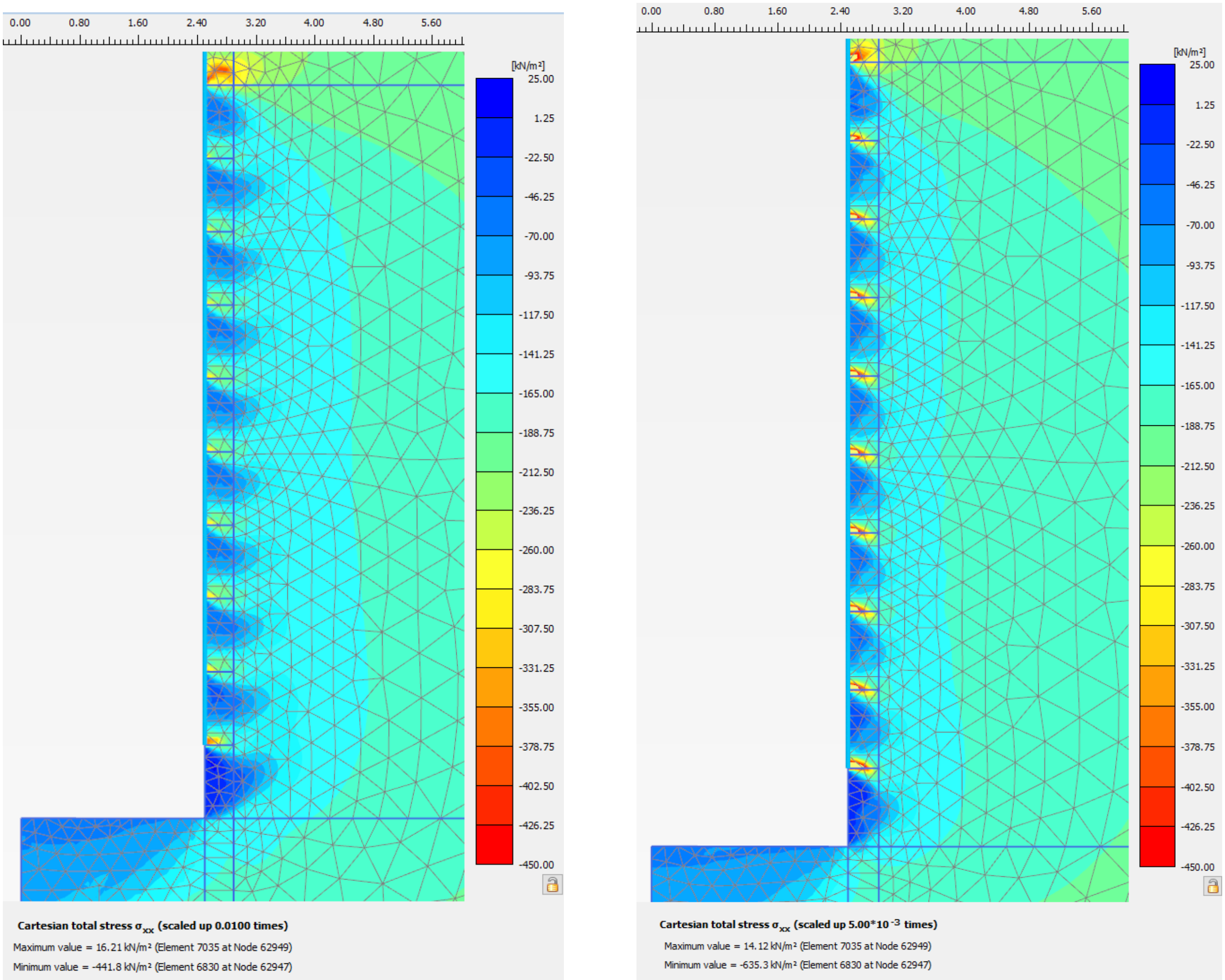

(a) Same cohesion case.

(b) Higher cohesion case.

Figure 7.17: Radial stress field obtained in Plaxis 2D for the enhanced Soil method at excavation phase 10.

The results reported in Figure 7.18 show a peculiar pattern. The plastic points are not limited to the tunnel face or to the excavation boundary. Indeed, a significant part of the plasticisation develops inside the enhanced soil layer, even in zones located beyond the face of the last excavation step. This behaviour can be related to the high stiffness assigned to the enhanced region, and due to that, this layer attracts a larger part of the stress during excavation. However, the plastic point in the layer must not be interpreted as the plastification of the pipes.

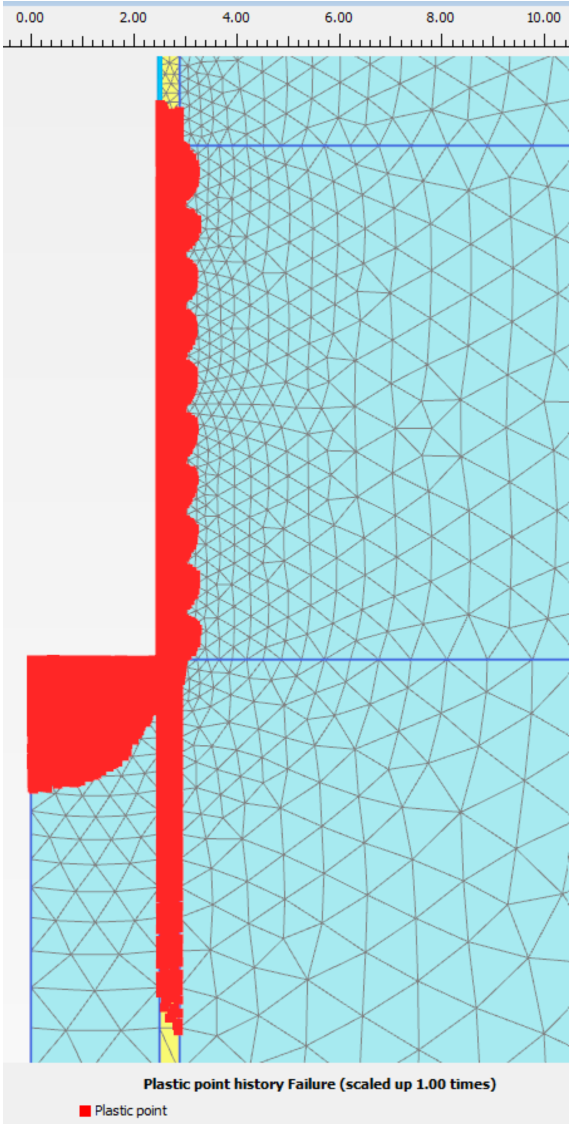

(a) Same cohesion case.

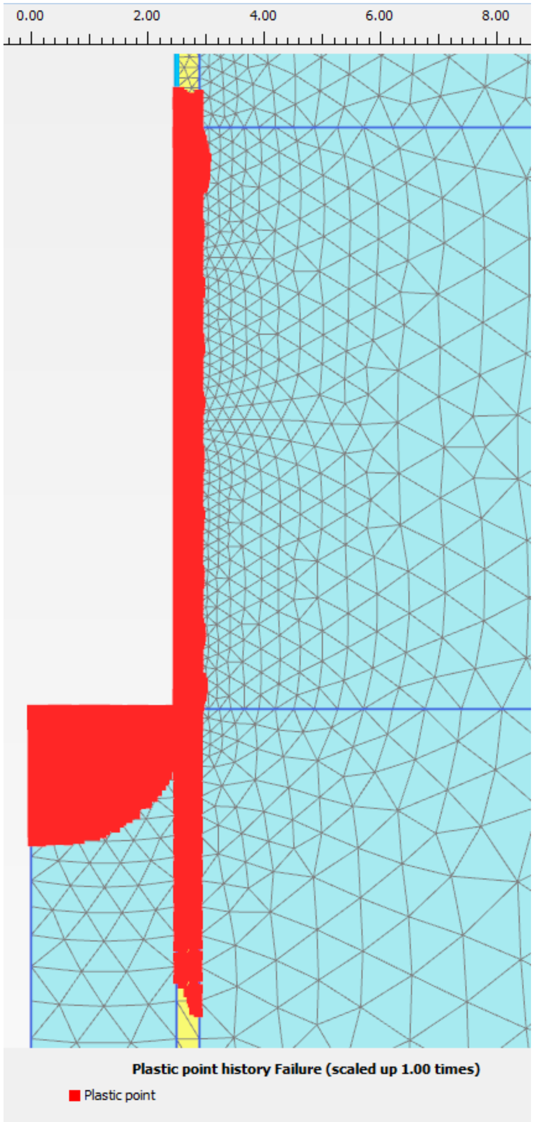

(b) Higher cohesion case.

Figure 7.18: Plastic points obtained in Plaxis 2D for the enhanced soil method at excavation phase 10.

7.3 Chapter conclusion

This chapter aims to present, both graphically and numerically, the results obtained from all the simulations introduced in the previous chapters. First, the analytical results are reported, including the free soil response, the case with lining, and the longitudinal displacement profile. The results obtained with Lagamine are then presented, with particular attention to the linear elastic equivalent volume approach and the corresponding displacement values. Subsequently, the results from Plaxis 2D are reported. In this case, in addition to the linear elastic equivalent volume approach, which was implemented in both numerical software programs, the results obtained from the other two methods are also presented, namely the anisotropic material approach and the enhanced soil approach. These two approaches were developed only in Plaxis 2D. Overall, the different models show noticeably different responses in terms of maximum deformation, radial displacement, and stress distribution. However, the detailed interpretation of these differences is not addressed in this chapter. The more extensive comments, comparisons, and critical analyses are instead developed in the following chapter, which is specifically dedicated to the comparison and discussion of the results.

8 Comparison and discussion

In this chapter, the results obtained from the different analyses are examined through graphical and numerical comparisons. The first step focuses on validating the FEM models against the analytical solution, mainly for the free soil response, in order to assess the consistency and reliability of the two numerical environments.

The displacement values obtained with Plaxis 2D and Lagamine are then compared for the linear elastic equivalent volume approach only. Subsequently, for greater consistency, the overall assessment of all the implemented pipe umbrella models is carried out entirely within Plaxis 2D.

The effects of the pipe umbrella system are mainly evaluated and discussed through the longitudinal profiles of radial displacement obtained after the ten excavation steps, which provide a global view of the deformation response.

In addition, a parametric assessment is performed based on the maximum radial displacement recorded in each simulation, taking as reference the configuration with lining only, without the pipe umbrella system. These elements made it possible to draw some important conclusions.

8.1 Analytical and 2D FEM comparisons

The first comparison concerns the Ground Reaction Curve, which represents a fundamental step in the validation of the model. In order to obtain the GRC, the lining was not activated and the ground was allowed to reach full deconfinement. The response was evaluated at a point sufficiently far from the model boundaries and far enough from the excavation face, so that the result could be considered representative of the ground behaviour without the influence of support elements.

As shown in Figure 8.1, the GRC obtained from the analytical model, Lagamine, and Plaxis 2D follows almost the same trend. This agreement confirms that the analytical formulation and the FEM models describe the same ground response under the defined assumptions. The small differences between the FEM and analytical curves are mainly related to the way the results are extracted in the numerical models. In particular, displacements are obtained at nodes, while stresses are evaluated at stress points or integration points, which do not coincide exactly with the same geometrical position.

This result is important because the GRC defines the mechanical response of the ground. Therefore, the correspondence between the analytical and numerical curves represents a first validation of the mathematical consistency of the models. This means that the simple analytical GRC can be enough to quickly determine the ground response.

Furthermore, if differences appear in the following analyses, they should not be directly attributed to an error in the basic formulation of the ground response, but rather to the additional modelling assumptions introduced later.

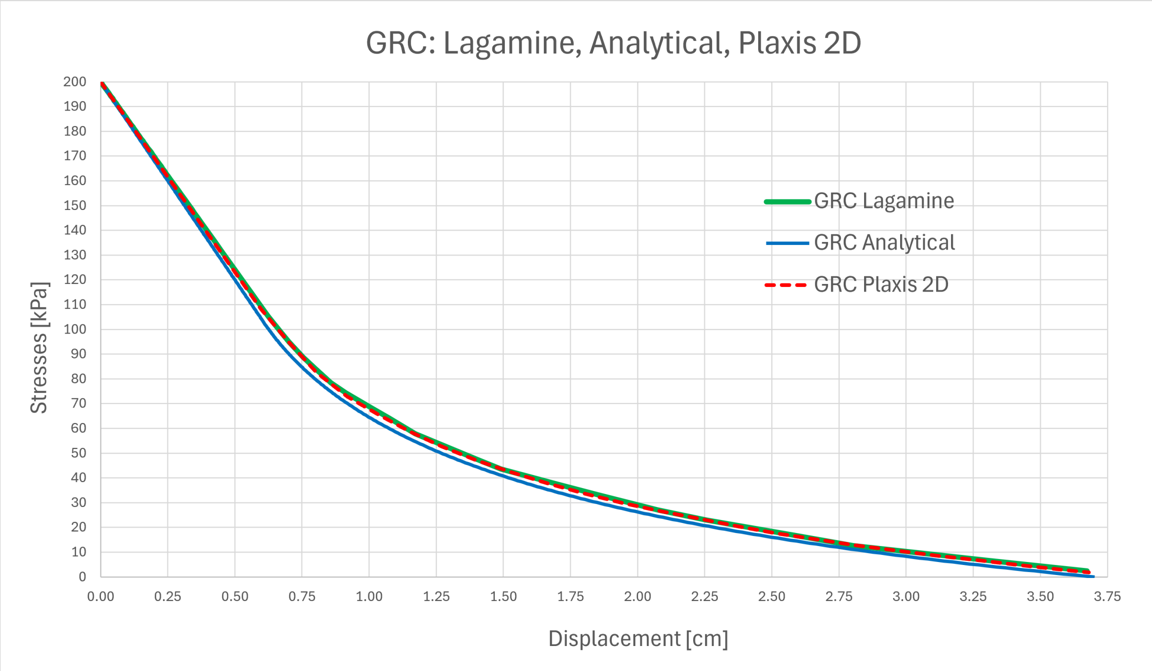

Figure 8.1: Comparison between the Ground Reaction Curves obtained from the analytical model, Lagamine and Plaxis 2D.

The second comparison concerns the Longitudinal Displacement Profile of free soil, without any support or pre-support, shown in Figure 8.2. The comparison was carried out between the analytical solution, the Lagamine and the Plaxis 2D. The analytical LDP is based on an approximate formulation, while the FEM result is obtained directly from the numerical simulation. For this reason, the numerical profile can be considered more reliable and representative of the actual longitudinal development of the displacement. In the graphs, the distance equal to zero corresponds to the tunnel face.

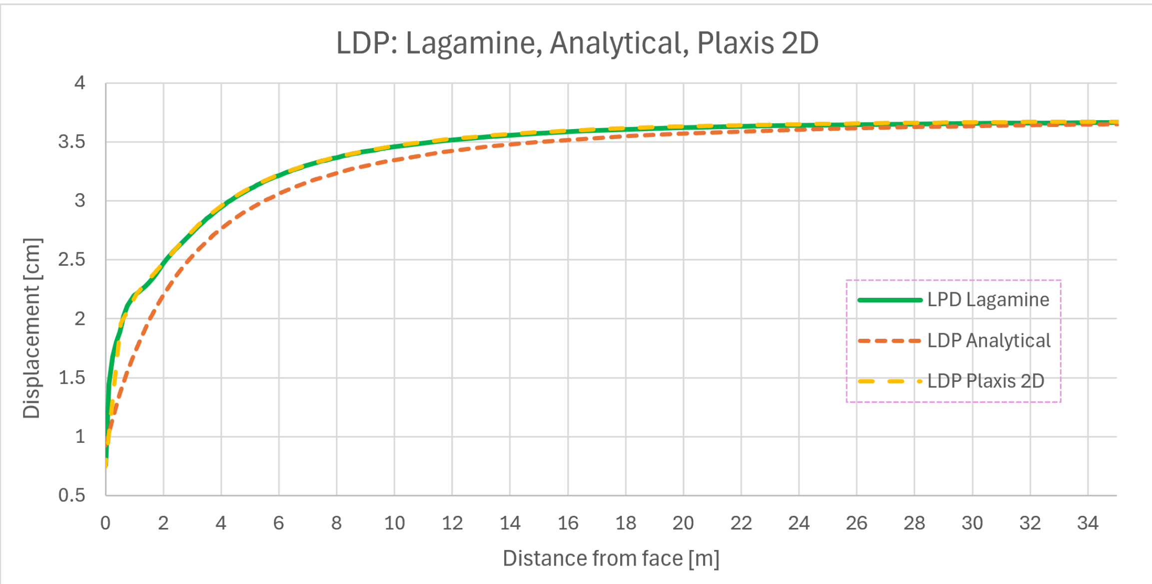

Figure 8.2: Comparison between the longitudinal displacement profiles at the tunnel wall obtained from the analytical model, Lagamine and Plaxis 2D. Distance=0 represents the tunnel face.

The two curves show the same general evolution, the displacement increases steeply close to the excavation face and progressively tends towards an asymptotic value far behind the face.

The analytical curve slightly underestimates the displacement in the first part of the profile, but it correctly reproduces the overall shape and the final order of magnitude.

The model chosen for the representation of the analytical LDP significantly influences the GRC-SRC intersection point and the solution of the problem. That explains the large difference in terms of displacement between the FEM and analytical models for the same unsupported one metre of soil, indeed

$$u_{R,analytic} = 1.71 \text{ cm}, \qquad u_{R,FEM} = 1.01 \text{ cm}.$$

The main reason for this initial difference could be explained by the fact that the FEM computes this curve from the stiffness properties of the ground, whereas the approach proposed by Panet–Corbetta uses generally calibrated parameters, such as a_0. It could be interesting to recalibrate different initial values of m and a_0 for the purpose of obtaining a closer agreement. However, considering the initial assumptions defined in this work and the objectives of this thesis, this procedure is not investigated in further detail.

Thus, the analytic solution represents undoubtedly a valid tool to compare results and define the order of magnitude of the project values, but it depends too much on the adopted strategy and the assumptions made.

8.2 Lagamine and Plaxis 2D comparison

For the unreinforced ground response case the comparison of the results between Lagamine and Plaxis 2D has already been discussed in the previous section. Thus, the following part focuses only on the results obtained for the linear elastic equivalent volume method, considering that this is the only method implemented in both FEM software.

In general, it can be observed that the longitudinal deformation pattern at the tunnel wall is quite similar in the two models (Figure 8.3). The first excavation face is located at a longitudinal distance of 75 m.

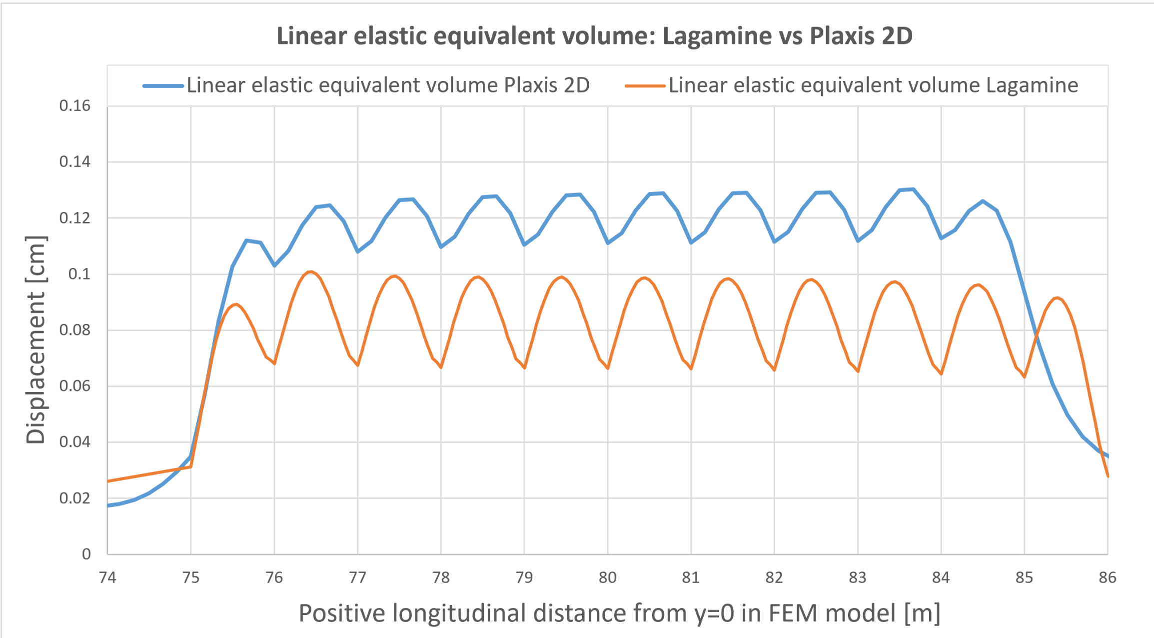

Figure 8.3: Comparison between Lagamine and Plaxis 2D longitudinal displacement profile at the tunnel wall for the linear elastic equivalent volume approach at the 10th excavation step. Distance=75 represents the first excavation face.

The shapes of the displacement patterns are similar and what is more important, the order of magnitude of the maximum radial displacement is comparable:

$$u_{R,\text{Lagamine}} = 0.10 \text{ cm}, \qquad u_{R,\text{Plaxis,2D}} = 0.13 \text{ cm}.$$

However, some differences between the two models are still present. These differences are mainly related to the mesh, the way in which the excavation stage is represented, and the different numerical formulation adopted by the two software packages; despite that, small differences in the final values can be considered acceptable. From a visual point of view, the two results remain consistent in terms of the overall deformation pattern, even though the local distribution is not exactly the same. One more excavation step has been mistakenly performed in the Lagamine model, but this does not influence the results.

8.3 Different 2D FEM methods comparison (Plaxis 2D only)

As anticipated in the previous section, Lagamine and Plaxis 2D have provided similar results. Nevertheless, the majority of the pipe umbrella models have been developed on Plaxis 2D, and so, to guarantee consistency and a better comparability of the results, only the Plaxis 2D ones are proposed hereby for the final comparison among the different methods.

It must be noted that the main quantity used for the comparison remains the radial displacement at the tunnel wall. This choice is made because the stress fields obtained inside the equivalent modelled layer are influenced by the simplified representation of the pipe umbrella. These stresses are useful to observe the general redistribution of stresses, but they are not interpreted as direct physical pressures acting in the real reinforced ground.

For all the models and configurations, the radial displacement is extracted along the tunnel wall, corresponding to

$$r = R = 2.5 \text{ m}.$$

All the reported results in Figure 8.4 are plotted for the 10th and last excavation phase. The first excavation face is located at a longitudinal distance of 75 m.

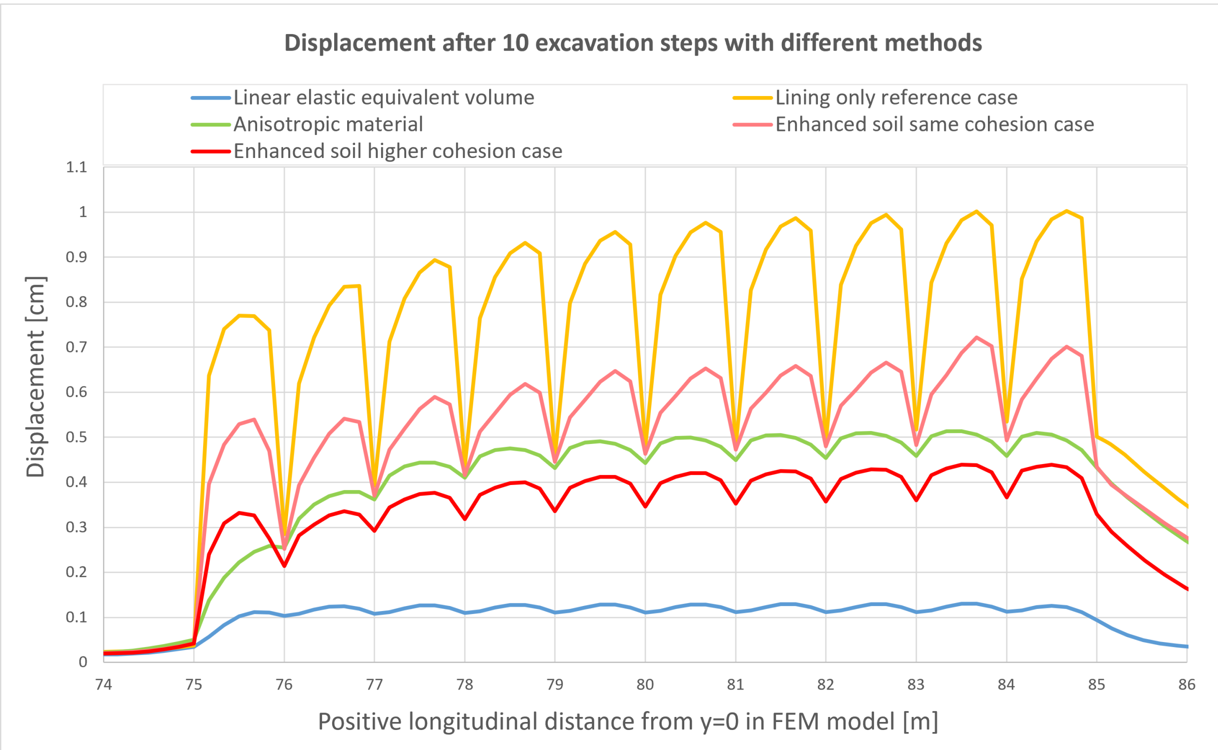

Figure 8.4: Comparison of the longitudinal displacement profile of the tunnel wall at the 10th excavation phase of all the methods. Distance=75 represents the first excavation face.

The comparison in terms of displacements gives some interesting observations. The case of lining-only is characterized by relatively large deformations, not only locally in the unsupported soil region, which is clearly visible through the individual deformation curves, but also at the global scale. In this case, the displacement generated during the first excavation stages does not differ significantly from the one obtained in the final stages. Therefore, the initial condition at 75 m does not seem to strongly affect the general response of the soil. The difference between the first excavated metre, which may still be influenced by the boundary conditions, and a later undisturbed excavation phase is then quite limited.

For the enhanced soil cases, the displacement is much smaller and scaled down compared with the lining-only case. However, the general trend remains similar. The local deformation curves associated with the unsupported meter are still clearly visible and are quite homogeneous in terms of intensity. In particular, their magnitude does not change significantly between the initial and final excavation stages. The method is less able to capture the directional effect introduced by the pipes.

The anisotropic material case appears to be an interesting approach. The deformation curves are flatter than in the previously described cases, but the overall response still seems realistic and mechanically plausible. The main difference appears in the global longitudinal behaviour. Indeed, unlike the other curves, this one increases more progressively and does not show the same initial peaks, which makes it more interesting not because of a higher reduction of displacements, but because it changes the deformation profile more coherently with the longitudinal response. This particular behaviour may indicate a more consistent representation of the pipe umbrella effect, since in this model the reinforced direction is introduced through the Young's modulus along the pipe axis. For this reason, the displacement profile seems to follow a more global deformation trend, which may be closer to the flexural behaviour expected from a beam-like element.

A different response is observed for the linear elastic equivalent volume. In this case, the computed displacement is much smaller than in the other models. The global displacement profile is more compressed, and the local deformation curves of the unsupported soil are less pronounced, with almost the same intensity throughout the excavation sequence. Such small displacements correspond to high stress levels if compared in the GRC. This suggests that this modelling approach may be too stiff and may not fully capture the expected behaviour of a soil reinforced by a pipe umbrella system. This could be explained by the fact that this approach is fast and simple and replaces the ground with an isotropic element characterized by very high stiffness in all directions, and it is likely unable to capture the preferential longitudinal behaviour of the pipes.

This consideration is also confirmed by the comparison between the longitudinal displacement profile of the free soil and that of the ground reinforced only by the pipe umbrella, without the contribution of the lining, shown in Figure 8.5. In both cases, the internal pressure was progressively reduced to zero to observe the free response of the ground. Despite the absence of the support, the model with the linear elastic equivalent volume method reaches a maximum displacement of only about 0.16 cm. The displacement obtained for the one unsupported metre is 0.13 cm, which is not far from the value obtained with no lining. This means that there is not a smooth development in the longitudinal displacement profile, because the majority of it is developed within the very first meter. This highlights once more the high stiffness of the equivalent region.

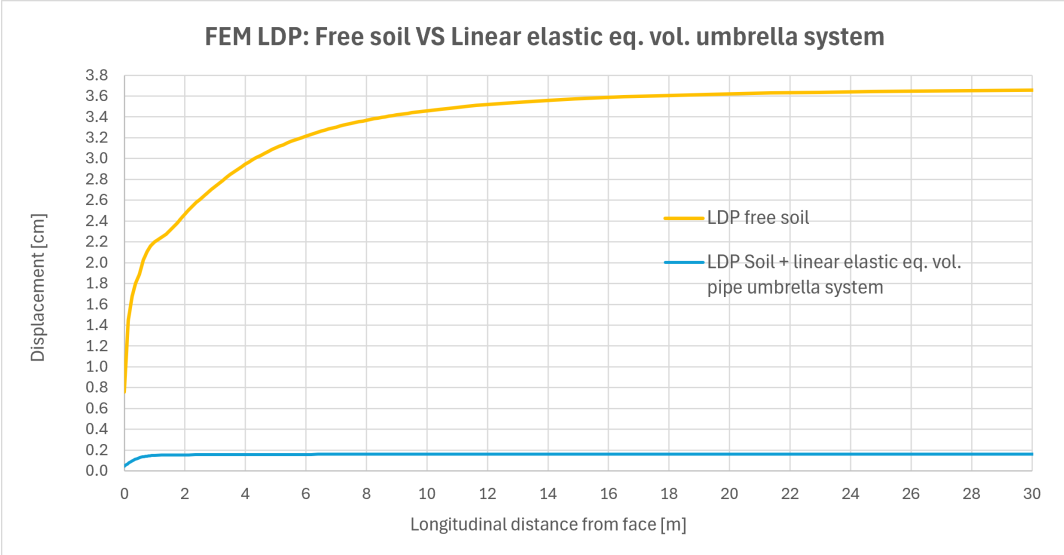

Figure 8.5: Longitudinal displacement profile at the tunnel wall of the free soil and of the soil reinforced by the pipe umbrella represented through the linear elastic equivalent volume approach. No lining contribution is included. Distance=0 represents the tunnel face.

8.4 Design parameters

8.4.1 Equivalent deconfinement from soil GRC

As defined in Section 3.4, the comparison between the different modelling strategies is also expressed in terms of an equivalent deconfinement ratio λ_{eq}, which, for the previously defined reason, is obtained from the maximum displacement rather than from the local stress field of each reinforced model.

The resulting value of λ_{eq} is therefore an equivalent indicator referred to the free-ground response. It allows the different approaches to be compared using the same reference GRC of the soil itself, which has been previously checked through the comparison between the analytical model and the two-dimensional unsupported models.

Thus, the software outputs allow the deconfinement ratio to be related directly to the radial displacement at the tunnel wall. The resulting curve is shown in Figure 8.6.

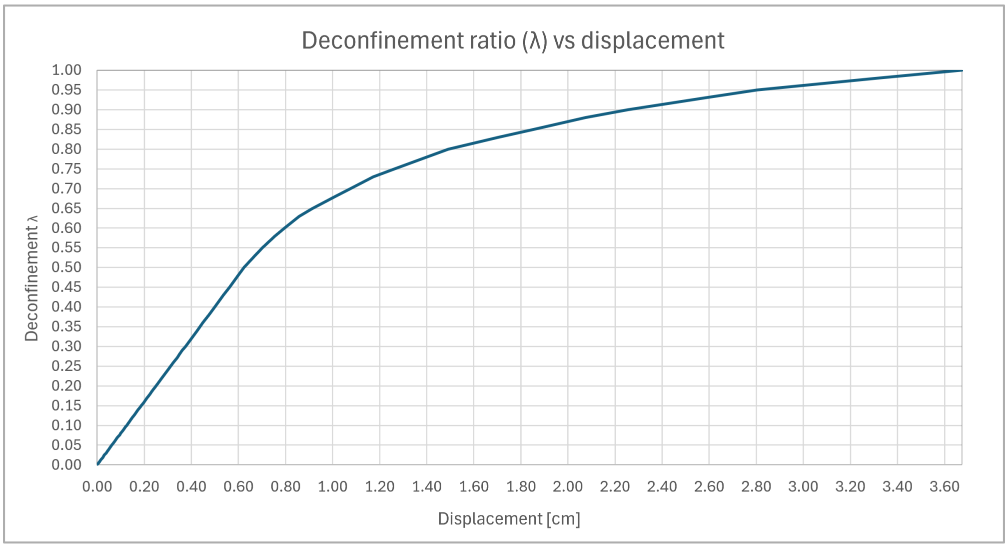

Figure 8.6: Deconfinement ratio at the tunnel wall as a function of the radial displacement obtained from the soil unsupported models.

The maximum displacements shown in the result chapter and the relative equivalent deconfinements obtained from each simulation are reported in Table 8.1.

Table 8.1: Equivalent deconfinement values obtained from the reference soil Ground Reaction Curve for the selected cases.

Case	λ_{eq}	u_R [cm]
Linear elastic equivalent volume	0.104	0.1310
Enhanced soil – high cohesion	0.355	0.4403
Homogenised anisotropic material	0.410	0.5144
Enhanced soil – same cohesion	0.550	0.7193
Reference case lining only	0.680	1.0030

A lower value of λ_{eq} means that the reinforced model shows a smaller displacement. When this displacement is projected onto the free-ground GRC, it corresponds to a lower level of deconfinement. Therefore, lower λ_{eq} values indicate a stronger effect of the pre-support.

Based on these results, it is possible to define the percentage reduction in terms of both deconfinement and displacement with respect to the reference case, represented by the lining only model (Table 8.2).

Table 8.2: Reduction of the equivalent deconfinement ratio and radial displacement with respect to the lining-only reference case.

Case	Reduction of λ_{eq} [%]	Reduction of u_R [%]
Linear elastic equivalent volume	84.7	86.9
Enhanced soil – high cohesion	47.8	56.1
Homogenised anisotropic material	39.7	48.7
Enhanced soil – same cohesion	19.1	28.3

These values should only be used to compare the different models, and they should not be interpreted as the efficiency of the pipe umbrella system representations.

8.4.2 Equivalent deconfinement from reinforced free response

As anticipated in the methodology, an equivalent deconfinement ratio can also be obtained from a new Ground Reaction Curve computed for the soil reinforced only by the pipe umbrella, without activating the lining. The internal pressure was progressively reduced to zero, allowing the reinforced ground to deform freely up to the equilibrium condition.

The comparison between the free-soil GRC and the GRC obtained with the linear elastic equivalent volume approach with no lining activation is shown in Figure 8.7. The two curves are almost overlapping, and only the zoomed view shows a small difference at the beginning of the response. It can be seen that the reinforced curve remains within the elastic range. This confirms that the equivalent volume, even without the presence of the main support, strongly reduces the deformation by introducing a high isotropic stiffness in the reinforced region.

From this modified GRC, the radial stresses can be extracted and used to evaluate an equivalent deconfinement ratio in terms of pressure. However, this procedure was applied only to the linear elastic equivalent volume approach, which is unable in this case to provide a sufficiently clear indication. That is why this second approach is not used for the final comparison of all the 2D methods, but only as an additional interpretation of this specific model.

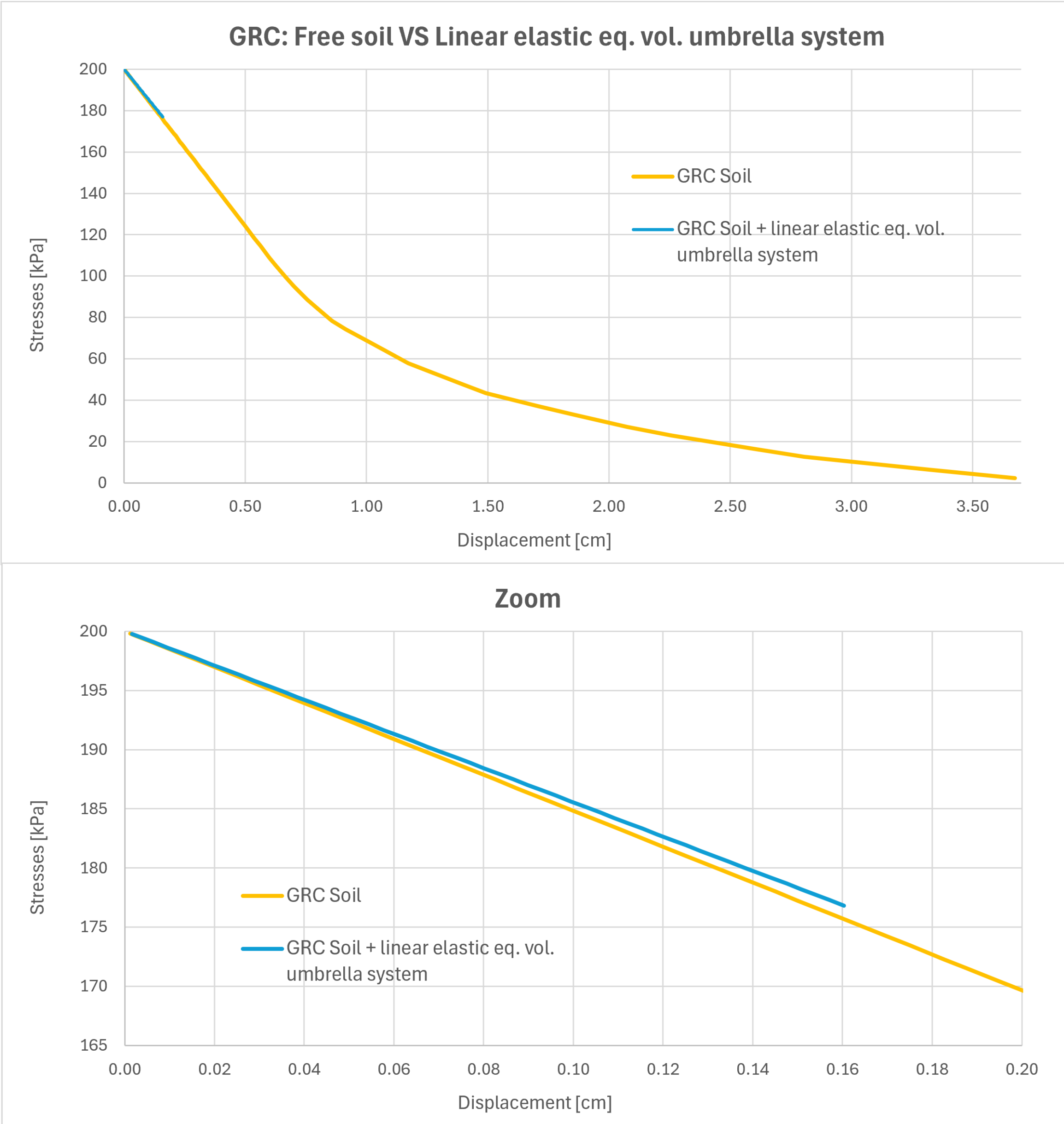

Figure 8.7: Ground reaction curve of the free soil and of the soil reinforced by the pipe umbrella represented through the linear elastic equivalent volume approach. No lining contribution is included in both cases.

8.5 Chapter conclusion

In this chapter, a critical analysis of the results has been developed. Therefore, the aim was not only to present the numerical and graphical comparisons, but also to interpret the possible reasons why each method exhibits a specific behaviour. In order to provide an additional parametric comparison with potential design relevance, the influence of each method on the equivalent deconfinement derived from the soil Ground Reaction Curve was also analysed, taking the lining-only configuration as the reference case. Overall, it was observed that the basic free soil response is practically identical in all models. The linear elastic equivalent volume approach shows a high stiffness and the lowest deformation levels, while the anisotropic material approach is able to reproduce the axial improvement in performance introduced by the pipes. Finally, the enhanced soil approach leads to reduced deformation magnitudes, although its response depends significantly on the adopted mechanical parameters.

9 Conclusions and perspectives

The results indicate that some of the proposed 2D strategies are able to reproduce, at least partially, the global influence of the pipe umbrella system on the deformation response of the tunnel. The comparison also shows that the results strongly depend on the adopted equivalent representation.

The linear elastic equivalent volume approach shows a very stiff response. Although this method is simple to implement and effective in reducing displacements, it may overestimate the reinforcement effect. The anisotropic material approach, instead, provides a better interpretation of the directional effect of the pipes, due to its mechanical formulation. The enhanced soil approach also reproduces the general improvement of the ground response and reduces the deformations, but it does not explicitly capture the increase of flexural stiffness along the pipe axis. Based on these results, it is therefore appropriate to further investigate strategies capable of introducing an anisotropic behaviour in the model, since this aspect appears to be relevant for representing the mechanical contribution of the pipes.

As a future perspective, it would be interesting to compare the results obtained in this thesis with those derived from a 3D numerical model based on the same assumptions, initial conditions, excavation stages and support sequence. This would provide a more complete basis for comparison and would make it possible to identify which of the methods implemented in this thesis is more suitable to reproduce the behaviour of the reinforced tunnel.

Further developments could also consider more realistic initial conditions, such as gravity and an anisotropic stress state. These aspects were not introduced in the present project, but they could be useful to extend the applicability of the proposed models to different tunnelling conditions.

References

Bae, G. J., Shin, H. S., Sicilia, C., Choi, Y. G., & Lim, J. J. (2005). Homogenization framework for three-dimensional elastoplastic finite element analysis of a grouted pipe-roofing reinforcement method for tunnelling. *International Journal for Numerical and Analytical Methods in Geomechanics*, *29*(1), 1–24. doi: 10.1002/nag.402

Barla, M. (2010). *Elementi di meccanica e ingegneria delle rocce.* Torino: CELID.

Bentley Systems. (2025). PLAXIS 3D Help: Parameters of the Jointed Rock model [Computer software manual]. Retrieved from `https://docs.bentley.com/LiveContent/web/PLAXIS%203D-v2025.1.3/Help/en/z_legacy_files/2283626/GUID-6A9B6678-24B7-4D90-A1BB-100C24B7BDAA.html` (Accessed: 2026-05-27)

Carranza-Torres, C., & Diederichs, M. (2009). Mechanical analysis of circular liners with particular reference to composite supports: combining shotcrete and steel sets. *Tunnelling and Underground Space Technology*, *24*, 431–449. doi: 10.1016/j.tust.2009.02.001

Elyasi, A., Javadi, M., Moradi, T., Moharrami, J., Parnian, S., & Amrac, M. (2016). Numerical modeling of an umbrella arch as a pre-support system in difficult geological conditions: a case study. *Bulletin of Engineering Geology and the Environment*, *75*, 211–221. doi: 10.1007/s10064-015-0738-5

Grasso, P., Mahtab, A., Ferrero, A. M., & Pelizza, S. (1991). The role of cable bolting in ground reinforcement. In *Soil and rock improvement in underground works* (Vol. 1, pp. 127–138). Milano.

Grasso, P., Mahtab, A., Pelizza, S., & Rabajoli, G. (1993). Considerations for design of shallow tunnels. In *International conference on underground transportation infrastructures* (pp. 138–146). Toulon.

Hoek, E. (2004). *Numerical modeling for shallow tunneling in weak rock.* Discussion Paper 3.

Morovatdar, A., Palassi, M., & Ashtiani, R. S. (2020). Effect of pipe characteristics in umbrella arch method on controlling tunneling-induced settlements in soft grounds. *Journal of Rock Mechanics and Geotechnical Engineering*, *12*, 984–1000. doi: 10.1016/j.jrmge.2020.05.001

Neuner, M., Schreter, M., Gamnitzer, P., & Hofstetter, G. (2020). On discrepancies between time-dependent nonlinear 3d and 2d finite element simulations of deep tunnel advance. *Computers and Geotechnics*, *119*, 103355. doi: 10.1016/j.compgeo.2019.103355

Panet, M. (1995). *Le calcul des tunnels par la méthode convergence-confinement.* Paris: Presses de l'École Nationale des Ponts et Chaussées.

Panet, M., & Sulem, J. (2022). *Convergence-confinement method for tunnel design.* Springer Nature Switzerland AG. doi: 10.1007/978-3-030-93193-3

Ranjbarnia, M., Fakher, M., & Sayyah, M. (2018). Convergence-confinement analysis of tunnels considering the umbrella arch system. *Tunnelling and Underground Space Technology*, *82*, 39–49. doi: 10.1016/j.tust.2018.07.033

Schumacher, F. P., & Kim, E. (2013). Modeling the pipe umbrella roof support system in a western us underground coal mine. *International Journal of Rock Mechanics and Mining Sciences*, *60*, 114–124. doi: 10.1016/j.ijrmms.2012.12.037

Song, K.-I., Cho, G.-C., Chang, S.-B., & Lee, I.-M. (2013). Beam–spring structural analysis for the design of a tunnel pre-reinforcement support system. *International Journal of Rock Mechanics and Mining Sciences*, *59*, 139–150. doi: 10.1016/j.ijrmms.2012.12.017

Svoboda, T., & Masin, D. (2009). Comparison of displacement field predicted by 2d and 3d finite element modelling of shallow natm tunnels in clays. *geotechnik*, *34*(2), 115–126. doi: 10.1002/gete.201000009

Viggiani, C. (1993). *Fondazioni.* Napoli: CUEN.

Volkmann, G. M., & Schubert, W. (2007). Geotechnical model for pipe roof supports in tunnelling. In J. Bartak, I. Hrdina, G. Romancov, & J. Zlamal (Eds.), *Underground space – the 4th dimension of metropolises: Proceedings of world tunnel congress 2007 (prague, czech republic, 5–10 may 2007)* (pp. 755–760). London: Taylor & Francis Group. doi: 10.1201/NOE0415408073.ch125

Wu, Y.-H., Liu, X.-R., Lin, X.-T., Zhang, Z., & Yao, Y.-Y. (2024). Study on mechanical characteristics of pipe umbrella with micro-arch effect. *Tunnelling and Underground Space Technology*, *145*, 105578. doi: 10.1016/j.tust.2023.105578

Zarei, H., Moarefvand, P., & Salmi, E. F. (2019). Numerical modeling of umbrella arch technique to reduce tunnelling induced ground movements. *Environmental Earth Sciences*, *78*, 291. doi: 10.1007/s12665-019-8302-4

Zhang, Z., Li, H., Liu, H., Li, G., & Shi, X. (2014). Load transferring mechanism of pipe umbrella support in shallow-buried tunnels. *Tunnelling and Underground Space Technology*, *43*, 213–221. doi: 10.1016/j.tust.2014.05.018